Hyperbolic L-spaces from a contact geometry perspective

by

Isacco Nonino

A thesis submitted in fulfilment of the requirements
for the degree of

Doctor of Philosophy

at the

School of Mathematics & Statistics
College of Science & Engineering
University of Glasgow

September 2026

To my father, who always believed in me.

Abstract

Thurston's seminal work on the geometrization conjecture shows that 3-manifolds admit a rich variety of geometric structures. In a different direction, the foundational result of Martinet [Mar71] establishes that every closed, orientable 3-manifold supports a *contact structure*. Within contact topology, there is a fundamental dichotomy between *tight* and *overtwisted* contact structures. While overtwisted structures are completely classified [Eli89], tight contact structures are considerably more rigid and remain far less understood. The classification of tight contact structures has therefore been a central problem in low-dimensional topology over the past decades. Early progress focused on model cases such as the 3-sphere [Eli92], solid tori and lens spaces [Hon00a, Hon00b], and has since expanded to include broad classes of Seifert fibered manifolds [EH01b, GS03, Wu06, GLS07, Tos20]. However, tight contact structures on hyperbolic 3-manifolds remain largely unexplored. In this thesis, we investigate the classification problem for tight contact structures on hyperbolic 3-manifolds. In particular, we present the first classification result for an infinite family of *hyperbolic L-spaces*, obtained in joint work with Hyunki Min [MN26]. We then turn to the study of symplectic fillability within this setting. It is known that not every tight contact structure is symplectically fillable [EH02], and understanding this distinction is a subtle and important problem. Building on previous constructions, we develop an algorithmic obstruction to (weak) symplectic fillability for families of contact structures arising from rational surgeries on L-space knots [Non24].

Contents

Acknowledgements

In all honesty, I have never believed too much in the vastly accepted concept of "the journey is more important than the destination". I have never felt this was true, and I would argue that both the journey and the destination are equally important in their own distinct way.

What I do think is correct is that very often during the journey we focus on the destination – and once we reached our goal, we tend to focus on the journey that led us there. If while we walk we stare at the horizon looking for a glimpse of the finishing line, when we sit down at the end of a long trip we wonder about all the small things that happened along the way. During these years, I have definitely spent a lot of time thinking of finally completing my PhD. Now that this thesis has finally come to be, I cannot avoid thinking about all the steps that allowed me to create such a complex work.

The first person that I should definitely thank, and to whom I owe much of what I am and of what I believe in, is my father. Thanks to your (maybe not so much) subtle exposure to the beauty of critical thinking, I grew up with the idea that, at the end of the day, there is nothing more important than creating something that nobody else has yet considered to create, and that everything deserves to be studied and analyzed, because it is only through comprehension that we can give full respect to the things that surround us. You are not here to read this, but if I am here to write this it is all thanks to you.

I also need to thank my sister Monica. Your presence always gave me stability and, when no one else was left for me to look up to, you gave me the possibility to keep feeling supported and understood, and gave me the idea that, at the end of the day, there is a chance that being an adult is not so bad.

I should probably thank all my friends back in the old, sleepy town of Udine, who were always there for me, and that never left my side, even when I left their place. I know you would get scared by finding your name associated to a mathematics work, but well, thanks to Jacopo, Mattia, Luca, Giovanni, Barbon, Viola, Marta, Andrea, Carlo, Stefano and many others.

I also would like to thank all the people that shared so many terrifying university classes with me. From hot, sunny days in Padua to cold, rainy days in Bonn, everyone of you played a role in leading me here. So thanks to Marta for long studying sessions that showed me the beauty of working closely with someone, thanks to Giacomo & Giacomo, thanks to Pietro, Andrea, Lucia, Matteo, Luca, thanks to Mara, Samuele, Guglielmo, Jordan, Jacopo and again, many others. And thanks to Aru, who gave me hope that one day, maybe, I would be as cool as her.

And now for these last 4 years. When I came to Glasgow, I was, for the third time in my life, completely changing the fabric of my daily existence. I was scared, and somehow not fully convinced I would find a place where my heart could feel warm.

Well, I was wrong.

I want to thank everyone at the Maths department here in Glasgow for being amazing colleagues, and more often than not, amazing friends. So thanks to Philipp, for being the best possible flatmate one could hope for, and for sharing so many thoughts with me. Thanks to JJ, for being such a great person and always available for a hike, or for a climb, or for watching some random football match. Thanks to Sage, for having been such an incredible friend. Although we will probably be continents apart, your wise words will always be with me. And yes, we are very good at basketball. Thanks to Gabriel for being such a wholesome presence, thanks to Parth for being genuine and always interesting, thanks to Susanna for bringing so much colour to our department, and thanks to Frieda, who made me remember how important is to cry, and to laugh, and how beautiful it is to do both. Thanks to Francesca, Alessandro, Sarah, Lewis, Ben, Marina, Francesco, Riccardo, Giulia, Franco, Simone, Daniel, Miguel, Livio, Luke, Lucia, Paula for sharing something so important with me: your time. I will always be grateful for that. Thanks to Ana and Andy, who always supported me as supervisors and looked after me. Thanks to Mark Powell, who believed in my qualities and discussed so much maths with me. Thanks to all my collaborators – Hyunki, Marc, Monika, Miguel, Daniel – for giving me the opportunity to create something together. Thanks to Alessio, Valentina, Magda, Alessandro and all the people I met at conferences, and made them more interesting.

Although this is a maths thesis, Glasgow – and my life, believe it or not! – is not just maths. I also want to thank Jen, whose artistic sense is much needed and whose smile is contagious. Thanks to Sara, Simona, Maider, Tatiana, Jack, Sam, Jason, Mitch, the huge basketball crew, and to everyone I had the chance to exchange a moment of life during these last years: you made my PhD experience easy to survive, and this is no simple feat.

Lastly, not for importance, I would like to thank Paula, whose presence on my side has allowed me to actually believe that, for some strange reason, I am good enough to be here, writing these acknowledgements.

These four years were a journey, and this is the destination. Now that I sit down, I look back and I think it was a great ride. So thanks to everyone, because this is a uniquely beautiful feeling, and should not be taken for granted.

Author's declaration

I declare that, except where explicit reference is made to the contribution of others, this dissertation is the result of my own work and has not been submitted for any other degree at the University of Glasgow or any other institution.

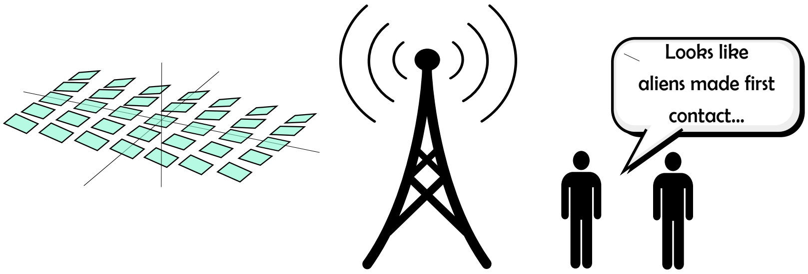

Chapter 1

Introduction

§ 1.1 | Hyperbolic L-spaces, a contact geometry approach

The nature of the research that we introduce in this thesis is dual and it builds on the important role that hyperbolic 3-manifolds, and specifically L-spaces, play in the context of contact geometry. Chapter 3 describes a complete classification result for (positive) tight contact structures on a family of hyperbolic L-spaces obtained as Dehn surgeries on the Whitehead link. This is the content of [MN26], written in collaboration with Hyunki Min. In some sense, this part is concerned with understanding *how many* distinct tight structures one can find for such manifolds. The main result of the first section is Theorem 3.1.3.

Theorem (3.1.3)**.** *Let $n \geq 5$ be an integer. Then $M(n,r)$ (this is the manifold obtained by (n,r)-surgery on the Whitehead link, see Figure 3.1) supports*

$$\begin{cases} \Psi(r) + 2\Phi(r) & r \in \mathcal{R}_+ \\ \Psi(r) & r \in \mathbb{Q}_- \end{cases}$$

tight contact structures up to isotopy, distinguished by their contact invariants in Heegaard Floer homology.

For the definition of $\mathcal{R}_+$ and $\mathbb{Q}_-$ see Chapter 3. There is also a section dedicated to some other contact-geometric *properties* of these structures. The main theorems in this part are Theorem 3.1.8 and Theorem 3.1.9.

Theorem (3.1.8)**.** *Let $n \geq 5$ be an integer and $r \in \mathcal{R}_+ \cup \mathbb{Q}_-$. Then every tight contact structure on $M(n,r)$ is Stein fillable.*

Theorem (3.1.9)**.** *Let $n \geq 5$ be an integer and $r \in \mathcal{R}_+ \cup \mathbb{Q}_-$. Then $M(n,r)$ supports* *at least*

$$\begin{cases} \Psi(r) + 2\Phi(r) - 6 & r \in \mathcal{R}_+ \\ \Psi(r) - 2 & r \in \mathbb{Q}_- \end{cases}$$

virtually overtwisted contact structures up to isotopy.

In the second part of this thesis, touching upon the connection with symplectic geometry, we investigate *symplectic fillability properties* of tight structures on hyperbolic L-spaces (see Definition 2.3.2)[1]. This is the content of [Non24]. Forgetting for a moment about the classification question we try to understand *what kind* of tight structures certain manifolds can admit. The main contribution we present in Chapter 4 is an algorithm that, given an L-space knot, can produce obstructions for symplectic fillability from its symmetrized Alexander polynomial. This is the content of Theorem 4.1.1, which we state here in a more concise form.

Theorem (4.1.1)**.** *Let K be an L-space knot, and let $K(n)$ be the manifold obtained by n-surgery on K, for $n \in \mathbb{N}$ square-free. We describe a set of inequalities involving only n and the exponents of the symmetrized Alexander polynomial of K. If such inequalities are not satified, then the manifold $K(n)$ has no weakly symplectically fillable contact structures.*

As an application, we prove that the hyperbolic L-space knots discussed in [BK22] produce an infinite family of hyperbolic L-spaces with tight contact structures having no weak symplectic fillings. Although our procedure is not new, but rather a generalised version of an already existing technique (see [LL19, KT17]), the family of knots we study is quite different from the ones previously analyzed in the literature. We describe this more in detail at the beginning of Chapter 4.

The motto of this thesis is that hyperbolic L-spaces are, from a contact geometry perspective, extremely important objects to study. We hope that the techniques discussed in Chapter 3 will be further used to study other families of manifolds and that the algorithm in Chapter 4 will be used for other families of L-space knots and links.

§ 1.2 | A history of contact geometry

In order to better understand the relevance of our contribution we provide a brief introduction to the past, the present and the future of the classification problem in contact geometry.

Since its introduction in the late nineteenth century, contact geometry has been studied from a wide range of perspectives. Owing to its polyhedric nature, it lies at the intersection of several areas of mathematics, including dynamical systems, symplectic geometry, and knot theory. This interplay is not merely tangential: contact

[1]Note, this family of hyperbolic L-spaces is not the same as the one considered in Chapter 3.

geometry has played a central role in the proof of deep results that, at first glance, appear unrelated to it. Notable examples include Eliashberg's proof of Cerf's "$\Gamma_4 = 0$" Theorem [Eli92].

As is the norm when dealing with specific structures on manifolds, a fundamental goal is their classification up to an appropriate notion of equivalence. For instance, in the study of smooth structures on topological manifolds, considerable effort has been devoted to understanding when two such structures are equivalent under diffeomorphism. In contact geometry one is naturally led to classify contact structures up to isotopy.[2]

A key feature of contact geometry is the existence of a fundamental dichotomy between two types of contact structures: *tight* and *overtwisted*. Given a 3-manifold M, a contact structure is called overtwisted if it contains an embedded overtwisted disc, that is, a disc whose boundary is everywhere tangent to the contact distribution and whose framing given by the contact planes agrees with the framing given by the disc (see Definition 2.2.4). Contact structures that do not contain such discs are called tight.

This is not just an ad hoc distinction: it has concrete consequences. Tight contact structures exhibit a strong form of rigidity, while overtwisted structures are considerably more flexible. For example, invariants of isotropic submanifolds (Definition 2.1.12) in tight manifolds are subject to stringent constraints, whereas these constraints can fail in the overtwisted setting. A similar contrast appears in the theory of convex surfaces (Definition 2.2.34), whose dividing multicurves (Definition 2.2.36) are much more restricted in tight manifolds (see Theorem 2.2.44).

This dichotomy is reflected in the classification problem. No tight contact structure can be isotopic to an overtwisted one, and vice versa, so the classification naturally splits into these two cases.

The overtwisted case is by now well understood. A fundamental result of Eliashberg [Eli89] (see Theorem 2.2.11) states that two overtwisted contact structures are isotopic if and only if they are homotopic as 2-plane fields. Since homotopy classes of 2-plane distributions can be studied using algebraic topology, this result reduces the classification of overtwisted contact structures to a purely algebraic-topological problem. Moreover, it implies that every 3-manifold admits an overtwisted contact structure.

In contrast, the classification of tight contact structures is significantly more subtle. Eliashberg's theorem does not extend to this setting; in fact, homotopic tight contact structures need not be isotopic. Plus, there might be homotopy classes of 2-plane fields not containing any tight contact structure. As a consequence, the classification problem cannot be reduced to purely topological data. This difficulty has led to the development of a variety of powerful techniques, including convex surface theory and

[2] This is not equivalent to classification up to *contactomorphism*: a contactomorphism induces an isotopy through contact structures if and only if it is smoothly isotopic to the identity, by Gray stability [Gra59].

invariants arising from Heegaard Floer homology, which provide tools to study the finer structure of tight contact manifolds.

A natural preliminary question is whether every 3-manifold admits a tight contact structure. Unlike the overtwisted case, the answer is negative. Etnyre-Honda [EH01b] showed that $\overline{\Sigma(2,3,5)}$ (the Poincaré homology sphere with reverse orientation) admits no *positive* (see Remark 2.1.3) tight contact structure. The manifold $\overline{\Sigma(2,3,5)}\#\Sigma(2,3,5)$ carries no tight contact structure (neither positive nor negative). More generally, [LS09] shows that there exist infinite families of Seifert fibered spaces that do not admit positive tight contact structures.

On the other hand, (positive) tight contact structures have been classified for several classes of 3-manifolds, including most (but not all) atoroidal Seifert fibered spaces and certain toroidal manifolds [CGH09, EH01b, Eli92, Etn00, Gir99, Gir01, GS03, GLS07, HKM02, Hon00a, Hon00b, Kan97, Tos20, Wu06]. We will discuss some of these results in Chapter 3.

In contrast, the situation for hyperbolic 3-manifolds remains largely open. This is particularly unsatisfactory, as most prime 3-manifolds are hyperbolic [Thu82]. In particular, it is not known whether every hyperbolic 3-manifold admits a tight contact structure.

Following the work of Thurston and Eliashberg [ET98] hyperbolic 3-manifolds admitting taut foliations (see Definition 2.4.2) also admit *universally tight* (see Definition 2.2.12) contact structures. Universally tight structures are tight. Consequently, in order to find potential counterexamples to the existence of tight structures, one is led to consider manifolds that do not admit taut foliations.

A natural class of candidates is given by hyperbolic L-spaces. These are rational homology spheres with particularly simple Heegaard Floer homology (see Definition 2.4.1), generalizing the notion of lens spaces. By results of [OS04a], L-spaces do not admit taut foliations. Moreover, the *L-space conjecture* (see Conjecture 2.4.3) predicts that they are precisely the 3-manifolds without coorientable taut foliations.

This makes hyperbolic L-spaces a compelling setting in which to investigate the existence and classification of tight contact structures. One possible strategy is to attempt to construct counterexamples to the existence question by studying tight contact structures on such manifolds.

The work presented in this thesis is motivated by the central role that hyperbolic L-spaces play in this context.

§ 1.3 | Thesis structure

Chapter 2 contains preliminary notions that should help the reader for the rest of the thesis. We first introduce contact structures and discuss their basic properties. We also define certain types of submanifolds which will be relevant for our work. We conclude it by introducing briefly the notions of fillability that will be relevant for the last part of the thesis and the necessary Heegaard Floer theoretic results.

Chapter 3 is dedicated to proving the classification result for hyperbolic L-spaces obtained by Dehn surgeries on the Whitehead link.

Finally, Chapter 4 is devoted to describing the algorithm to obstruct symplectic fillability for L-space knots.

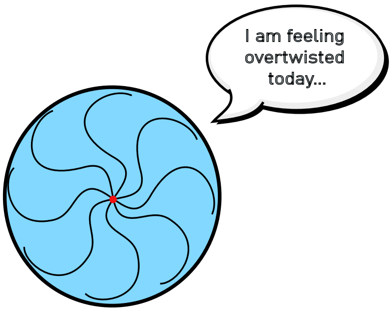

Chapter 2

Background knowledge

This section is intended to be a short but substantially complete introduction to contact geometry. We refer the reader to [Gei08] for details and further expositions. For more background knowledge in specific topics, like convex surface theory and symplectic fillability, we refer the reader to the corresponding sections, where more advanced results are presented.

§ 2.1 | Contact structures: definitions and basic properties

Fix M a smooth, odd-dimensional manifold and consider its tangent bundle TM. We will study smooth sub-bundles ξ of codimension 1 in TM. We refer to such codimension 1 objects as *fields of hyperplanes*, or codimension 1 *distributions*. Informally, one can think of these sub-bundles as a consistent choice of a hyperplane ξ_p in T_pM for all points $p \in M$.

In general, in order to study and describe a hyperplane field we write it as the kernel of a differential 1-form. More precisely, we always write

$$\xi = \ker \alpha,$$

where α is a smooth 1-form on M. This can be always done locally and if the distribution is coorientable[1], even globally [Gei08]. The description in terms of differential forms becomes quite handy when studying contact structures.

Remark 2.1.1. Note that if $\xi = \ker \alpha$ then $\xi = \ker \lambda\alpha$ for any other choice of 1-form $\lambda\alpha$, where λ is a non-vanishing real valued function.

Contact structures are special types of hyperplane fields. More precisely they are *maximally non-integrable* hyperplane fields. By this we mean that *no codimension 1 submanifold N of M has the property*

$$T_qN = \xi_q$$

[1] By this we mean there is an orientable line field transverse to ξ, i.e. we are orienting the *normal bundle* of ξ.

for all $q \in N$. Roughly speaking, the contact hyperplane field always cuts through codimension 1 submanifolds in some interesting way, and it is never completely tangent to them. This is an intuitive condition, but it is quite hard to work with. Looking at the identification

$$\xi = \ker \alpha,$$

we can model the non-integrability condition as

$$\alpha \wedge (d\alpha)^n \neq 0$$

everywhere. This is also commonly referred to as the *contact condition.*

Definition 2.1.2 (Contact structure). Let M be a $2n+1$ dimensional smooth manifold. A (coorientable) *contact structure* on M is a maximally non-integrable hyperplane field $\xi = \ker \alpha \subset T_M$, that is, the 1-form α satisfies

$$\alpha \wedge (d\alpha)^n \neq 0.$$

The form α is the *contact form* and the pair (M, ξ) is a *contact manifold.*

Remark 2.1.3 (Orientations). Note that $\alpha \wedge (d\alpha)^n$ is a *volume form*, since its a non-vanishing $(2n+1)$-form. In particular, for this to exist M needs to be orientable. The contact condition is independent of the specific choice of α. Any other choice must be of the form $\lambda\alpha$ where λ is a non-vanishing real valued function on M. It's a simple calculation to show that

$$(\lambda\alpha) \wedge (d(\lambda\alpha))^n = \lambda\alpha \wedge (\lambda d\alpha + d\lambda \wedge \alpha)^n = \lambda^{n+1}\alpha \wedge (d\alpha)^n \neq 0.$$

The above equality shows that if $n+1$ is even then the sign of the volume form is independent of the choice of α but is rather a property of ξ. So in such cases the contact structure induces a natural orientation on M. If M comes equipped with an orientation, we say that the contact structure is positive if the two agree, negative otherwise.

Example 2.1.4 (Standard contact structures on $\mathbb{R}^{2n+1}$). On $\mathbb{R}^{2n+1}$ with Cartesian coordinates $(x_1, \cdots, x_n, y_1, \cdots, y_n, z)$ the 1-form

$$\alpha = dz + \sum_{j=1}^{n} x_j dy_j$$

defines a contact form. The contact structure $\xi = \ker \alpha$ is called the *standard contact structure on* $\mathbb{R}^{2n+1}$. See Figure 2.1 for a visual representation in $\mathbb{R}^3$.

Definition 2.1.5 (Contactomorphism). Two contact manifolds (M_1, ξ_1) and (M_2, ξ_2) are *contactomorphic* if there exists a diffeomorphism

$$f : M_1 \to M_2$$

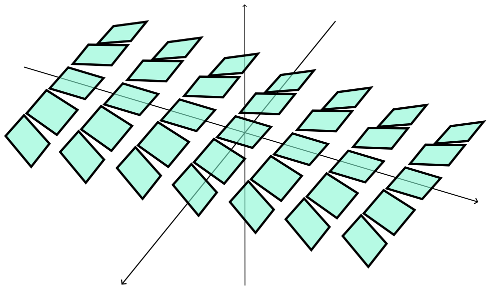

Figure 2.1: The standard contact structure on $\mathbb{R}^3$

so that

$$df(\xi_1) = \xi_2,$$

where $df : TM_1 \to TM_2$ denotes the differential of f. We normally denote two contactomorphic manifolds by $(M_1, \xi_1) \cong_{cont} (M_2, \xi_2)$.

Remark 2.1.6. If we write $\xi_1 = \ker \alpha_1$ and $\xi_2 = \ker \alpha_2$ then the above definition is equivalent to the existence of a nowhere vanishing real valued function λ so that

$$f^*\alpha_2 = \lambda\alpha_1.$$

Definition 2.1.7 (Contact isotopy)**.** We say that two contact structures ξ_1 and ξ_2 are *contact isotopic* if the hyperplane fields ξ_1 and ξ_2 are homotopic through contact-hyperplane fields.

A result standing at the foundations of contact geometry is *Gray stability theorem* [Gra59]. This result relates smooth isotopies of the underlying manifold with homotopies through distributions.

Theorem 2.1.8 (Gray stability theorem)**.** *Let ξ_t, $t \in [0, 1]$ be a smooth family of contact structures on a closed manifold M. Then there exists an isotopy ψ_t, $t \in [0, 1]$ of M such that*

$$d\psi_t(\xi_0) = \xi_t$$

for all $t \in [0, 1]$. The isotopy ψ_t is a contact isotopy of (M, ξ_0) to (M, ξ_1).

Remark 2.1.9. The assumption that M is closed is rather important. Theorem 2.1.8 does not hold for open manifolds [Tri06].

By Theorem 2.1.8, two contact structures on M are contact isotopic if and only if there is a smooth ambient isotopy of M carrying one structure to the other. There is also another structural result that relates contact structures locally.

Theorem 2.1.10 (Darboux's Theorem)**.** *Let α be a contact form on M^{2n+1} and p a point in M. Then there is a local chart $(x_1, \cdots, x_n, y_1, \cdots, y_n, z)$ on a neighbourhood*

$U_p \subset M$ of p such that $p = (0, \cdots, 0)$ and

$$\alpha|_U = dz + \sum_{j=1}^{n} x_j dy_j.$$

Recall that in Example 2.1.4 we called the structure defined by the right hand side of the equation the standard structure on $\mathbb{R}^{2n+1}$. Theorem 2.1.10 shows that locally all contact structures are contactomorphic to the standard contact structure on $\mathbb{R}^{2n+1}$. Hence, the relevant differences between contact structures are measured globally and not locally. The global behaviour is on the other hand controlled by the stability result in Theorem 2.1.8.

§ 2.1.1 | Submanifolds of contact manifolds

We now give some relevant definitions for submanifolds in contact manifolds. These will be important for defining certain type of contact structures, and are key for the work presented in this thesis.

Definition 2.1.11 (Contact submanifold)**.** Let (M, ξ) be a contact manifold. A submanifold M' of M with contact structure ξ' is called a *contact submanifold* of (M, ξ) if $TM' \cap \xi|_{M'} = \xi'$.

Definition 2.1.12 (Isotropic submanifold)**.** An embedding $\iota \colon L \longrightarrow (M, \xi)$ is called an *isotropic embedding* if $\iota(L)$ is an *isotropic submanifold*, i.e. the contact structure ξ is tangent everywhere to $\iota(L)$.

Remark 2.1.13. The most relevant example of isotropic embeddings are *Legendrian embeddings* of links.

Definition 2.1.14 (Characteristic foliation)**.** The *characteristic foliation* S_ξ of a hypersurface S in (M, ξ) is the singular 1-dimensional foliation of S defined by the distribution $(TS \cap \xi|_S)^\perp$.

Remark 2.1.15. Here $(T_pS \cap \xi_p)^\perp$ denotes the symplectically orthogonal complement to the (non-constant rank) distribution $(T_pS \cap \xi_p)$ with respect to $d\alpha$. The distribution $(T_pS \cap \xi_p)$ spans either the full tangent space at p or it is a codimension 1 subspace both of T_pS and ξ_p. If $(T_pS \cap \xi_p)$ is the full tangent space T_pS then the orthogonal complement is simply $\{\mathbf{0}\}$. Otherwise, $(T_pS \cap \xi_p)^\perp$ is a 1-dimensional subspace in $(T_pS \cap \xi_p)$. If M is 3-dimensional and S is a surface, we have that $(T_pS \cap \xi_p)^\perp = (T_pS \cap \xi_p)$ at the points p for which the intersection is 1-dimensional.

In short, the characteristic foliation is the singular foliation dictated by the contact structure restricted on the hypersurface. As we will see, the characteristic foliation of a surface in a contact 3-manifold encodes a lot of information about the contact structure.

§ 2.2 | Contact structures on 3-manifolds

Although contact structures can be defined in all odd dimensions, we are mainly interested in 3-dimensional manifolds. This has been, by far, the most studied area of contact geometry. In recent times the interest in higher dimensional contact manifold has consistently increased (see for example [BEM15, CPP15, MNW13]). From now onwards, we will assume that $2n + 1 = 3$, and all our definitions are done in this dimension. Most of them can be generalised – with some modifications – to higher dimensions.

The first key result in 3-dimensional contact geometry is due to Martinet [Mar71].

Theorem 2.2.1 (Martinet)**.** *Every closed, orientable 3-manifold M admits a contact structure.*

There are multiple ways to prove Theorem 2.2.1. One can interpret it as a consequence of the Lickorish-Wallace theorem and the fact that S^3 admits a contact structure combined with the following theorem.

Theorem 2.2.2. *Let ξ_0 be a contact structure on a 3-manifold M_0. If M is the manifold obtained from M_0 via Dehn surgery along a knot K, then M admits a contact structure ξ which coincides with ξ_0 away from the neighbourhood of K where the surgery is performed.*

Theorem 2.2.1 tells us that a closed contact 3-manifold always admits a contact structure. There is another existence result for contact structures on (closed, orientable) 3-manifolds.

Theorem 2.2.3 (Lutz-Martinet theorem)**.** *Every cooriented tangent 2-plane field on a closed, orientable 3-manifold is homotopic to a contact structure*

For the proof, see [Gei08] and references therein. Hence for 3-manifolds not only contact structures always exist, but they are also as frequent as possible. Every homotopy class of 2-plane fields contains a contact structure. To further investigate the nature of contact structures in these homotopy classes of 2-plane fields we ought to introduce the most important dichotomy of contact structures on 3-manifolds.[2] This was introduced by Eliashberg in [Eli89]. We are referring to the division into *tight* and *overtwisted* contact structures. Informally, a contact structure "twists enough" so that no surface is completely tangent to the distribution. However, it could "twists too much".

Definition 2.2.4 (Overtwisted disc)**.** An embedded 2-disc D in a contact 3-manifold (M, ξ) is an *overtwisted disc* if its boundary $\partial\Delta$ is a Legendrian curve for ξ with $tb = 0$ (see Definition 2.2.19 below), and the characteristic foliation of D contains only a singular point in the interior of the disc.

[2] As mentioned before, this is not restricted to dimension 3 – the generalisation to higher dimension is discussed, for example, in [BEM15].

Remark 2.2.5. As mentioned in [Gei08], the additional requirement that the characteristic foliation only contains a singular point is superfluous. Whenever the boundary of an embedded disc satisfies the conditions in Definition 2.2.4, we can isotope the disc relative to the boundary to a disc with the correct characteristic foliation (or to a disc containing an overtwisted disc in its interior). Hence nowadays an the expression "overtwisted disc" really means an embedded disc Δ with $\partial\Delta$ Legendrian curve with $tb = 0$. The last condition means that $\partial\Delta$ has contact framing coinciding with the Seifert framing.

Definition 2.2.6 (Overtwisted contact structure)**.** A contact structure on a 3-manifold is called *overtwisted* if it contains an overtwisted disc.

Definition 2.2.7 (Tight structure)**.** A contact structure is called *tight* if it is not overtwisted.

Remark 2.2.8. The contact structure defined in Example 2.1.4 is tight. This was first proved by Bennequin in [Ben83].

Example 2.2.9 (Overtwisted contact structure on $\mathbb{R}^3$). We can define the contact structure ξ_{ot} on $\mathbb{R}^3$ given by $\ker \alpha_{ot}$ where

$$\alpha_{ot} = \cos(r)dz + r\sin(r)d\theta$$

in cylindrical coordinates. ξ_{ot} is overtwisted, as we can find an evident overtwisted disc in $D = \{r \leq \pi, z = 0\}$, since $\xi|_{r=\pi} = \ker(-dz) = \langle\{\partial_x, \partial_y\}\rangle$.

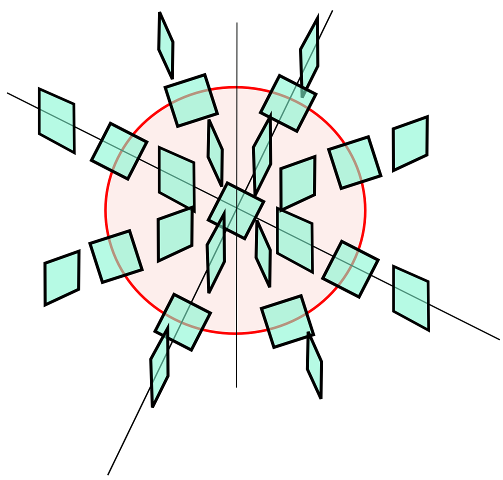

Figure 2.2: The overtwisted contact structure ξ_{ot} on $\mathbb{R}^3$, together with the overtwisted disc in red.

Example 2.2.10. On $S^3 \hookrightarrow \mathbb{C}^2$ we can define the contact structure $\xi_{std} = \ker\alpha$, where

$$\alpha = \sum_{i=1}^{2} x_i dy_i - y_i dx_i.$$

ξ_{std} is tight, and has the property that $(S^3 \setminus \{pt\}, \xi_{std}|) \cong_{cont} (\mathbb{R}^3, \xi_{std})$, where the latter is the standard structure on $\mathbb{R}^3$ defined in Example 2.1.4. Here (S^3, ξ_{std}) is the *standard tight sphere*, and thanks to Eliashberg [Eli92] we know that up to isotopy ξ_{std} is the unique tight structure on S^3.

As mentioned in Chapter 1, we are interested in classifying contact structures on 3-manifolds. We introduced a dichotomy splitting them into tight and overtwisted. The following result due to Eliashberg [Eli89] essentially says that the isotopy classification of overtwisted structures is equivalent to the homotopy classification of 2-plane fields.

Theorem 2.2.11 (Classification of overtwisted contact structures)**.** *The obvious inclusion map:*

$$i : \mathcal{E}^{ot}(M) \to Distr(M),$$

induces a bijection at the level of path components. Here $\mathcal{E}^{ot}(M)$ is the space of overtwisted structures on M, and $Distr(M)$ is the space of hyperplane fields.

In short: Theorem 2.2.11 says that every 2-plane field is homotopic to an overtwisted structure and two homotopic (via 2-plane fields) overtwisted contact structures are also isotopic (via contact structures). It is evident that this result reduces the classification problem for overtwisted contact structures to a topological problem substantially disjoint from contact geometry. On the other hand, tight contact structures are harder to study, as an adapted version of Theorem 2.2.11 does not hold.[3]

Inside the family of tight contact structures there is a relevant subfamily composed by the so called *universally tight structures*.

Definition 2.2.12 (Universally tight structures)**.** A tight contact manifold (M, ξ) is *universally tight* if the contact manifold $(\widetilde{M}, \widetilde{\xi})$ is tight. Here $\widetilde{M}$ is the universal cover of M and $\widetilde{\xi}$ is the pullback of ξ under the covering map.

In opposition to universally tight structures we have the *virtually overtwisted* ones.

Definition 2.2.13 (Virtually overtwisted)**.** A tight contact manifold (M, ξ) is *virtually overtwisted* if there exists a finite cover M' so that the pull-back contact structure ξ' on M' is overtwisted.

Note that if M is compact, residual finiteness implies that the universal cover is tight if and only if every finite cover is tight [Hon00a]. Hence the two definitions above are truly mutually exclusive for the manifolds we consider.

§ 2.2.1 | Submanifolds of contact 3-manifolds

We will now introduce certain submanifolds of contact 3-manifolds that play a relevant role in our work. We start with 1-dimensional submanifolds, i.e. links in contact 3-manifolds. As mentioned before, there are two special types of links.

[3]The quickest way to see this is to note that there are 3-manifolds without tight structures [LS09].

Definition 2.2.14 (Legendrian link)**.** A *Legendrian link* in a contact 3-manifold (M, ξ) is (the image of) a Legendrian embedding $\gamma : \bigsqcup S^1 \to (M, \xi)$. This means that the embedding satisfies $d\gamma(\theta) \in \xi_{\gamma(\theta)}$ for all $\theta \in \bigsqcup S^1$.

Definition 2.2.15 (Transverse link)**.** A *transverse link* in (M, ξ) is (the image of) an embedding $\gamma : \bigsqcup S^1 \to M$ that is everywhere transverse to ξ. More precisely, $d\gamma(\theta) \notin \xi_{\gamma(\theta)}$ for $\theta \in \bigsqcup S^1$.

As proved in [Gei08, Corollary 2.5.9], any two Legendrian knots have contactomorphic neighbourhoods. A model for this neighbourhood is given by

$$L = S^1 \times \{0\} \hookrightarrow S^1 \times \mathbb{R}^2$$

where the latter is given the contact structure

$$\ker(\cos\theta dx - \sin\theta dy), \tag{2.1}$$

where the θ coordinate parametrises the knot and (x, y) are coordinates on $\mathbb{R}^2$.

Legendrian links in $(\mathbb{R}, \xi_{std})$ are normally represented via their *front projection.*

Definition 2.2.16 (Front projection)**.** The *front projection* of an embedding $\gamma(\theta) = (x(\theta), y(\theta), z(\theta))$ in $(\mathbb{R}^3, \xi_{std})$ is the projection in $\mathbb{R}^2$ given by $(y(\theta), z(\theta))$.

If we have a Legendrian link in $(\mathbb{R}^3, \xi_{std})$, then

$$dy(\theta) = 0 \implies dz(\theta) = 0,$$

meaning that the front projection has a singularity at $(y(\theta), z(\theta))$. Usually we assume that a Legendrian link is *generic*, meaning that the front projection only has isolated singularities – which we call *cusps.* In practice, such singular points in a front projection correspond to cusps at vertical tangencies. This is probably the most recognizable feature of front projection diagrams of Legendrian links.

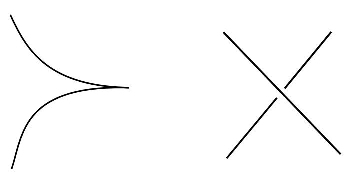

Figure 2.3: A cusp on the left, a crossing in the front projection of a Legendrian link on the right.

As per transverse links, they also are usually drawn via their front projection. Given a link $\gamma(\theta) = (x(\theta), y(\theta), z(\theta))$ in $(\mathbb{R}^3, \xi_{std})$, if we require it to be positively transverse to the contact structure [4] then $dz + xdy > 0$. Hence, if dy vanishes then $dz > 0$, if

[4]Here by positively transverse we mean $\alpha(d\gamma(\theta)) > 0$ for all θ.

$dy > 0$ then $x > -dz/dy$ and if $dy < 0$ then $x < -dz/dy$. Basically this implies that there are no vertical downward tangencies and there is a forbidden crossing in a front projection of a positively transverse link.

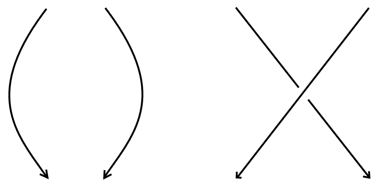

Figure 2.4: Forbidden front projections of a positively transvere link.

A very useful result is the following genericity theorem.

Theorem 2.2.17 (Legendrian and transverse approximation)**.** *Let K be a link in (M^3, ξ). Then K can be C^0 approximated by a Legendrian link isotopic to K and by a positively transverse link isotopic to K.*

In some sense this shows that even though the conditions for a link to be Legendrian or transverse look quite restrictive, they are remarkably generic objects. We now focus on Legendrian and transverse *knots*. Given a null-homologous Legendrian knot K in M, we can associate two classical knot invariants, the *Thurston-Bennequin number* and the *rotation number*.

Definition 2.2.18 (Contact framing)**.** Let K be a Legendrian knot in (M, ξ). By definition, $T_pK \subset \xi_p$ for all $p \in K$. Then the normal bundle of K splits as a Whitney sum of trivial line bundles:

$$\nu(K) \cong (TM|_K)/(\xi|_K) \oplus (\xi|_K)/TK.$$

We define the *contact framing* of K to be the trivialisation of $\nu(K)$ defined by this splitting.

More informally, the contact framing is just the framing specified by a parallel curve to K obtained by pushing K in a direction transverse to ξ. Expressed in the language of Definition 2.2.18, this curve represents a section of the factor $(TM|_K)/(\xi|_K)$.

Recall that a null-homologous knot has a topological framing – called the surface framing – given by a Seifert surface.

Definition 2.2.19 (Thurston Bennequin number)**.** Let K be a null-homologous knot in (M, ξ). The *Thurston-Bennequin number* of K, denoted by $tb(K)$, is the twisting of the contact framing with respect to the surface framing of K.

Equivalently, given K' a curve obtained by pushing K along a vector field transverse to ξ, $tb(K)$ equals $lk(K, K')$. We can give K any orientation – K' is given the corresponding orientation so that K, K' are isotopic as Legendrians. Since the linking number does not change by switching orientation, the Thurston-Bennequin invariant is *independent* of the choice of orientation on K. Note moreover that $tb(K)$ is invariant under Legendrian isotopies – i.e., isotopies of the knot K through Legendrian knots.

Given a Legendrian knot K in $\mathbb{R}^3$, its Thurston-Bennequin number can be read off from the front projection defined in Definition 2.2.16. More precisely, we have [Gei08, Proposition 3.5.9] that

$$tb(K) = \text{writhe}(K_F) - \frac{1}{2}\#(\text{cusps}(K_F)),$$

where here we denote by K_F the front projection of K.

As per the second invariant associated to K, we start by taking an oriented Seifert surface Σ of K so that the orientation on K equals the orientation as the boundary of Σ. Since Σ is a surface with boundary, we can choose a trivialization $\xi|_\Sigma \cong \Sigma \times \mathbb{R}^2$ [5] and let $\pi\colon \xi|_\Sigma \to \mathbb{R}^2$ be the projection onto the second factor.

Definition 2.2.20 (Rotation number)**.** Let K be a null-homologous Legendrian knot in M. Let $\gamma : S^1 \to M$ be a parametrisation of K. The *rotation number* of K *with respect to* Σ, denoted by $r(K, \Sigma)$ is the degree of the map $\pi \circ \gamma\colon S^1 \to R^2 \setminus \{0\}$. This is equal to the winding number of $\pi(d\gamma/dt)$ around the origin.

Roughly speaking, $r(K, \Sigma)$ is the obstruction to extending the non-zero section of $\xi|_K$ given by $\gamma'(t)$ to a non-zero section of ξ along Σ. Note that, in contrast with the Thurston-Bennequin number, the rotation number does depend on the orientation of K. If $\overline{K}$ is the inverse of K, the rotation number satisfies $r(\overline{K}, \Sigma) = -r(K, \Sigma)$, where the two Seifert surfaces have opposite orientations.

A priori, the rotation number of K depends on the specific choice of Σ and on the chosen trivialisation. In reality it is independent of the choice of trivialisation. Moreover, under certain assumptions (see for example [Gei08, Section 3.5]) we can show that it is independent from the choice of Σ as well. In that case we can simply speak of a rotation number $rot(K)$. This happens for example when the Euler class of ξ is trivial[6] – e.g., for (S^3, ξ_{std}) or $(\mathbb{R}^3, \xi)$. Given an (oriented) Legendrian knot K in $(\mathbb{R}^3, \xi_{std})$ we can compute the rotation number of K from its front projection as

$$rot(K) = \frac{1}{2}(c_- - c_+),$$

where c_- resp. c_+ is the the number of downward resp. upward cusps.

Arguably the most relevant relation between Thurston Bennequin number and rotation number of a knot K is the *Bennequin inequality*.

[5]To see this, note that the surface with boundary retracts to a bouquet of circles and every orientable plane bundle over S^1 is trivial.

[6]Here we mean the Euler class of ξ viewed as sub-bundle of $TM \to M$.

Theorem 2.2.21 (Bennequin Inequality)**.** *Let K be a null-homologous (oriented) Legendrian knot in a tight contact 3-manifold (M,ξ). Let Σ be a Seifert surface for K, oriented compatibly. Then we have*

$$tb(K) + |rot(K,[\Sigma])| \le -\chi(\Sigma), \tag{2.2}$$

where the latter is the Euler characteristic of the Seifert surface.

The Bennequin inequality represents a perfect example of the rigid nature of tight contact structures. Legendrian submanifolds need to satisfy the above bound. On the other hand, Legendrian knots in overtwisted contact structures *need not satisfy* the Bennequin bound. In fact there are always knots that break it, see [Etn13]. One can interpret this as follows: using an overtwisted disc one can *destabilize* (the opposite of the operation described before Lemma 2.2.24 below) a Legendrian knot as much as desired, with the effect of increasing the Thurston-Bennequin number and breaking the inequality in (2.2).

We now turn our attention to transverse knots and their invariant. Let K be a null-homologous (positively) transverse knot in (M,ξ) and and Σ a Seifert surface for K. Choose a non-zero section of $\xi|_\Sigma$ and push K in the direction of the section to obtain a positively transverse knot K'.

Definition 2.2.22 (Self-linking number)**.** The *self-linking number* of K is defined as $sl(K,\Sigma) = lk(K,K')$.

Note that, as for the Thurston-Bennequin number, $sl(K)$ does not really depend on the orientation of K (although here we are requiring the knots to be positively transverse anyway). As before, one can show the self-linking number is independent of the choice of trivialization and, under certain assumptions, does not depend on the Seifert surface as well. In this case we write $sl(K)$ instead of $sl(K,\Sigma)$. This will certainly be the case for knots in $\mathbb{R}^3$ or S^3.

Given a transverse knot K in $(\mathbb{R}^3,\xi_{std})$ we can compute the self-linking number $sl(K)$ via the front projection. In particular, we have

$$sl(K) = \text{writhe}(K_F),$$

where again K_F denotes the front projection of K.

Legendrian and transverse knots are closely related to each other. Roughly speaking, one can always pass from a Legendrian knot to a transverse one (and vice-versa) by pushing off in a certain direction. In fact, a Legendrian knot K has both a *positive* and a *negative transverse push-off*. For the construction of these, see [Gei08, Discussion after Remark 3.1.2]. We have the following property for transverse push-offs of a Legendrian knot K.

Proposition 2.2.23. *Let K be a null-homologous (oriented) Legendrian knot K, together with a compatible Seifert surface Σ. Let $K_\pm$ be the positive or negative transverse push-off of K. We have that:*

$$sl(K_\pm, \Sigma) = tb(K) \mp rot(K, [\Sigma]).$$

Note that the above formula makes sense because Σ is a Seifert surface for $K_\pm$ as well – these knots are topologically isotopic to K.

There is a local operation for Legendrian knots (and links) that is vastly used. Such operation is called *stabilization*. By considering its standard neighbourhood one can identify any Legendrian link component L locally with the x axis in $\mathbb{R}^3$. Stabilization is a local operation performed as shown in Figure 2.5. The modification on the top right-side is called the positive stabilization and usually denoted by L_+. The modification on the bottom right-side is known as negative stabilization and usually denoted as L_-.

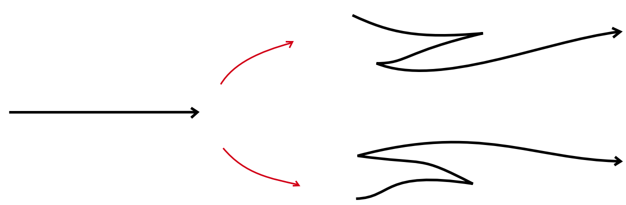

Figure 2.5: Stabilizations of Legendrian knots.

Lemma 2.2.24 (Effect of stabilizations)**.** *The effect of stabilizations on the classical invariants are as follows*

$$\mathrm{tb}(L_{\pm 1}) = \mathrm{tb}(L) - 1$$

and

$$\mathrm{rot}(L_\pm) = \mathrm{rot}(L) \pm 1.$$

§ 2.2.2 | Convex surfaces

Important objects in 3-dimensional contact geometry are *convex surfaces*. In Chapter 3 we will use tools coming from convex surface theory to obtain a classification result for tight contact structures.

Our setting is, as always, a contact 3-manifold (M, ξ) with $\xi = \ker \alpha$, ξ oriented and cooriented. Let S be an oriented surface embedded in M.

Definition 2.2.25 (Characteristic foliations of a surface)**.** Let $\Sigma \subset (M, \xi)$ be an embedded surface and ω an area form on Σ. The *characteristic foliation* of Σ, denoted by Σ_ξ is the singular foliation dictated by the vector field X on Σ which satisfies

$$\iota_X \omega = \alpha|_\Sigma.$$

Remark 2.2.26. Note that different choices of area form ω and different choices of contact form α for the cooriented contact structure ξ differ by a positive function. Thus the equivalence class of the singular foliation dictated by X depends only on Σ and ξ.

Recall that in Definition 2.1.14 we defined the characteristic foliation of an hypersurface. Given a point $p \in \Sigma$, we have $\alpha_p(X) = \omega_p(X_p, X_p) = 0$, so $X_p \in \xi_p$, and $X_p = 0$ iff $\xi_p = T_p\Sigma$. In words, for each non-singular point of X the foliation defined in 2.2.25 spans the line $T_p\Sigma \cap \xi_p$, consistently with Definition 2.1.14.

Recall the following definition.

Definition 2.2.27 (Divergence)**.** The *divergence* of a vector field X with respect to Σ is the real-valued function on Σ satisfying

$$\mathrm{div}_\omega(X) \cdot \omega = \mathcal{L}_X\omega = d(\iota_X\omega).$$

Remark 2.2.28. Note that the set of points on Σ for which the divergence is non-vanishing only depends on X up to non-zero scalar multiplication.

We have the following result about vector fields defining characteristic foliations on embedded surfaces.

Lemma 2.2.29. *A vector field X defines the characteristic foliation Σ_ξ – for some contact structure ξ defined on a neighbourhood of Σ – if and only if $X_p = 0$ implies $div_\omega(X) \neq 0$ at p.*

Hence, not all foliations on Σ dictated by a vector field can represent the characteristic foliation of Σ in a contact manifold. However, as long as the above condition is satisfied, the foliation is a model for a characteristic foliation of Σ.

Note that the foliation determines the contact structure on a neighbourhood of Σ.

Proposition 2.2.30. *Given Σ_0 resp. Σ_1 in contact manifolds (M_0, ξ_0) resp. (M_1, ξ_1). Assume there is a diffeomorphism $\varphi : \Sigma_0 \to \Sigma_1$ carrying the foliation of Σ_0 to the foliation of Σ_1. Then there exist a contactomorphism*

$$\widetilde{\varphi}\colon N(\Sigma_0) \to N(\Sigma_1)$$

extending φ.

Hence, the diffeomorphism type of the characteristic foliation is everything that one needs to know to identify the contact structure on a neighbourhood of an embedded surface. Although characteristic foliations – and their properties – have been extensively used as a tool to study contact structures in full generality [Eli89] it turns out that one can potentially reduce the complexity of the problem by instead studying a more combinatorial object called the *dividing set*. For this to exist, we require that the embedded surface is convex.

Definition 2.2.31 (Contact vector field)**.** A *contact vector field* v is a vector field whose flow preserves ξ. In formulas, if $\xi = \ker\alpha$ and ϕ_t is the flow of v then the flow preserves ξ if we have $\phi_t^*\alpha = f\alpha$ for some non-vanishing function f.

Remark 2.2.32. Since $\mathcal{L}_v(\alpha) = \frac{d}{dt}\phi_t^*(\alpha)|_{t=0}$, v is contact if and only if $\mathcal{L}_v(\alpha) = g\alpha$ for some function g.

Remark 2.2.33. Probably the most relevant example of a contact vector field is the *Reeb vector field* R of α, i.e. the unique vector field with $\alpha(R) = 1$ and $\iota_R d\alpha = 0$.

Definition 2.2.34 (Convex surface)**.** A surface $\Sigma \subset (M, \xi)$ is *convex* if there is a contact vector field v with $v \pitchfork \Sigma$.

Convex surfaces can be characterized as follows.

Proposition 2.2.35. *A surface $\Sigma \subset (M, \xi)$ is convex if and only if there is an embedding $i\colon \Sigma \times \mathbb{R} \hookrightarrow M$ with $\Sigma = i(\Sigma \times \{0\})$ such that $i^*(\xi)$ is $\mathbb{R}$-invariant.*

Given Proposition 2.2.35, we can write the contact structure on the vertically-invariant neighbourhood of Σ convex as

$$\alpha = \mu + f\,dt,$$

where μ and f are respectively a 1-form and a real-valued function on Σ. The contact condition translates to

$$f\,d\mu - df \wedge \mu > 0$$

on Σ. Recall that we have given Σ an area form ω. Then the characteristic foliation is determined by $\iota_X\omega = \mu$, and hence Σ_ξ is singular precisely at the points for which $\mu = 0$.

Definition 2.2.36 (Dividing multicurve)**.** Let Σ be a surface with singular foliation $\mathcal{F}$. A multi-curve $\Gamma \subset \Sigma$ transverse to $\mathcal{F}$ *divides* $\mathcal{F}$ if Σ admits a volume form ω and a vector field v dictating $\mathcal{F}$ such that $\Sigma \setminus \Gamma = \Sigma_+ \sqcup \Sigma_-$ with $\pm\mathcal{L}_v\omega > 0$ on $\Sigma_\pm$ and v points outwards with respect to Σ_+ along Γ.

The following theorem links the notion of a convex surface and the existence of a dividing multicurve.

Theorem 2.2.37. *Let $\Sigma \subset (M, \xi)$ be an orientable surface. If Σ has boundary, we require it to be a Legendrian submanifold. Then Σ is convex if and only if the characteristic foliation Σ_ξ admits dividing curves.*

We can construct, for a convex surface Σ, a dividing multicurve Γ_Σ as follows. Recall that $\Sigma \times \mathbb{R}$ has a model neighbourhood with contact vector field ∂_t – see the discussion after Proposition 2.2.35. Then $v_p \in \xi_p$ if and only if $f = 0$. Hence we can identify Γ_Σ

with $\{p \in \Sigma |\ v_p \in \xi_p\}$. Note this is non-empty. If f is nowhere vanishing, then we can take normalize α to $\alpha' = \mu' + dt$, with $\mu' > 0$. But then

$$\int_{\partial\Sigma} \alpha' = \int_{\Sigma} d\alpha' = \int_{\Sigma} d\mu' > 0,$$

which is clearly a contradiction whenever $\partial\Sigma = \emptyset$ or Legendrian.

So the dividing multicurve of a convex surface consists of the points where the contact planes contain the "vertical" direction.

Example 2.2.38. Let $(\mathbb{R}^3, \xi_r)$ be the tight contact $\mathbb{R}^3$ with contact structure defined by

$$\xi_r = \ker(dz + r^2 d\theta).$$

Then the unit sphere $S^2 \hookrightarrow \mathbb{R}^3$ is convex and it is divided by the equator $\Sigma_{S^2} = \{z = 0\}$.

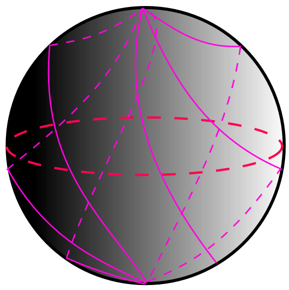

Figure 2.6: Convex unit sphere showing characteristic foliation and dividing set.

In order for the dividing multicurves to be a relevant invariant for a convex surface, we need the following essential uniqueness result.

Proposition 2.2.39. *Let Σ be convex with two sets of dividing curvex Γ_0 and Γ_1. Then Γ_0 and Γ_1 are isotopic through curves transverse to Σ_ξ.*

Convex surfaces are, in some sense, everywhere. More precisely, any surface with *Morse-Smale* characteristic foliation has dividing curves and hence it is convex [Gir91]. Moreover, the dividing set Γ actually encodes everything that one needs to understand the contact structure near Σ. If Σ is convex with dividing set Γ and $\mathcal{F}$ is any foliation divided by Γ, then Σ may be perturbed to have characteristic foliation $\mathcal{F}$.

Theorem 2.2.40 (Genericity of convex surfaces)**.** *Given a closed, orientable surface $\Sigma \subset (M, \xi)$ there is a C^∞-small perturbation Σ' of Σ so that Σ'_ξ is Morse-Smale. Moreover, if a surface $\Sigma \subset (M, \xi)$ has Morse-Smale characteristic foliation then Σ is convex.*

Theorem 2.2.41 (Giroux flexibility)**.** *Let $\iota \colon \Sigma \to M$ be an embedding of Σ into (M, ξ) with convex image, and let $\mathcal{F}$ be a foliation of Σ divided by $\iota^{-1}(\Gamma_\Sigma)$. Given any neighbourhood U of $\iota(\Sigma)$ in M there is an isotopy $H_s : \Sigma \to M$ supported inside U so that*

$H_0 = \iota$, each $H_s(\Sigma)$ is convex with dividing set Γ_Σ, H_s fixes the dividing curves $\iota^{-1}(\Gamma_\Sigma)$ for all s and $H_1(\mathcal{F})$ is the characteristic foliation of $H_1(\Sigma)$.

Theorem 2.2.41 affirms that, as long as a singular foliation $\mathcal{F}$ is divided by the same set of multicurves of $\mathcal{F}_\Sigma$ then we can find a contact isotopy contained in a neighbourhood of Σ so that the end of the isotopy has characteristic foliation $\mathcal{F}$. Note that thanks to Gray stability 2.1.8 and isotopy extension, we can also view this as a modification of the contact structure itself and not of the surface. Both are perfectly valid interpretations.

Convex surfaces posess a lot of key features that play an important role in understanding contact structures on 3-manifolds. We will now list some basic properties that will become relevant in Chapter 3.

Theorem 2.2.42 (Legendrian realisation principle – LeP [Hon00a, Kan97])**.** *Let $\Sigma \subset (M, \xi)$ be a convex surface, and let $C \subset \Sigma$ be a multicurve which is transverse to Γ_Σ. Let C be non-isolating, i.e. every component of $\Sigma \setminus C$ intersects Γ_Σ. Then there is an isotopy H_s of Σ through convex surfaces –supported on a small neighbourhood $\Sigma \subset U$ and fixing the dividing set– such that $H_s(C)$ is always transverse to Γ_Σ and $H_s(C)$ is Legendrian.*

Proposition 2.2.43 (Honda [Hon00a])**.** *Let C be a closed Legendrian curve transverse to Γ_Σ. Then*

$$tw(C, \Sigma) = -\frac{1}{2}|C \cap \Gamma_\Sigma|,$$

where the latter denotes the geometric intersection and tw is the twisting number[7] *of the curve with respect to the surface Σ.*

One of the most important features of convex surfaces is that we can give a concrete characterization of those who possess a tight neighbourhood.

Theorem 2.2.44 (Giroux's Criterion)**.** *Let $\Sigma \subset (M, \xi)$ be a convex closed surface. Then Σ has a tight neighbourhood if and only if $\Sigma = S^2$ and Γ_Σ is* connected *or $\Sigma \neq S^2$ and Γ_Σ has* no null-homotopic components*.*

It is evident that the above result is relevant for the classification of contact structures on 3-manifolds. Whenever we find a convex surface that violates the criterion in Theorem 2.2.41 we can immediately conclude the contact structure is overtwisted.

Remark 2.2.45*.* Theorem 2.2.41 applies to convex surfaces with Legendrian boundary as well – in this case only the second obstruction is relevant, meaning a convex surface with Legendrian boundary has a tight neighbourhood iff Γ_Σ has no contractible components.

[7] This is the integer difference between the number of twists in the normal framing induced by the contact structure and the number of twists given by the surface Σ.

§ 2.3 | Symplectic fillability

Although tight versus overtwisted is the most important dichothomy in contact topology, there are other distinctions we can make between tight structures that somehow allow us to measure how rigid they are.

Recall the following definition.

Definition 2.3.1 (Symplectic structure)**.** A *symplectic structure* on a smooth $2n$ manifold M is a differential 2-form ω that is closed and non-degenerate, i.e. $d\omega = 0$ and if there exist an $X \in T_p$ so that $\omega_p(X, Y)$ for all $Y \in T_pM$, then $X = 0$. (M, ω) is called a symplectic manifold.

We can establish a hierarchy between tight contact structures on a 3-manifold M by looking at their relationship with the symplectic structures on 4-manifolds X filling M.

Definition 2.3.2 (Weakly symplectically fillable)**.** A contact manifold (M, ξ) is *weakly symplectically fillable* if there exists a compact symplectic 4-manifold (X, ω) so that $\partial X = M$ and $\omega|_\xi > 0$.

Definition 2.3.3 (Strongly symplectically fillable)**.** A weakly symplectically fillable contact manifold is said to be *strongly symplectically fillable* if (X, ω) as in Definition 2.3.2 is compact and there exists a transverse vector field v to M pointing out of X along M so that the flow of v dilates ω.

Recall that a *Stein domain* is a complex 4-manifold (W, J) equipped with a smooth proper Morse function $\phi\colon W \to \mathbb{R}$ that is bounded below and such that the form $w_\phi(v, w) = -d(d\phi \circ J)(v, w)$ is non-degenerate. The function ϕ is called a *plurisubharmonic exhaustion*.

Definition 2.3.4 (Stein fillable)**.** If a contact manifold (M, ξ) is a regular level-set of a Stein domain (W, J), i.e. the preimage $\phi^{-1}(c)$ for c a regular value, then we say (M, ξ) is *Stein fillable*.

We can describe the hierarchy induced by fillability properties as follows:

$$\text{Stein fillable} \subsetneq \text{Strongly fillable} \subsetneq \text{Weakly fillable} \subsetneq \text{Tight}.$$

The properness of the above inclusions has been proved in different steps. In [EH02] Etnyre and Honda produced the first example of tight structures with no weak symplectic fillings. Eliashberg showed in [Eli96] that there are weakly fillable structures on T^3 that are not strongly fillable. Ghiggini [Ghi05] constructed examples of strongly fillable structures that are not Stein fillable.

We will refer to the above hierarchy again in Chaper 4, where we investigate fillability properties of certain 3-manifolds.

§ 2.4 | Around Heegaard Floer homology: L-spaces, contact invariants and correction terms

In this section we introduce the notions related to Heegaard Floer homology that we will need in this thesis. It is not our scope to fully discuss the theory of Heegard Floer homology. For this, see the original work of [OS04c, OS05a] or [LS07a], and [Juh15] for a modern survey.

§ 2.4.1 | L-spaces

The main characters of this thesis are members of a very specific class of 3-manifolds, *L-spaces*. We give here some basic definitions and properties of such spaces to help the reader navigate through the next chapters.

Definition 2.4.1 (L-space)**.** An L-space is a rational homology sphere such that the free rank of its Heegaard Floer homology equals the order of its first (integral) singular homology group.

In a broad sense Heegaard Floer homology gives (a collection of) invariants of closed oriented 3-manifolds (for its original formulation see [OS04c, OS04b]). There are different variants of such homology theory; the one we will mainly use and consider is the simplest one and usually denoted by $\widehat{HF}(Y)$. The condition in Definition 2.4.1 can be rewritten as

$$rk\widehat{HF}(Y) = |H_1(Y;\mathbb{Z})|.$$

The class of L–spaces includes all lens spaces and is closed under connected sum as well as orientation reversal. One of the most relevant questions regarding L-spaces is the so-called "L-space conjecture". In order to state it, we need the following definition.

Definition 2.4.2 (Taut foliation)**.** Given a connected, closed 3-manifold M a smooth, oriented, cooriented codimension 1 foliation $\mathcal{F}$ is taut if it has the property that every leaf meets a transverse circle.

Conjecture 2.4.3 (L-space conjecture)**.** *Suppose Y is an irreducible rational homology 3-sphere. Then the following are equivalent.*

- *Y is* not *a L-space*
- *Y admits a taut foliation*

Remark 2.4.4. There is another (conjectured) equivalent property, namely "left-orderability" of $\pi_1(Y)$ – we will not discuss this here.

One of the directions has been shown to hold.

Theorem 2.4.5 ([OS04a])**.** *If Y is a rational homology L-space then Y does not admit taut foliations.*

§ 2.4.2 | Contact invariants in Heegaard Floer homology

In this subsection, we review some useful properties of contact invariants in Heegaard Floer homology. For our purposes, the key fact is that associated to a contact manifold (M, ξ) there exists an invariant $c(\xi)$ – called the *contact invariant* or *contact class* – that encodes relevant properties of the contact manifold [OS05a]. Roughly speaking, this invariant in Heegaard Floer homology is defined exploiting the correspondence between contact structures and *open book decompositions* [Gir02].

Theorem 2.4.6 (Properties of contact invariant [OS05a, Ghi06])**.** *The Heegaard Floer contact invariant $c(\xi) \in \widehat{\mathrm{HF}}(-M)$ of (M, ξ) satisfies the following properties.*

- *If (M, ξ) is overtwisted, then $c(\xi) = 0$.*
- *If (M, ξ) is strongly fillable, then $c(\xi) \neq 0$.*
- *Let L be a Legendrian knot in (M, ξ) and (M_L, ξ_L) the result of Legendrian surgery on L. If $c(\xi) \neq 0$, then $c(\xi_L) \neq 0$.*

There also have been several studies when a positive contact surgery preserves non-vanishing contact invariants, see [LS04, LS07b, Gol15, MT18]. In this thesis, we only need the result for the right-handed trefoil.

Theorem 2.4.7 (Contact invariant and surgeries on the RH trefoil [LS04, MT18])**.** *Let L be a Legendrian right-handed trefoil in (S^3, ξ_{std}) with $tb(L) = 1$. For any $r \in \mathbb{Q} \setminus \{0\}$, contact (r)-surgery (see Definition 3.2.16) on L produces a tight contact structure with non-vanishing contact invariant.*

§ 2.4.3 | Correction terms

Another object that will be relevant in this thesis – more specifically in Chapter 4 – is the d-invariant. Recall that the d-invariant (introduced in [OS03]) for a rational homology 3-sphere Y with a given $Spin^c$ structure t is the so called *correction term*. In short, $d(Y, t)$ is the minimal degree of any non-torsion class in $HF^+(Y, t)$ coming from $HF^\infty(Y, t)$ [OS03].[8]

This invariant is additive with respect to connected sums and is a rational homology cobordism invariant – in fact, it is a useful obstruction for existence of rational homology cobordisms of $Spin^c$ three-manifolds. This invariant has been successfully used for answering a number of questions in three-dimensional topology and knot theory, and provides a good obstruction to the existence of negative definite fillings of 3-manifolds. For applications of d-invariants, see for example [OS06, MO07, LS07a, OS12b]. In this thesis we use the following obstruction for a certain 3–manifold to bound a negative definite 4-manifold.

[8]These are two different variants of Heegaard Floer homology of Y, see [OS03].

Theorem 2.4.8 ([OS12a, Theorem 2]). *Let Y be a rational homology sphere with $|H_1(Y;\mathbb{Z})| = \delta$. If Y bounds a negative definite 4-manifold X, and if either δ is square-free or there is no torsion in $H_1(Y;\mathbb{Z})$, then:*

$$\max_{t \in \mathrm{Spin}^c(Y)} 4d(Y,t) \geq \begin{cases} 1 - \frac{1}{\delta} & \text{if } \delta \text{ is odd,} \\ 1 & \text{if } \delta \text{ is even.} \end{cases}$$

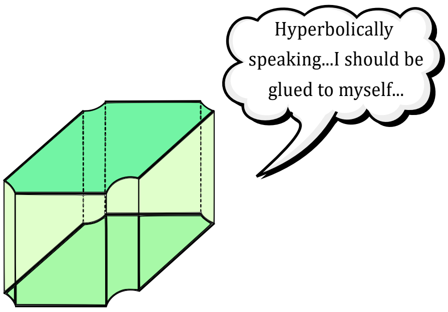

Chapter 3

Tight contact structures on an infinite family of hyperbolic L-spaces

The content of this chapter is almost entirely taken from [MN26], with some minor changes made to fit the text more seamlessly in the fabric of this thesis.

§ 3.1 | Classification problem: the landscape and our contribution

Recall that a cooriented contact 3-manifold (M, ξ) is *overtwisted* if it contains an overtwisted disk (see Definition 2.2.4) and *tight* if it does not contain an overtwisted disk – see Definitions 2.2.7 and 2.2.6. Recall also that [Eli89] reduced the (isotopy) classification problem for overtwisted contact structures (see Theorem 2.2.11) to a homotopy problem for distributions. Hence recent studies focus solely on the classification of (positive) tight contact structures.

Since tight contact structures respect the *prime decomposition* of 3-manifolds by the work of Colin [Col97] (see also [DG07, Hon02]), it is sufficient to consider the classification of tight contact structures on prime manifolds. The geometrization of 3-manifolds implies that a prime 3-manifold is either Seifert fibered (and atoroidal), toroidal or hyperbolic. For Seifert fibered spaces with two singular fibers, tight contact structures were completely classified, see [Eli92, Etn00, Gir00, Hon00a]. For Seifert fibered spaces with three singular fibers, there have been several classification results, see [EH01b, GLS07, GS03, Tos20, Wu06] for example. For the toroidal case, tight contact structures were classified on torus bundles over S^1 and S^1-bundles over a surface, see [Gir99, Gir00, Gir01, Hon00b, Kan97]. Honda, Kazez and Matić [HKM02] showed that there exist infinitely many tight contact structures up to isotopy on toroidal manifolds and Colin, Giroux and Honda [CGH09] showed that a closed orientable irreducible 3-manifold supports infinitely many tight contact structures up to isotopy if and only if it is toroidal.

For hyperbolic manifolds, much less is known although "most" prime 3-manifolds fall into this category [Thu82]. Honda, Kazez and Matić [HKM03] partially classified tight contact structures on hyperbolic surface bundles over S^1 when the contact structures have an *extremal* relative Euler class, meaning that the Euler class of the contact structure – recall this is a cohomology class in $H^2(M;\mathbb{Z})$ – evaluated on a fiber surface is maximal.[1] Later, Conway and Min [CM20] classified tight contact structures on (most) surgeries on the figure eight knot in S^3, a family which contains infinitely many hyperbolic 3-manifolds.

The goal of [MN26] is to study hyperbolic *L-spaces* (see Definition 2.4.1). In general, it is hard to construct a universally tight contact structure on an L-space because an L-space does not admit a *taut foliation* (see Definition 2.4.2 and Theorem 2.4.5). Recall that a taut foliation is a codimension 1 foliation of a closed manifold with the property that every leaf meets a transverse circle. The point is that taut foliations can be perturbed into universally tight contact structures [ET98]. There are some non-hyperbolic L-spaces (*e.g.* lens spaces) that support a universally tight contact structure while it is not known for hyperbolic L-spaces yet. Thus it is natural to ask whether there is a hyperbolic L-space that supports a universally tight contact structure, which can be considered as a contact topology version of the *L-space conjecture* ([BGW13, Juh15]).

We conjectured in [MN26] that a hyperbolic 3-manifold is an L-space if and only if it does not support a universally tight contact structure. Shortly after, Baldwin-Sivek-Zung [BSZ25] constructed hyperbolic L-spaces with universally tight contact structures using pseudo-Anosov flows and cylindrical contact homology techniques. Although the conjecture in [MN26] has been shown to be false, a new version is proposed in [BSZ25]. This refined conjecture stems from the work of [Hoz20, Mas24] on bi-contact geometry.

Question 3.1.1. *Is there a hyperbolic L-space with both positive and negative universally tight contact structures?*

In [MN26], we classify tight contact structures on an infinite family of hyperbolic L-spaces. Although we could not show that they are all virtually overtwisted, we show that most of them are. We point out that [BSZ25] does not prove that the manifolds considered in [MN26] have universally tight contact structures.

Let $M(n,r)$ be the result of (n,r)-surgery on the Whitehead link (see Figure 3.1). We will classify tight contact structures on $M(n,r)$ for surgery coefficients

$$n \in \mathbb{Z}, n \geq 5,$$
$$r \in \mathcal{R}_+ \cup \mathbb{Q}_-,$$

where $\mathbb{Q}_-$ is the set of negative rational numbers and

$$\mathcal{R}_+ = ([2,4) \cup [5,\infty)) \cap \mathbb{Q}.$$

[1] Maximality is described by the condition

$$\langle e(\xi), \Sigma_t \rangle = \pm(2g-2)$$

for $t \in [0,1]$ and g the genus of the surface.

Remark 3.1.2. The reasons we restrict to $n \geq 5$ and to $\mathcal{R}_+, \mathbb{Q}_-$ are different in nature and will be discussed during this chapter.

Recall that the Whitehead link is a hyperbolic L-space link – i.e. all sufficiently large surgeries on all components of the link are L-spaces. In particular, Liu [Liu17, Proposition 6.4] showed that $M(r_1, r_2)$ is an L-space if and only if $r_1, r_2 > 0$. Moreover, there are only finitely many – 26, to be precise – isolated exceptional Dehn fillings[2] of the Whitehead link [Mar21, Thu22]. Thus our family of $M(n, r)$ contains infinitely many hyperbolic L-spaces.

Before stating the results, we define two functions $\Phi(r)$ and $\Psi(r)$. For $0 < r \leq 1$, we write the negative continued fraction of $-\frac{1}{r}$ as follows:

$$-\frac{1}{r} = [r_0, \ldots, r_n] = r_0 - \cfrac{1}{r_1 - \cfrac{1}{\ddots - \cfrac{1}{r_n}}},$$

where $r_0 \leq -1$, and $r_i \leq -2$ for $i = 1, \ldots, n$. Then define

$$\Phi(r) = |r_0(r_1 + 1) \cdots (r_n + 1)|\,.$$

We define Φ on all of $\mathbb{Q}$ by setting $\Phi(r + 1) = \Phi(r)$. Then we define $\Psi(r)$ for $r \in \mathbb{Q}$ by

$$\Psi(r) = \begin{cases} 0 & r = 1 \\ \Phi(\frac{1}{1-r}) & r \neq 1 \end{cases}$$

Now we are ready to state the main theorem of this chapter.

Theorem 3.1.3 (Main theorem)**.** *Let $n \geq 5$ be an integer. Then $M(n, r)$ supports*

$$\begin{cases} \Psi(r) + 2\Phi(r) & r \in \mathcal{R}_+ \\ \Psi(r) & r \in \mathbb{Q}_- \end{cases}$$

tight contact structures up to isotopy, distinguished by their contact invariants in Heegaard Floer homology.

Remark 3.1.4. For $n > 2$ and $r \geq 1$ (resp. $r < 1$), we can construct at least $\Psi(r)+2\Phi(r)$ (resp. $\Psi(r)$) tight contact structures on $M(n, r)$ even if $n < 5$ or $r \notin \mathcal{R}_+$ (resp. $r \notin \mathbb{Q}_-$), see § 3.3. However, there could be more.

We will prove Theorem 3.1.3 by estimating an upper bound using convex surface decompositions, and realizing this upper bound via contact surgery. We construct tight contact structures in Section 3.3 by using contact surgery diagrams and distinguish them by using the contact invariant in Heegaard Floer homology. In Section 3.4, we use a convex decomposition for a punctured genus one surface bundle over S^1 with a pseudo-Anosov monodromy, which was first introduced by Etnyre and Honda [EH01a]

[2] By this we mean Dehn fillings of the complement that do not produce a hyperbolic manifold.

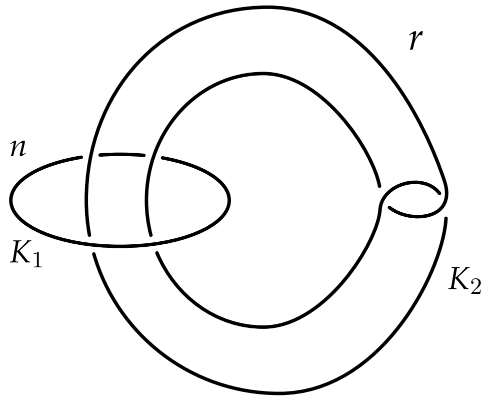

Figure 3.1: (n, r)-surgery on the Whitehead link.

and developed by Conway and Min [CM20] for the figure-eight knot complement. One of the important additions of [MN26] is to generalize this technique for any pseudo-Anosov monodromy ϕ with $-1 < c(\phi) < 1$ where $c(\phi)$ is the fractional Dehn twist coefficient [GO89, HKM07, HM18] of ϕ. We expect this technique will apply to various monodromies and lead to the classification of tight contact structures on a broad class of hyperbolic 3-manifolds.

Recall that $M(n, 0)$ is a torus bundle over S^1 (see § 3.4.1). Since $\Phi(m) = 1$ and $\Psi(m) = 2$ for any integer $m > 2$ and $\Psi(m) = |m-1|$ for any integer $m < 0$, we have the following results for integer surgeries.

Corollary 3.1.5. *Let $n \geq 5$ and $m \neq 1, 4$ be integers. Then $M(n, m)$ supports*

$$\begin{cases} |m-1| & m < 0, \\ \infty & m = 0, \\ 3 & m = 2, \\ 4 & m > 2,\, m \neq 4 \end{cases}$$

tight contact structures up to isotopy.

As mentioned in Remark 3.1.4 in the missing integral cases we can still construct certain tight contact structures using our techniques. The upper bound is however considerably harder to obtain for $m = 1, 4$, and we currently cannot show that it matches the lower bound. Recall also that $M(5, \frac{5}{2})$ is the Weeks manifold, known to have the smallest volume among closed hyperbolic 3-manifolds [GMM09]. Since $\Phi(\frac{5}{2}) = 2$ and $\Psi(\frac{5}{2}) = 3$, we obtain the following result.

Corollary 3.1.6 (Tight structures on Weeks manifold)**.** *The Weeks manifold supports seven (positive) tight contact structures up to isotopy.*

Remark 3.1.7. Corollary 3.1.6 refers to the Weeks manifold with its standard positive orientation. We do not classify positive tight contact structures on the Weeks manifold with its opposite orientation. In general, it would be an interesting question to classify positive tight contact structures on $-M(n,r)$ – or, equivalently, negative tight contact structures on $M(n,r)$. This classification could have interesting consequences for bi-contact geometry and the theory of projectively Anosov flows, following the work of [Hoz20, Mas24].

In addition to classifying tight contact structures, we also determine whether these tight contact structures are Stein fillable (see Definition 2.3.4).

Theorem 3.1.8. *Let $n \geq 5$ be an integer and $r \in \mathcal{R}_+ \cup \mathbb{Q}_-$. Then every tight contact structure on $M(n,r)$ is Stein fillable.*

Lastly, we consider what we can say about universal tightness for structures on $M(n,r)$. We provide a lower bound on the number of tight contact structures on $M(n,r)$ that are virtually overtwisted.

Theorem 3.1.9. *Let $n \geq 5$ be an integer and $r \in \mathcal{R}_+ \cup \mathbb{Q}_-$. Then $M(n,r)$ supports at least*

$$\begin{cases} \Psi(r) + 2\Phi(r) - 6 & r \in \mathcal{R}_+ \\ \Psi(r) - 2 & r \in \mathbb{Q}_- \end{cases}$$

virtually overtwisted contact structures up to isotopy.

Remark 3.1.10. There are some cases (*e.g.* $2 \leq r \in \mathbb{Z}$) in which $\Psi(r) + 2\Phi(r)$ is smaller than 6. In these cases, our techniques cannot determine neither virtual overtwistedness nor universal tightness for any structure.

§ 3.2 | More contact topology preliminaries

For the basic 3-dimensional contact topology the reader is referred to Chapter 2 and to [Etn03, Gei08]. For convex surface theory, we refer to [Etn, Hon00a] and for Heegaard Floer homology to [OS04b, OS04c]. In this section, we briefly review the results that we will frequently use.

§ 3.2.1 | More on convex surfaces

Let (M,ξ) be a contact 3-manifold, where $\xi = \ker \alpha$. Recall that a contact vector field is a vector field whose flow preserves ξ (Definition 2.2.31). An orientable surface Σ is called convex if there exists a contact vector field transverse to Σ (see Definition 2.2.34). If Σ has boundary, then we assume that $\partial\Sigma$ is Legendrian with negative twisting number with respect to the surface framing. According to Theorem 2.2.41 (the boundary case is proven by Kanda [Kan97]), for any embedded surface Σ there is a C^∞-small isotopy (rel boundary) that isotopes Σ into a convex surface.

Given a convex surface Σ, recall that the *dividing set* Γ_Σ is a set of points on Σ where the contact vector field X is tangent to ξ (see the discussion after Definition

2.2.36). The dividing set divides Σ into two regions:

$$\Sigma \setminus \Gamma_\Sigma = R_+ \cup R_-$$

where $R_+ = \{p \in \Sigma : \alpha(v_p) > 0\}$ and $R_- = \{p \in \Sigma : \alpha(v_p) < 0\}$. If Σ has Legendrian boundary, then $tb(\partial\Sigma) = -\frac{1}{2}|\Gamma_\Sigma \cap \partial\Sigma|$ and $rot(\partial\Sigma) = \chi(R_+) - \chi(R_-)$. Recall that we can compute the twisting number of a Legendrian curve with respect to a specific framing as in Proposition 2.2.43.

Let G be an embedded graph on a convex surface Σ. Thanks to Theorem 2.2.42, if $\Sigma \setminus G$ is connected, G can always be realized as a Legendrian graph. This implies any non-separating curve on Σ can be realized as a Legendrian curve. Honda [Hon00a] showed that if two convex surfaces intersect transversely along a Legendrian curve L, the dividing curves of the two surfaces interleave and we can obtain a new convex surface by *rounding the edge*, see Figure 3.2.

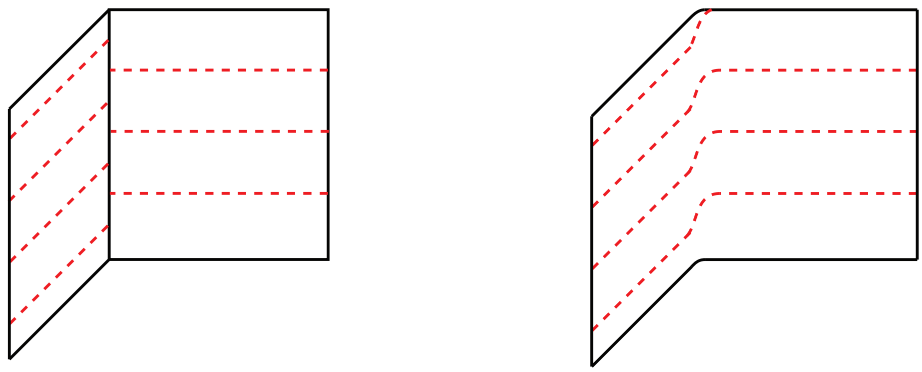

Figure 3.2: Rounding an edge between two convex surfaces.

We can modify a dividing set in a systematical way.

Definition 3.2.1 (Bypass attachment)**.** Let Σ be an oriented convex surface with a dividing set Γ_Σ and D be a half-disk with boundary given by two legendrian arcs a and b, i.e $\partial D = a \cup_\partial b$ with $\mathrm{tb}_D(a) = -1$ and $\mathrm{tb}_D(b) = 0$. Suppose $\alpha = D \cap \Sigma$ intersects Γ_Σ in three points $\{p, q, r\}$ and $\partial\alpha = \{p, r\}$ are elliptic singularities of D. By Giroux's flexibility Theorem 2.2.41, we can C^∞-small isotope D for q to be a unique hyperbolic singularity. We call D a *bypass* and the sign of the hyperbolic singularity is called the *sign* of a bypass.

Honda proved in [Hon00a] that there is a one-sided neighborhood $\Sigma \times [0, 1]$ of $\Sigma \cup D$ such that $\Sigma \times \{0, 1\}$ is convex and the dividing set on $\Sigma \times \{1\}$ is modified as shown in Figure 3.4. We say $\Sigma \times \{1\}$ is obtained from $\Sigma \times \{0\}$ by a bypass attachment along α. Note that a bypass can be on either side of a surface and it gives a different effect on the dividing set.

Let us investigate the effect of bypass attachment to a torus in detail. First, we introduce the Farey graph. We define the graph inductively. Let $\mathbb{D}$ be the Poincaré

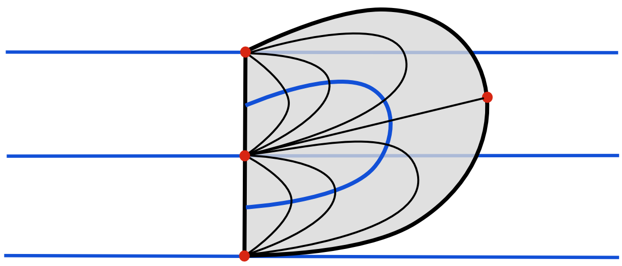

Figure 3.3: A model for the (front) bypass attachment.

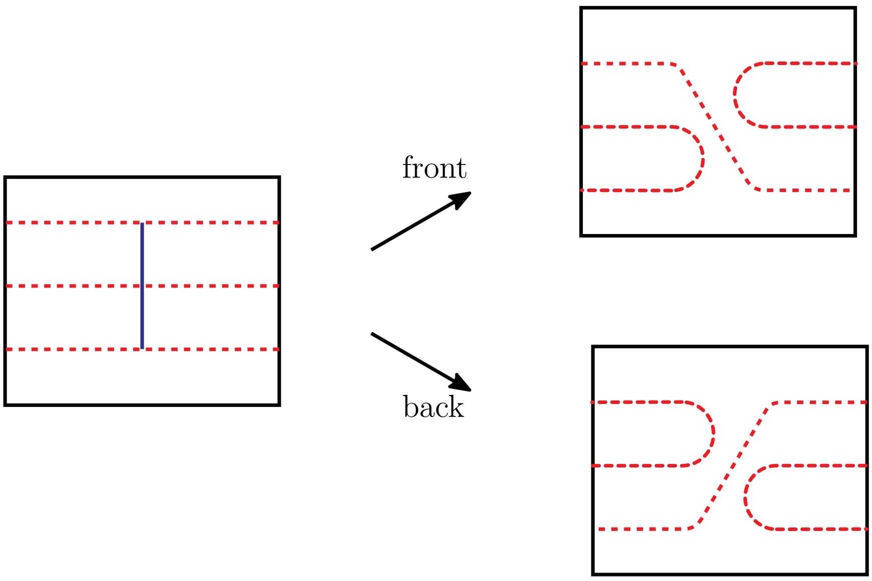

Figure 3.4: Bypass attachments

disk. Start with the top-most vertex labeled $0 = \frac{0}{1}$ and the bottom-most vertex labeled $\infty = \frac{1}{0}$ and connect them by a geodesic. Given two vertices in the right half plane which are already labeled $\frac{a}{b}$ and $\frac{c}{d}$, choose a vertex on $\partial\mathbb{D}$ in the middle of the vertices and label it as $\frac{a+c}{b+d}$. Then connect it with the other two vertices by geodesics. For the left half plane, we treat ∞ as $-\infty = \frac{-1}{0}$. See Figure 3.5.

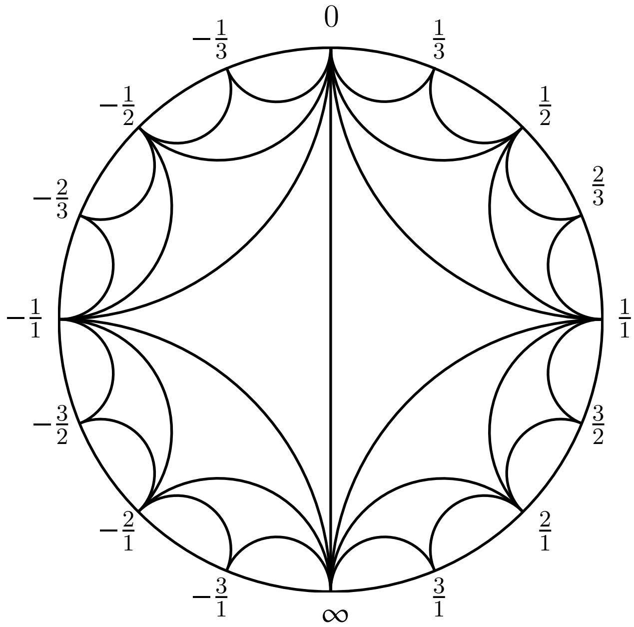

Figure 3.5: The Farey graph.

Now consider a convex torus T^2 in standard form, with two parallel dividing curves and characteristic foliation given by *ruling curves*. Choose a homology basis for T^2 as $(\binom{1}{0}, \binom{0}{1})$. Denote the slope of curves parallel to $\binom{p}{q}$ by $\frac{p}{q}$.

Theorem 3.2.2 (Honda [Hon00a]). *Let s, r be the dividing slope and the ruling slope of T^2 respectively. After a bypass attachment along a ruling curve, we obtain a new convex torus with two dividing curves with slope s', where s' is the vertex on the Farey graph anticlockwise of r and clockwise of s. In addition, s' is closest to r with an edge to s.*

Remark 3.2.3. In Theorem 3.2.2, we use the slope convention $\frac{p}{q} = \binom{p}{q}$ since $\frac{\text{meridian}}{\text{longitude}}$ is our slope convention for a solid torus. If we use the slope convention $\frac{q}{p} = \binom{p}{q}$, then we should reverse the words "clockwise" and "anticlockwise". Also, Theorem 3.2.2 assumes that we attach a bypass from the front. If we attach a bypass from the back, then we should reverse the words "clockwise" and "anticlockwise".

We need to guarantee the existence of bypasses to utilize them. There are several ways to find bypasses.

Theorem 3.2.4 (Imbalance principle [Hon00a]). *Let Σ and $A = S^1 \times [0, 1]$ be convex surfaces with Legendrian boundary. Suppose $\Sigma \cap A = S^1 \times \{0\}$ and $\mathrm{tw}(S^1 \times \{0\}) < \mathrm{tw}(S^1 \times \{1\}) \leq 0$. Then there is a bypass for Σ along $S^1 \times \{0\}$.*

Theorem 3.2.5 (Disk imbalance [Hon00a])**.** *Let Σ be a convex surface and D be a convex disk with a Legendrian boundary. Suppose $\Sigma \cap D = \partial D$. If $\mathrm{tb}(\partial D) < -1$ then there is a bypass for Σ along ∂D.*

Theorem 3.2.6 (Bypass rotation [HKM05])**.** *Suppose that there is a bypass for Σ from the front along an attaching arc γ. If γ' is a Legendrian arc as in Figure 3.6, then there exists a bypass for Σ from the front along γ'.*

Theorem 3.2.7 (Bypass slide [Hon00a])**.** *Suppose that there is a bypass for Σ from the front along an attaching arc γ. If γ' is a Legendrian arc that is isotopic to γ relative to Γ_Σ, then there is a bypass for Σ from the front along γ'.*

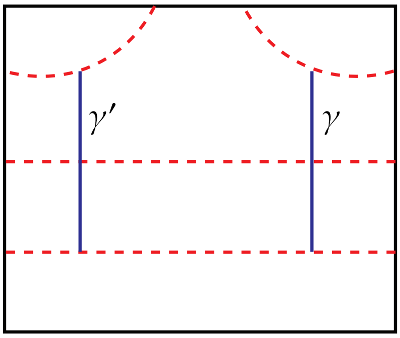

Figure 3.6: The two attaching arcs involved in a bypass rotation.

§ 3.2.2 | Contact structures on $T^2 \times I$ and solid tori

We quickly recall some facts about the contact geometry of $T^2 \times I$ and $S^1 \times D^2$.

Definition 3.2.8 (Basic slice)**.** A tight contact structure ξ on $T^2 \times I$ is called a *basic slice* if

1. $\partial(T^2 \times I) = T_0 \cup T_1$ is two standard convex tori with dividing slopes s_0 and s_1, respectively,
2. s_0 and s_1 are connected by an edge in the Farey graph, and
3. the slope of the dividing curves on any convex torus T parallel to the boundary is clockwise of s_0 and anticlockwise of s_1 in the Farey graph. This condition is called *minimal twisting*.

Honda [Hon00a] studied various properties of basic slices. Here, we review the classification of basic slices up to isotopy.

Theorem 3.2.9 (Classification of basic slices [Hon00a])**.** *There are exactly two basic slices up to isotopy fixing the characteristic foliation on the boundary. These two tight contact structures are distinguished by their relative Euler class. They are called positive and negative basic slices and denoted by $B_+(s_0, s_1)$ and $B_-(s_0, s_1)$, respectively.*

We now review Giroux torsion. Let $k \in \frac{1}{2}\mathbb{N}$. Consider the contact structure $\xi^k = \ker(\sin(2\pi kz)dx + \cos(2\pi kz)dy)$ on $T^2 \times [0,1]$, where (x,y) are the coordinates on T^2 and z is the coordinate on $[0,1]$.

Definition 3.2.10 (Giroux torsion)**.** We call ξ^k a *Giroux k-torsion layer* and if we have a contact structure (M,ξ) into which $(T^2 \times [0,1], \xi^k)$ embeds, we say (M,ξ) contains *Giroux k-torsion.* We will use the phrase (M,ξ) has *exactly Giroux k-torsion* to the situation where one can embed $(T^2 \times [0,1], \xi^k)$ into (M,ξ) but not $(T^2 \times [0,1], \xi^{k+\frac{1}{2}})$. If $k = 1/2$, then we call ξ^k a *half Giroux torsion.* We say (M,ξ) has *no (half) Giroux torsion* if $(T^2 \times [0,1], \xi^k)$ does not embed in (M,ξ) for any $k \in \frac{1}{2}\mathbb{N}$.

Now we consider $(T^2 \times \mathbb{R}, \sin(2\pi kz)dx + \cos(2\pi kz)dy)$ and perturb $T^2 \times \{0\}$ and $T^2 \times \{1\}$ so that they become convex with two dividing curves of slope 0. Let ξ_c^k be the resulting contact structure on $T^2 \times [0,1]$.

Definition 3.2.11 (Giroux torsion layer)**.** We call the structure ξ_c^k a *convex Giroux k-torsion layer.* Notice that inside of $(T^2 \times [0,1], \xi_c^k)$ there is a basic slice with one boundary component agreeing with $T^2 \times \{0\}$ and having boundary slope 0 and ∞. This will either be a positive or a negative basic slice. By reversing the coorientation of ξ_c^k, if necessary, we can assume it is positive.

Theorem 3.2.12 (Uniqueness of Giroux torsion layers [Hon00a])**.** *For $k \in \frac{1}{2}\mathbb{N}$, there are exactly two convex Giroux k-torsions $\pm\xi_c^k$, up to isotopy rel. boundary, on $T^2 \times [0,1]$ with convex boundary having two dividing curves, both of slope 0. The two contact structures are contactomorphic.*

Remark 3.2.13. In this chapter, since we only consider contact manifolds with convex boundary, we just use the term *Giroux k-torsion* for convex Giroux k-torsion. However, readers should notice that the original Giroux torsion has pre-Lagrangian [3] torus boundary.

Next, we will review the classification of tight contact structures on a solid torus. Consider a solid torus with a fixed longitude. Here, our slope convention is $\frac{\text{meridian}}{\text{longitude}}$. We denote by $N(s)$, a solid torus with convex boundary having two dividing curves of slope s.

Theorem 3.2.14 (Classification of tight contact structures on a solid torus [Gir00, Hon00a])**.** *Let (p,q) be a pair of relatively prime integers satisfying $q > -p \geq 1$ and*

$$\frac{q}{p} = [r_0, \cdots, r_k]$$

for $r_i \leq -2$. Then there exist exactly

$$|(r_0+1)\dots(r_{k-1}+1)r_k|$$

[3] A *pre-Lagrangian submanifold* L is the diffeomorphic image of a Lagrangian submanifold $\widetilde{L}$ in the symplectization SM of (M,ξ) under the projection $\pi\colon SM \to M$.

tight contact structures on $N(\frac{p}{q})$ *up to isotopy fixing the characteristic foliation on the boundary.*

Now we consider a solid torus with a different meridional slope. Take a core of $N(s)$ and perform an r-surgery on it. Then we obtain a solid torus with dividing slope s and meridional slope r. Denote it by $N_r(s)$. From Theorem 3.2.14, we can deduce the following result.

Proposition 3.2.15 ([CM20]). *Let* (p, q) *be a pair relatively prime integers. Then there exist* $\Phi(\frac{p}{q})$ *tight contact structures on* $N_{p/q}(\infty)$ *up to isotopy fixing the characteristic foliation on the boundary.*

§ 3.2.3 | Contact surgery

Let L be a Legendrian knot in a contact 3-manifold (M, ξ) and N a standard neighborhood of L (see the discussion after Definition 2.2.15).

Definition 3.2.16 (Contact surgery). *Contact* $(\frac{p}{q})$*-surgery* on L is defined as follows: let (μ, λ) be a meridian and contact framing of L, respectively. $(M_{(p/q)}(L), \xi_{(p/q)})$ is obtained by cutting N from M and re-gluing it via a diffeomorphism of ∂N sending μ to $p\mu + q\lambda$ and then by extending the contact structure $(M \setminus N, \xi)$ to the entire $M_{(p/q)}(L)$.

In general the extension is not unique since there could be distinct tight contact structures on N with a given boundary condition. For $\frac{p}{q} = \pm 1$, the extension is unique [Gir00, Hon00a] and -1 contact surgery is a special case which normally referred to as *Legendrian surgery.* Legendrian surgery is extremely well-behaved with respect to tight contact structures.

Theorem 3.2.17 (Legendrian surgery preserves tightness [Wan15]). *If* (M, ξ) *is obtained by Legendrian surgery on tight* (M', ξ')*, for* M' *a closed, oriented 3-manifold, and* ξ' *a positive co-oriented contact structure, then* (M, ξ) *is tight.*

Remark 3.2.18. The strength of Theorem 3.2.17 extends to fillability properties as well. In fact, it is known that Legendrian surgery preserves (weak/strong/Stein) fillability of contact structures [EH01a, Eli90, Wei91].

If we only focus on the tight contact structures on N, Theorem 3.2.14 provides the number of all possible extensions.

Theorem 3.2.19 (Counting contact surgeries [DG04]). *Let* L *be a Legendrian knot in* (M, ξ) *and* p, q *be relatively prime integers satisfying* $\frac{p}{q} < 0$. *The number of tight contact structures induced by contact* $(\frac{p}{q})$*-surgery on* L *is*

$$|(r_0 + 1) \cdots (r_n + 1)|$$

where

$$\frac{p}{q} = r_0 + 1 - \frac{1}{r_1 - \frac{1}{r_2 \dots - \frac{1}{r_n}}} = [r_0 + 1, r_1, \cdots, r_n]$$

for $r_i \leq -2$.

If $\frac{p}{q} > 0$, use $\frac{p}{q-kp}$ instead where k is a positive integer such that $q - kp < 0$.

In [DGS04], Ding, Geiges and Stipsicz exhibited an algorithm that converts any contact surgery diagram into a (± 1)-surgery diagram. We briefly recall it here.

Algorithm 3.2.20 (Conversion for contact surgeries)**.** We split the algorithm in two options, depending wether $\frac{p}{q}$ is positive or negative.

- contact $(\frac{p}{q})$-surgery with $\frac{p}{q} < 0$:
  1. Stabilize[4] L $|r_0 + 2|$ times. Let this be L_0.
  2. For $i = 1, \dots, n$, let L_i be the Legendrian push-off of L_{i-1} and stabilize it $|r_i + 2|$ times.
  3. Then a contact $(\frac{p}{q})$-surgery on L corresponds to a contact (-1)-surgeries on a link $(L_0, \dots, L_n)$.
- contact $(\frac{p}{q})$-surgery with $\frac{p}{q} > 0$:
  1. Choose a positive integer k such that $q - kp < 0$. Let $r' = \frac{p}{q-kp}$.
  2. Let $L_1, \dots, L_k$ be k successive Legendrian push-offs of L.
  3. Then a contact $(\frac{p}{q})$-surgery on L corresponds to $(+1)$-surgeries on $L, L_1, \dots, L_{k-1}$ and a contact (r')-surgery on L_k.

Sometimes, a contact surgery produces an overtwisted contact structure.

Proposition 3.2.21. *Consider contact* (r)*-surgery on a Legendrian knot* L*. If*

- $r = 0$ *and* L *is any Legendrian knot,*
- $0 < r < 1$ *and* L *is a Legendrian unknot with* $\mathrm{tb} = -1$*,*

then we get an overtwisted contact structure.

Proof. If $r = 0$ and L is any Legendrian knot we are creating an obvious overtwisted disc which will bounded by the meridian of the glued in solid torus, which has slope 0 with respect to the contact framing. As per the second point a quick proof can be found in [CK24, Lemma 3.2]. One can see this also as a consequence of $\frac{1}{k}$ $(k \geq 2)$ surgeries on a $tb = -1$ unknot being overtwisted [Ona18]. □

[4] See Chapter 2, Figure 2.5

§ 3.3 | The lower bounds

In this section, we will construct $2\Phi(r)+\Psi(r)$ isotopy classes of tight contact structures on $M(n,r)$ for $n > 2$ and $r \geq 1$ and $\Psi(r)$ isotopy classes of tight contact structures for $n > 2$ and $r < 1$ using contact surgery diagrams. We first construct distinct contact structures counted by Ψ and then consider contact structures counted by Φ. After that, we will show that the contact structures counted by Ψ are distinct from the ones counted by Φ. For this section we expect the reader to be familiar with elementary modifications of surgery descriptions. We believe [GS99] is a perfect reference for all these operations.

§ 3.3.1 | Tight contact structures counted by Ψ.

Consider the surgery diagram for $M(n,r)$ shown in Figure 3.1. A left-handed Rolfsen twist [GS99] on K_1 turns the diagram into the one in Figure 3.7. We then perform a sequence of inverse slam–dunk moves [GS99] to turn K_1 into a chain of unknots. Since we have

$$-\frac{n}{n-1} = [\overbrace{-2,\cdots,-2}^{n-1}],$$

there are $n-1$ components in the chain of the unknots and the surgery coefficients are all -2, see Figure 3.8. We can turn this diagram into a contact surgery diagram as shown in Figure 3.9. Applying the algorithm described in Section 3.2.3, we can convert the diagram into a (± 1)-contact surgery diagram. Notice that there are choices of stabilizations during the conversion.

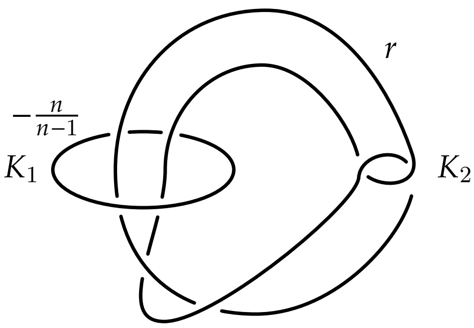

Figure 3.7: A surgery diagram for $M(n,r)$.

Proposition 3.3.1. *The contact surgery diagram in Figure 3.9 induces a tight contact structure for any choice of stabilizations for any $r \neq 1$.*

Proof. We first consider the case $r > 1$. Fix a choice of stabilizations. Since $r > 1$, the contact surgery coefficient on the trefoil component in Figure 3.9 is positive. Thus there exists a single link component L having contact surgery coefficient $(+1)$ after the

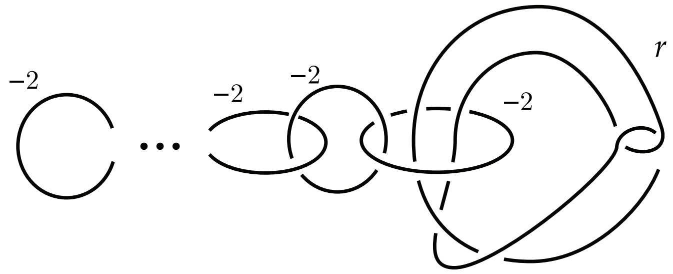

Figure 3.8: The result of inverse slam–dunk moves.

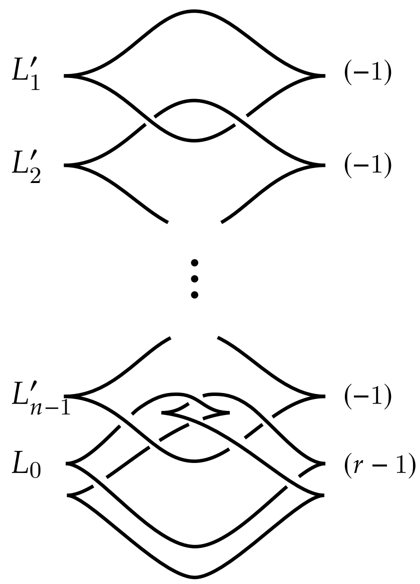

Figure 3.9: A contact surgery diagram for tight contact structures on $M(n,r)$ counted by Ψ.

conversion, and all other components have the contact surgery coefficient (-1). Let $(S^3_2(L), \xi_L)$ be the result of a contact $(+1)$-surgery on L. L is a Legendrian right-handed trefoil with $\mathrm{tb}(L) = 1$, hence the Heegaard Floer invariant of ξ_L is non-vanishing by Theorem 2.4.7. Since the contact structure on $M(n, r)$ is constructed from $(S^3_2(L), \xi_L)$ by Legendrian surgeries on the other link components, the Heegaard Floer invariant of the resulting contact structure is non-vanishing by Theorem 2.4.6. Thus the contact structure on $M(n, r)$ is tight.

Now we consider the case $r < 1$. Fix a choice of stabilizations. Since $r < 1$, the contact surgery coefficient on the trefoil component in Figure 3.9 is negative. Thus this contact surgery diagram represents a Stein fillable contact structure and hence it is tight. □

Proposition 3.3.2. *The contact surgery diagram in Figure 3.9 induces $\Psi(r)$ pairwise non-isotopic tight contact structures for any $r \in \mathbb{Q}$, distinguished by their Heegaard Floer invariants.*

Remark 3.3.3. As it will be clear from the proof, we are actually distinguishing the contact structures by looking at Chern classes of specific Stein structures. By work of [Pla04] this also implies that the contact invariants in Heegaard Floer homology of the contact structures are distinct.

Proof. We first consider the case $r > 1$. We will use the same notations used in Proposition 3.3.1. As we discussed in the proof of Proposition 3.3.1, there exists a single link component L with the contact surgery coefficient $(+1)$ after the conversion, and all other components have the contact surgery coefficient (-1). Thus there exists a Stein cobordism W (see Definition 2.3.4) from $S^3_2(L)$ to $M(n, r)$ induced from the contact surgery diagram. We claim that different choices of stabilizations give rise to non-isomorphic Stein structures and by [Pla04, Theorem 2] applied to W, with boundary $S^3_2(L)$ and $M(n, r)$ the induced contact structures on $M(n, r)$ are also non-isotopic, distinguished by their Heegaard Floer invariants. To prove the claim, fix two different choices of stabilizations. Suppose $L_1, \ldots, L_m$ are the push-offs of L after the conversion. Since each L_i is rationally null-homologous [BE12] in $S^3_2(L)$, we can calculate its rational rotation number in $(S^3_2(L), \xi_L)$. Recall that a stabilization behaves precisely the same way as in the null-homologous case (Lemma 2.2.24), i.e. $\mathrm{rot}_{\mathbb{Q}}(S_\pm(L)) = \mathrm{rot}_{\mathbb{Q}}(L) \pm 1$ (cf. [BE12, Lemma 1.3]).

Since we chose different sets of stabilizations, there exists at least one index i such that the values of $\mathrm{rot}_{\mathbb{Q}}(L_i)$ are different. Now we compare the first Chern class of the Stein structure J on W induced by the surgery diagrams. Using the formula from [LW19, Lemma 4.1], we obtain

$$\langle c_1(J), [\Sigma_i \cup 2 \cdot C_i] \rangle = 2 \cdot \mathrm{rot}_{\mathbb{Q}}(L_i),$$

where Σ_i is a rational Seifert surface of L_i, C_i is the core of the Weinstein 2-handle

[Wei91] attached along L_i. Note that the knots L_i are rationally null-homologous in $S^3_2(L)$, which has first homology isomorphic to $\mathbb{Z}_2$, and hence have order 2. We can conclude the two different values of $\mathrm{rot}_{\mathbb{Q}}(L_i)$ lead to non-isomorphic Stein structures on W, proving the claim.

By Proposition 3.3.1, all contact structures are tight for any choices of stabilizations. Hence we are only left to show that there exist $\Psi(r)$ different choices of stabilizations for the contact surgery diagram in Figure 3.9. According to the algorithm in Section 3.2.3, if $r > 1$, a contact $(r-1)$-surgery on L is equivalent to a contact $(+1)$-surgery on L and $(-\frac{r-1}{r-2})$-surgery on its push-off. Consider the negative continued fraction expansion $-\frac{r-1}{r-2} = [r_0, r_1, \ldots, r_k]$. Then the number of stabilization choices for a contact $(-\frac{r-1}{r-2})$-surgery is $|r_0(r_1+1)\cdots(r_k+1)|$, which is $\Phi(\frac{r-2}{r-1}) = \Phi(\frac{1}{1-r}) = \Psi(r)$.

If $r = 1$, we have $\Psi(1) = 0$ and the contact surgery diagram produces an overtwisted contact structure by Proposition 3.2.21.

Lastly, we consider the case $r < 1$. As discussed in Proposition 3.3.1, since all contact surgery coefficients are negative, the surgery diagram represents a Stein manifold (X, J) and the first Chern class of the Stein structure will evaluate to $\mathrm{rot}(L_i)$ on the set of generators of $H_2(X; Z)$ given by the cores of 2-handles and the Seifert surfaces for the attaching spheres, see [Gom98]. Since we chose different sets of stabilizations, there exists at least one index i such that the values of $\mathrm{rot}(L_i)$ are different. Thus, the two different values of $\mathrm{rot}(L_i)$ lead to non-isomorphic Stein structures. Now it remains to show that there exist $\Psi(r)$ different choices of stabilizations for the contact surgery diagram in Figure 3.9. Consider the negative continued fraction expansion $r-1 = [r_0, r_1, \ldots, r_k]$. According to the algorithm in Section 3.2.3, the number of stabilization choices for a contact $(r-1)$-surgery is $|r_0(r_1+1)\cdots(r_k+1)|$, which is $\Phi(\frac{1}{1-r}) = \Psi(r)$. □

§ 3.3.2 | Tight contact structures counted by Φ.

Since the Whitehead link is symmetric, we can switch the link components via isotopy and obtain the diagram in the first drawing of Figure 3.10. Perform a left-handed Rolfsen twist on K_2, and we obtain a surgery diagram as shown in the right drawing of Figure 3.10. After realizing this link as a Legendrian link, we obtain a contact surgery diagram shown in Figure 3.11. Applying the algorithm from Section 3.2.3, we can convert the diagram into a (±1)-contact surgery diagram. Again, there are choices of stabilizations during the conversion.

The proofs of Proposition 3.3.4 and 3.3.6 are essentially identical to the proofs of Proposition 3.3.1 and 3.3.2, respectively. Since they do not introduce any relevant ideas, we do not spell them out here.

Proposition 3.3.4. *The contact surgery diagram in Figure 3.11 induces a tight contact structure for any choices of stabilizations for $r \geq 1$.* □

Remark 3.3.5. In [MN26] we claim that thanks to Proposition 3.2.21, the surgery

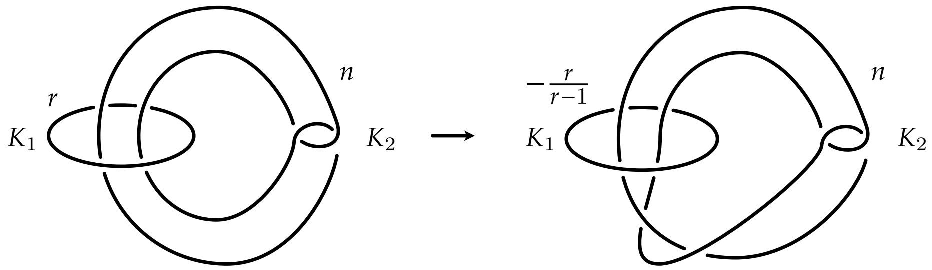

Figure 3.10: Another surgery diagram for $M(n,r)$.

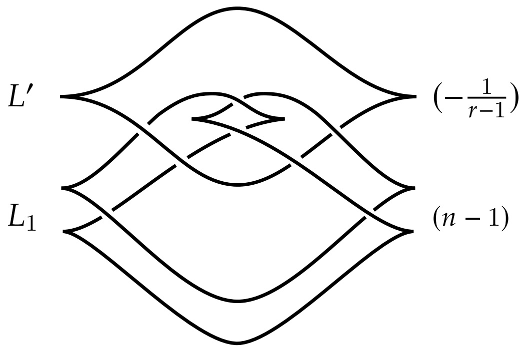

Figure 3.11: A contact surgery diagram for tight contact structures on $M(n,r)$ counted by Φ.

diagram in Figure 3.11 results in overtwisted contact structures if $r < 0$. Although the surgery on L' is indeed overtwisted, we cannot conclude directly that $(n-1)$ surgery on L_1 does not produce a tight structure. The overtwisted disc exhibited in the proof of [CK24, Lemma 3.2] might be destroyed by the $(n-1)$ surgery on L_1. Overtwistedness of the structures described by the diagram in Figure 3.11 however follows from the upper bound we construct in Section 3.4.

Proposition 3.3.6. *The contact surgery diagram in Figure 3.11 induces* $2\Phi(r)$ *pairwise non-isotopic tight contact structures for* $r \geq 1$*, distinguished by their Heegaard Floer invariants.*

§ 3.3.3 | Distinguishing contact structures counted by Ψ and Φ

So far, we have constructed tight contact structures on $M(n,r)$ using contact surgery diagrams. However, since we have used different surgery diagrams for the ones counted by Ψ and Φ, respectively, we constructed two distinct manifolds diffeomorphic to $M(n,r)$. To compare the isotopy classes of the contact structures on each manifold, we push them to a fixed manifold and determine their first Chern classes.

Proposition 3.3.7. *For* $n > 2$ *and* $r \geq 1$*,* $M(n,r)$ *supports at least* $\Psi(r) + 2\Phi(r)$ *pairwise non-isotopic tight contact structures, distinguished by their Heegaard Floer invariants.*

Proof. In the previous subsections, we denoted by $M(n,r)$ any 3-manifolds constructed from the surgery diagrams in Figure 3.1, 3.8, 3.9, 3.10, and 3.11, but here we will distin-

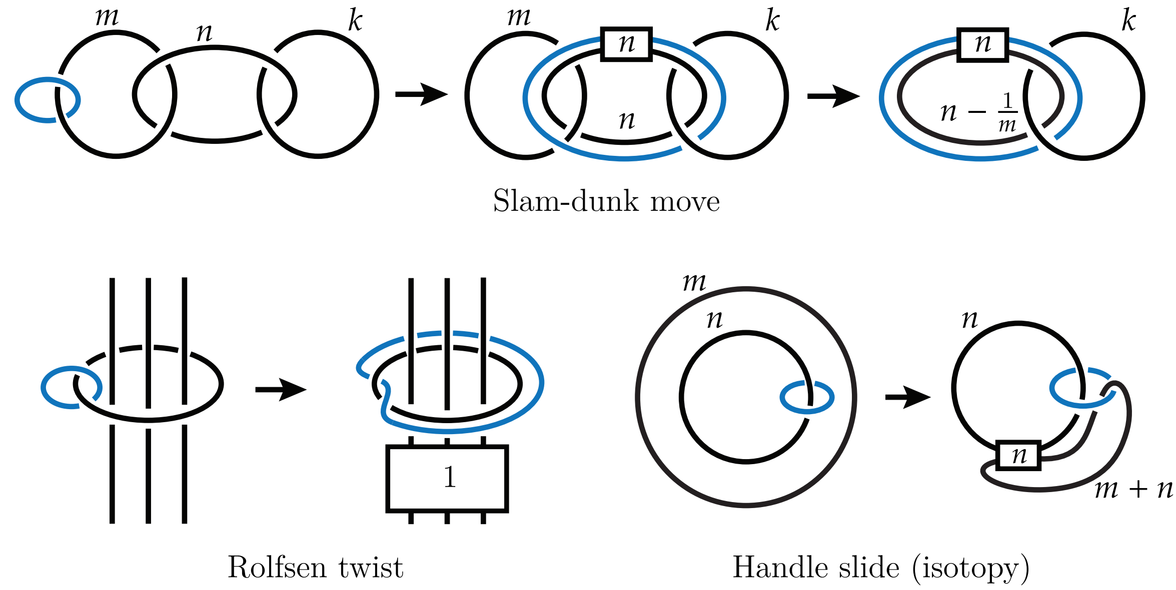

Figure 3.12: Various surgery operations. In all the pictures the first blue curve is a meridian (generator) and we trace its image under the different moves. On top we have a slam-dunk move, on the bottom left a Rolfsen twist and in the bottom right a handle slide.

guish them. Let $M(n,r)$ be the 3-manifold constructed from the surgery diagram shown in Figure 3.1, and M_1 a manifold constructed from the (± 1)–contact surgery diagram which is converted from Figure 3.9 using the algorithm in Section 3.2.3, and M_2 a manifold constructed from the (± 1)–contact surgery diagram converted from Figure 3.11. It is routine to check that we can return back from these (± 1)–contact surgery diagrams to the surgery diagram in Figure 3.1 by using isotopies (handle slides), slam–dunk moves and Rolfsen twists. Since each of these operations induces a diffeomorphism, we obtain diffeomorphisms $f^i \colon M_i \to M(n,r)$ for $i = 1, 2$.

Pick contact structures (M_1, ξ_1) and (M_2, ξ_2) counted by Ψ and Φ, respectively. We claim that the contact structures $f^1_*(\xi_1)$ and $f^2_*(\xi_2)$ on $M(n,r)$ are not isotopic. Together with Proposition 3.3.2 and 3.3.6, the claim completes the proof.

We will show the claim by calculating the first Chern classes of the contact structures. We start with calculating $H_1(M(n,r))$. Let μ and ν be the meridians of K_1 and K_2 in Figure 3.1, respectively. Since the linking number between the components of the Whitehead link is 0, we have

$$H_1(M(n,r)) = \langle \mu, \nu \mid n\mu = 0, p\nu = 0 \rangle = \mathbb{Z}_n \oplus \mathbb{Z}_p.$$

where $r = \frac{p}{q}$. Next, we will compute the Poincaré dual of $c_1(f^1_*(\xi_1))$ and express it in terms of $[\mu]$ and $[\nu]$. Consider the contact (± 1)–surgery diagram for (M_1, ξ_1). Let $-\frac{r-1}{r-2} = [r_1, \ldots, r_k]$, L_0 the Legendrian trefoil in Figure 3.9, and $L_1, \ldots, L_k$ its push-offs after the conversion. We also denote the Legendrian unknots in Figure 3.9 by $L'_1, L'_2, \cdots, L'_{n-1}$ from the bottom to the top. According to the results from [DGS04, Gom98], we have

$$\mathrm{PD}\,(c_1(\xi_1)) = \sum_{i=0}^{k} \mathrm{rot}(L_i)[\mu_i] + \sum_{i=1}^{n-1} \mathrm{rot}(L_i')[\mu_i'], \tag{3.1}$$

where $\mathrm{rot}(L_i') = 0$ for $1 \leq i \leq n-1$, $\mathrm{rot}(L_0) = 0$ and $\mathrm{rot}(L_i)$ for $1 \leq i \leq k$ depends on the choice of stabilizations. We now keep track of this homology class under the diffeomorphisms induced by surgery operations.

First, consider the chain of unknots $L_1', \ldots, L_{n-1}'$. We apply slam-dunk moves to remove all L_i' for $2 \leq i \leq n-1$. Suppose L_i' is the last component of the chain. We investigate the effect of a slam-dunk move to L_i'. We claim that the homology classes will change under the induced diffeomorphism as follows:

$$[\mu_i'] \mapsto -2[\mu_{i-1}'] - [\mu_{i-2}']$$

and all other $[\mu_j]$ and $[\mu_j']$ remain unchanged. To see this, slide μ_i' over L_{i-1}' and obtain a $(1,-2)$-cable of L_{i-1}' as shown in the top of Figure 3.12. Thus we have $[\mu_i'] = -2[\mu_{i-1}'] + [\lambda_{i-1}']$ where λ_{i-1}' is a Seifert longitude of L_{i-1}'. Then apply the slam-dunk move to L_i' and remove it. Since the slam-dunk move is a local operation, it only affects a small neighborhood of $D_i' \cup L_{i-1}'$ where D_i' is a Seifert disk of L_i'. Thus it does not change the isotoped μ_i'. Also, λ_{i-1}' is isotopic to $-\mu_{i-2}'$ since $\mathrm{lk}(L_i, L_{i-1}) = \mathrm{tb}(L_{i-1}) = -1$. Thus the result follows.

Now we turn our attention to $L_1, \ldots, L_k$. First, notice that the smooth surgery coefficient of L_0 is $2 = \mathrm{tb}(L_0) + 1$, and all other L_i is $\mathrm{tb}(L_i) - 1$. We slide L_k over L_{k-1} and L_k becomes a meridian of L_{k-1}. Since $\mathrm{lk}(L_k, L_{k-1}) = \mathrm{tb}(L_{k-1})$, the surgery coefficient becomes

$$\begin{aligned}(\mathrm{tb}(L_k) - 1) + (\mathrm{tb}(L_{k-1}) - 1) - 2\,\mathrm{tb}(L_{k-1}) &= \mathrm{tb}(L_k) - \mathrm{tb}(L_{k-1}) - 2 \\ &= r_k.\end{aligned}$$

The second equality follows from the fact that both $|r_k + 2|$ and $|\,\mathrm{tb}(L_k) - \mathrm{tb}(L_{k-1})|$ are the difference between the number of stabilizations on L_k and L_{k-1}. We keep sliding L_i over L_{i-1} for all $1 \leq i \leq k$ consecutively. Then we obtain a chain of unknots where $\mathrm{lk}(L_i, L_{i-1}) = -1$ for $1 \leq i \leq k$. Notice that the surgery coefficient of L_i is

$$\begin{cases} \mathrm{tb}(L_i) - \mathrm{tb}(L_{i-1}) - 2 = r_i & 2 \leq i \leq k, \\ \mathrm{tb}(L_i) - \mathrm{tb}(L_{i-1}) = r_i + 1 & i = 1, \\ \mathrm{tb}(L_i) + 1 = 2 & i = 0. \end{cases}$$

We can now perform a sequence of slam-dunk moves to eliminate all L_i for $1 \leq i \leq k$. Suppose L_i is the last component of the chain. As what we did to L_i' in the previous paragraph, we can keep track of the homology classes under the slam-dunk moves on

L_i and the homology classes change as follows:

$$\begin{cases} [\mu_i] \mapsto r_{i-1}[\mu_{i-1}] - [\mu_{i-2}] & 3 \leq i \leq k \\ [\mu_i] \mapsto (r_{i-1}+1)[\mu_{i-1}] - [\mu_{i-2}] & i = 2 \\ [\mu_i] \mapsto 2[\mu_{i-1}] & i = 1 \end{cases}$$

and all other $[\mu_j]$ and $[\mu'_j]$ remain unchanged.

Finally, we apply a right-handed Rolfsen twist along L'_1 and obtain the surgery diagram in Figure 3.1. As shown in the bottom left of Figure 3.12, the meridian μ'_1 becomes $(1,1)$-cable of L'_1 after the Rolfsen twist. Let λ'_1 be a Seifert longitude of L'_1. Since the linking number between the two link components is 0, the homology classes will change under the induced diffeomorphism as follows:

$$[\mu'_1] \mapsto [\mu'_1] + [\lambda'_1] = [\mu'_1] + [\mu_0] - [\mu_0] = [\mu'_1],$$

and $[\mu_0]$ remains unchanged.

We can now naturally identify μ_0 and μ'_1 with ν and μ, respectively. Altogether, we have

$$\begin{aligned} \mathrm{PD}\,(c_1(f^1_*(\xi_1))) &= f^1_*(\mathrm{PD}\,(c_1(\xi_1))) \\ &= f^1_*\left(\sum_{i=0}^{k} \mathrm{rot}(L_i)[\mu_i] + \sum_{i=1}^{n-1} \mathrm{rot}(L'_i)[\mu'_i]\right) \\ &= f^1_*\left(\sum_{i=0}^{k} \mathrm{rot}(L_i)[\mu_i]\right) \\ &= \sum_{i=0}^{k} \mathrm{rot}(L_i) \cdot f^1_*\left([\mu_i]\right) \\ &= 0[\mu] + m[\nu] \end{aligned}$$

for some $m \in \mathbb{Z}$. The first and fourth equalities follow from the naturality, the second equality follows from (3.1), the third equality follows from the fact that $\mathrm{rot}(L'_i) = 0$ for $1 \leq i \leq n-1$ and the fifth equality follows from the discussions about the effect of surgery operations in the previous paragraphs.

Similarly, we can calculate $c_1(f^2_*(\xi_2))$. Consider the contact (± 1)–surgery diagram for (M_2, ξ_2). Let L_1 be the Legendrian trefoil in Figure 3.11. Since we have

$$\frac{n-1}{1-(n-1)} = -\frac{n-1}{n-2} = [\overbrace{-2, \cdots, -2}^{n-2}],$$

there are $(n-2)$ push-offs of L_1 after the conversion. Denote them by $L_2, L_3, \cdots, L_{n-1}$. Recall that during the conversion, we stabilize L_2 once and push it off $n-3$ times.

Thus the rotation numbers of L_i are

$$\mathrm{rot}(L_1) = 0, \mathrm{rot}(L_2) = \mathrm{rot}(L_3) = \cdots = \mathrm{rot}(L_{n-1}) = \pm 1. \tag{3.2}$$

Let $L'_0, \ldots, L'_k$ be the Legendrian unknots obtained as pushoffs of the unknot L' in Figure 3.11 after the conversion. As before, we have

$$\mathrm{PD}\,(c_1(\xi_2)) = \sum_{i=1}^{n-1} \mathrm{rot}(L_i)[\mu_i] + \sum_{i=0}^{k} \mathrm{rot}(L'_i)[\mu'_i]. \tag{3.3}$$

We first consider $L_1, \ldots, L_{n-1}$. We start by sliding all L_i over L_1 for $2 \le i \le n-1$. This produces an unlink of $(n-2)$ components which are meridians of L_1 and the surgery coefficient of each component becomes -1. The handle-slide operation on L_i induces a diffeomorphism and the homology classes will change under this diffeomorphism as follows:

$$[\mu_1] \mapsto [\mu_1] + [\mu_i]$$

and all other $[\mu_j]$ and $[\mu'_j]$ remain unchanged. This is clear from the bottom right of Figure 3.12. Now apply right-handed Rolfsen twist along each L_i for $2 \le i \le n-1$ and get rid of it. As shown in the bottom left of Figure 3.12, each μ_i becomes a $(1,1)$-cable of L_i. Let λ_i be a Seifert longitude of L_i. Since λ_i is a meridian of L_1 and μ_i becomes contractible, the homology classes will change under the induced diffeomorphism as follows:

$$[\mu_i] \mapsto [\mu_i] + [\lambda_i] = [\mu_1]$$

and all other $[\mu_j]$ and $[\mu'_j]$ remain unchanged.

We now perform a sequence of handle-slides to make $L'_0, \ldots, L'_k$ a linear chain of unknots and then perform slam-dunk moves to get rid of all L'_i for $1 \le i \le k$. Thus we apply a similar argument as before to keep track of the homology classes. The only important fact here is that these operations only affect μ'_i and do not affect any μ_i.

Finally, we apply a right-handed Rolfsen twist along L'_0 and obtain the surgery diagram in the left of Figure 3.10. Then swap the link components and obtain the diagram in Figure 3.1. As in the case of ξ_1, this Rolfsen twist does not affect any homology class.

We can now naturally identify μ_1 and μ'_0 with μ and ν, respectively. Altogether, we have

$$\begin{aligned}
\mathrm{PD}\,(c_1(f_*^2(\xi_2))) &= f_*^2(\mathrm{PD}\,(c_1(\xi_2))) \\
&= f_*^2\left(\sum_{i=1}^{n-1}\mathrm{rot}(L_i)[\mu_i] + \sum_{i=0}^{k}\mathrm{rot}(L_i')[\mu_i']\right) \\
&= \sum_{i=2}^{n-1} \pm f_*^2\left([\mu_i]\right) + \sum_{i=0}^{k}\mathrm{rot}(L_i')\cdot f_*^2\left([\mu_i']\right) \\
&= \pm(n-2)[\mu] + h[\nu]
\end{aligned}$$

for some $h \in \mathbb{Z}$. The first equality follows from the naturality, the second equality follows from (3.3), the third equality follows from (3.2) and the fourth equality follows from the discussions about the effect of surgery operations in the previous paragraphs.

Since we assume $n > 2$, we can conclude that $f_*^1(\xi_1)$ and $f_*^2(\xi_2)$ are distinguished by their first Chern classes, which completes the proof of the claim. □

§ 3.4 | The upper bounds

In this section, we determine the upper bounds of the number tight contact structures on $M(n,r)$ for $n \geq 5$ and $r \in \mathcal{R}_+ \cup \mathbb{Q}_-$. Combining it with the lower bounds in Section 3.3, we complete the proof of Theorem 3.1.3.

§ 3.4.1 | Convex decompositions of $M(n,r)$

The first step is to decompose $M(n,r)$ into two pieces with convex (see Definition 2.2.34) torus boundary. Consider the surgery diagram for $M(n,r)$ shown in Figure 3.1. If we perform the surgery only on K_1, then the result will be $L(n,n-1)$. Moreover, it is well known (*c.f.* [Bak14, HMW92, Mor89]) that K_2 is a genus one fibered knot in $L(n,n-1)$. Let N be a neighborhood of K_2 in $L(n,n-1)$, C_n the complement of N, Σ a fiber surface (a once punctured torus) of C_n and ϕ_n the monodromy[5] of C_n. Then there is a symplectic basis of $H_1(\Sigma)$ such that the action of the monodromy ϕ_n on $H_1(\Sigma)$ is given by

$$\phi_n = \begin{pmatrix} -n+2 & 1 \\ -1 & 0 \end{pmatrix} = \begin{pmatrix} 1 & 0 \\ -1 & 1 \end{pmatrix}\begin{pmatrix} 1 & 1 \\ 0 & 1 \end{pmatrix}\begin{pmatrix} 1 & 0 \\ -1 & 1 \end{pmatrix}^{n-1}.$$

We can also assume that ϕ_n is the identity near the boundary. Notice that ϕ_n is pseudo-Anosov for $n \geq 5$ (this can be seen from the fact that the absolute value of the trace of ϕ_n is > 2) is and it's right-veering – this is not hard to check using the monodromy decomposition. The fractional Dehn twist coefficient (see [HKM07]) satisfies $c(\phi_n) \in (0,1)$ – this can again be seen by the monodromy presentation $D_\alpha D_\beta D_\alpha^{n-1}$ and the fact that we are also excluding boundary twisting. Since $M(n,r)$ is a Dehn filling of C_n,

[5] The monodromy ϕ_n is given by $D_\alpha D_\beta D_\alpha^{n-1}$, where D_α is a positive Dehn twist about α, and α, β are a choice of meridian and longitude for the punctured torus (see [Mor89, Bak14]).

we can write

$$M(n,r) = C_n \cup N_r$$

where N_r is a solid torus with the meridional slope r, with respect to the coordinate system induced by K_1. We can also write C_n as

$$C_n = \Sigma \times [0,1]/(x,1) \sim (\phi_n(x), 0).$$

Let ξ be a contact structure on $M(n,r)$ and L a Legendrian knot in N_r isotopic to the core of N_r. We can assume that N_r is a standard neighborhood of L after a perturbation, so ∂N is convex with two dividing curves of some slope s (again, we measure slopes on $\partial N_r = -\partial C_n$ using the coordinates induced by K_1). Let $C_n(s)$ and $N_r(s)$ denote C_n and N_r with contact structures with convex boundaries with two dividing curves of slope s.

As it is done in [CM20], we will *thicken* $C_n(s)$ into a standard form, which means finding $C_n(s') \subset C_n(s)$ such that $C_n(s) \setminus C_n(s') = T^2 \times I$. We say that $C_n(s)$ *thickens* to $C_n(s')$, or $C_n(s)$ *thickens to slope* s'.[6] Also, we say $C_n(s)$ *does not thicken* if $C_n(s)$ thickens to s' implies $s = s'$. We will thicken $C_n(s)$ by attaching bypasses to $-\partial C_n(s)$. We will find such bypasses by finding boundary parallel dividing arcs on a fiber surface $\Sigma \subset C_n(s)$. Due to our slope convention and the choice of orientation, the slope increases after attaching a bypass to $-\partial C_n(s)$.

Let $\mathcal{S}(r)$ be the set of slopes s that is clockwise of r, anticlockwise of ∞ on the Farey graph and connected to r by an edge. For $r \in \mathcal{R}_+$, we need the following two lemmas.

Lemma 3.4.1. *Suppose $n \geq 5$, $r \in \mathcal{R}_+$ and $s \in \mathcal{S}(r)$. Then $C_n(s)$ thickens to $C_n(\infty)$.*

Once we thicken $C_n(s)$ to $C_n(\infty)$, we will determine an upper bound for the number of tight contact structures on $C_n(\infty)$.

Lemma 3.4.2. *Suppose there is no boundary parallel half Giroux torsion in $C_n(\infty)$. Then there exist at most four tight contact structures on $C_n(\infty)$ up to isotopy (not fixing the boundary pointwise but preserving it setwise). Two of them thicken further to $C_n(1)$.*

Remark 3.4.3. Since we will classify tight contact structures on closed manifolds, which are obtained by gluing a solid torus to the boundary of $C_n(\infty)$, it is enough to classify tight contact structures on $C_n(\infty)$ up to isotopy fixing the boundary setwise.

For $r \in \mathbb{Q}_-$, we need the following two lemmas.

Lemma 3.4.4. *Suppose $n \geq 5$, $r \in \mathbb{Q}_-$, $s \in \mathcal{S}(r)$ and $s \neq 0$. Then $C_n(s)$ thickens to $C_n(1)$.*

[6] The terminology "thicken" might sound confusing, as $C_n(s)$ is actually getting smaller. What we are actually thickening is the solid torus N_r. This is however standard terminology, and we prefer to maintain it keeping in mind that our perspective is somehow reversed.

According to Lemma 3.4.4, we can write $C_n(s) = T \cup C_n(1)$ for $s < 0$, where $T = T^2 \times [0,1]$ with convex boundary and dividing slopes $s_0 = s$ and $s_1 = 1$.

Lemma 3.4.5. *Suppose there is no boundary parallel half Giroux torsion. Then there exist at most four tight contact structures on $C_n(-\frac{1}{k})$ for $k \in \mathbb{N}$ up to isotopy (not fixing the boundary pointwise but preserving it setwise). Moreover, the (possibly) tight contact structures on $C_n(-\frac{1}{k})$ are determined by their restriction to T.*

Remark 3.4.6. In fact, there are exactly three tight contact structures on $C_n(-1)$ without boundary parallel Giroux torsion but we will not use this fact in this thesis.

We also need to count the number of tight contact structures on $N_r(\infty)$ and $N_r(1)$ using Proposition 3.2.15.

Lemma 3.4.7. *For any $r \in \mathbb{Q}$, there are $\Phi(r)$ tight contact structures on $N_r(\infty)$ up to isotopy fixing the boundary pointwise (hence fixing the characteristic foliation).*

Also, there are $\Psi(r)$ tight contact structures on $N_r(1)$ up to isotopy fixing the boundary pointwise.

Combining these lemmas, we can obtain the upper bounds.

Theorem 3.4.8. *Suppose $n \geq 5$ and $r \in \mathcal{R}_+ \cup \mathbb{Q}_-$.*

- *$M(n,r)$ supports at most $2\Phi(r) + \Psi(r)$ tight contact structures up to isotopy if $r \in \mathcal{R}_+$.*
- *$M(n,r)$ supports at most $\Psi(r)$ tight contact structures up to isotopy if $r \in \mathbb{Q}_-$.*

Proof. We first consider the case $r \in \mathcal{R}_+$. By Lemma 3.4.1 and Lemma 3.4.2, $C_n(s)$ thickens to slope ∞ or 1 for any $s \in \mathcal{S}(r)$. Thus any tight contact structure on $M(n,r)$ can be decomposed as a union of a tight contact structure on $C_n(\infty)$ and a tight contact structure on $N_r(\infty)$, or a union of a tight contact structure on $C_n(1)$ and a tight contact structure on $N_r(1)$. In the case that $C_n(s)$ thickens to $C_n(\infty)$ and not further, there are at most two tight contact structures on $C_n(\infty)$ by Lemma 3.4.2. Also, there are $\Phi(r)$ tight contact structure on $N_r(\infty)$ by Lemma 3.4.7. These lead to $2\Phi(r)$ (possibly) tight contact structures on $M(n,r)$. In the case that $C_n(s)$ thickens to $C_n(1)$, we can decompose $N_r(1)$ into a union of $N_r(-1)$ and T, where $T = T^2 \times I$ with dividing slopes -1 and 1. By Lemma 3.4.5, a tight contact structure on $T \cup C_n(1) = C_n(-1)$ is completely determined by T. Also, there are $\Psi(r)$ tight contact structure on $N_r(-1) \cup T = N_r(1)$ by Lemma 3.4.7. These lead to the $\Psi(r)$ (possibly) tight contact structures on $M(n,r)$.

Next, we consider the case $r \in \mathbb{Q}_-$. By Lemma 3.4.4, $C_n(s)$ thickens to slope 1 for any $s \in \mathcal{S}(r)$ and $s \neq 0$. If $s = 0$, there is $N_r(s') \subset N_r(0)$ for $r < s' < 0$, so we can decompose $M(n,r)$ into $N_r(s')$ and $C_n(s')$. By Lemma 3.4.4, we can thicken $C_n(s')$ to slope 1. Thus any tight contact structure on $M(n,r)$ can be decomposed as a union of a tight contact structure on $C_n(1)$ and a tight contact structure on

$N_r(1)$. We can decompose $N_r(1)$ into a union of $N_r(-\frac{1}{m})$ and T, where $m \in \mathbb{N}$ and $T = T^2 \times I$ with dividing slopes $-\frac{1}{m}$ and 1. By Lemma 3.4.5, a tight contact structure on $T \cup C_n(1) = C_n(-\frac{1}{m})$ is completely determined by its restriction to T. Also, there are $\Psi(r)$ tight contact structure on $N_r(-\frac{1}{m}) \cup T = N_r(1)$ by Lemma 3.4.7. These lead to the $\Psi(r)$ (possibly) tight contact structures on $M(n, r)$. □

We will prove the above lemmas in Section 3.4.4.

§ 3.4.2 | Normalizing the dividing set on Σ

We begin by normalizing the dividing set Γ_Σ of Σ. Since we can freely modify the slopes of the Legendrian ruling curves on N (always keeping in mind that they cannot be parallel to Γ_{N_r}), we assume Σ is convex with Legendrian boundary. Recall that for us Σ is a once-punctured torus.

Etnyre and Honda [EH01a] normalized Γ_Σ for any pseudo-Anosov monodromy of a once-punctured torus bundle over S^1.

Proposition 3.4.9 (Etnyre and Honda [EH01a, Proposition 5.5]). *Suppose Γ_Σ consists of $k > 0$ properly embedded arcs and m closed curves. Then there is an isotopic copy of Σ such that one of the following holds.*

1. *k is odd.*
   - *$m = 1$ and all arcs are in the same isotopy class that is not boundary parallel.*
   - *$m = 0$ and there are three distinct isotopy classes of arcs that are not boundary parallel.*
   - *there is a boundary parallel arc (possibly with other dividing curves).*
2. *k is even.*
   - *there is a boundary parallel arc (possibly with other dividing curves).*

When $k \geq 3$, Etnyre and Honda [EH01a] further normalized the dividing set on Σ in the figure-eight knot complement. Their argument holds however for any pseudo-Anosov monodromy of a once punctured torus.

Let ϕ be a pseudo-Anosov monodromy of $C = \Sigma \times [0, 1]/(x, 1) \sim (\phi(x), 0)$. Consider the matrix representation of ϕ with respect to the symplectic basis of Σ. Then there are two eigenvectors v_a and v_r, where v_a is an attracting fixed point of ϕ and v_r is a repelling fixed point of ϕ. Denote by s_a and s_r the slopes of v_a and v_r, respectively. There are two distinguished paths P_c and P_a in the Farey graph where P_c is the (shortest) clockwise path from s_r to s_a and P_a is the (shortest) anticlockwise path from s_r to s_a.

Lemma 3.4.10 (Etnyre and Honda,[EH01a, Lemma 5.7]). *Suppose Γ_Σ consists of $k \geq 3$ properly embedded arcs and m closed curves. Then there is an isotopic copy of Σ such that one of the following holds.*

- *$m = 0$ and there are three distinct isotopy classes of arcs with slopes $\{a, b, c\}$ in P_c. Moreover, $\{a, b, c\}$ forms the maximal geodesic triangle in the Farey graph among geodesic triangles with vertices in P_c.*

- *$m = 0$ and there are three distinct isotopy classes of arcs with slopes $\{a, b, c\}$ in P_a. Moreover, $\{a, b, c\}$ forms the maximal geodesic triangle in the Farey graph among geodesic triangles with vertices in P_a.*

- *there is a boundary parallel arc (possibly with other dividing curves).*

In Lemma 3.4.10 we use "maximal geodesic triangle" meaning that it is the innermost geodesic triangle, i.e. closest to the center of the disk, and it cannot be enlarged while still keeping the vertices in P_c or P_a.

Etnyre and Honda further convert these dividing sets into a simpler form.

Lemma 3.4.11 (Etnyre and Honda [EH01a, Lemma 5.7])**.** *Suppose that Γ_Σ consists of n arcs and there are three distinct isotopy classes of arcs with slopes $\{a, b, c\}$ in P_a (resp. P_c). Without loss of generality, assume that a is the closest to s_r in the Farey graph. Then there is another isotopic copy of Σ such that*

- *Γ_Σ consists of one closed curve and n arcs with slope a.*

- *there is a boundary parallel arc (possibly with other dividing curves).*

Now we are ready to normalize the dividing set on Σ in our $C_n(s)$.

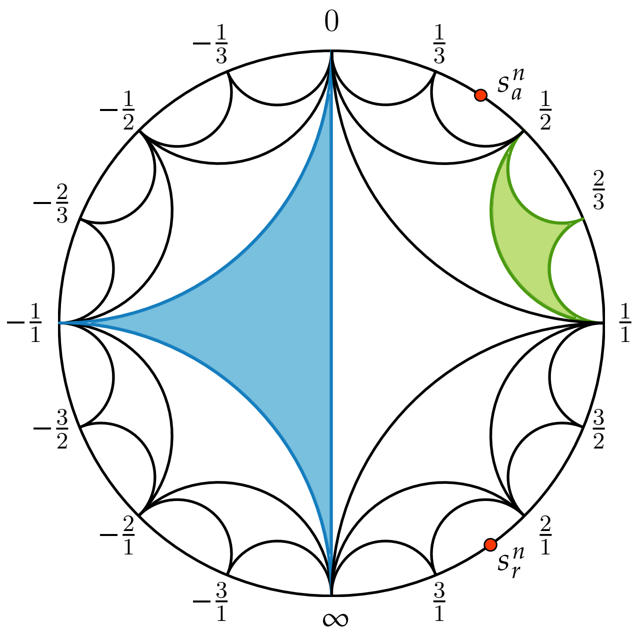

Figure 3.13: The Farey graph together with the slopes of the fixed points (the red dots) and the largest geodesic triangles in P_a (green triangle) and P_c (blue triangle).

Proposition 3.4.12. *Suppose $\Sigma \subset C_n(s)$ and Γ_Σ consists of $k \geq 2$ properly embedded arcs and m closed curves. Then there is an isotopic copy of Σ such that one of the following holds.*

1. *k is odd.*
   - *$m = 1$ and all dividing arcs have slope ∞.*
   - *$m = 0$ and there are three isotopy classes of dividing arcs with slopes $\{0, 1, \infty\}$, $\mathrm{mult}(1) = k - 2$ and $\mathrm{mult}(0) = \mathrm{mult}(\infty) = 1$. Here, $\mathrm{mult}(s)$ is the number of arcs with slope s.*
   - *there is a boundary parallel arc (possibly with other dividing curves).*
2. *k is even, and there is a boundary parallel arc (possibly with other dividing curves).*

Proof. Assume that any isotopic copy of Σ in $C_n(s)$ contains no boundary parallel dividing arcs. By Proposition 3.4.9, this implies that k is odd, since k even would imply the existence of a boundary parallel arc and contradict our assumption. We first calculate the slopes of the fixed points v_a^n and v_r^n of ϕ_n for $n \geq 5$ and obtain

$$s_a^n = \frac{2}{n - 2 + \sqrt{n^2 - 4n}} \quad \text{and} \quad s_r^n = \frac{2}{n - 2 - \sqrt{n^2 - 4n}}.$$

Briefly, to obtain the slopes of the fixed points, we compute the eigenvectors of the matrix ϕ_n and take their slope. Thus $0 < s_a^n < 1/2$ and $2 < s_r^n < \infty$. For any $n \geq 5$, the largest geodesic triangle with the vertices in P_c^n is $\{\infty, -1, 0\}$, and the largest geodesic triangle with the vertices in P_a^n is $\{\frac{1}{2}, \frac{2}{3}, 1\}$ (see Figure 3.13). By Lemma 3.4.10 and 3.4.11, there is an isotopic copy of Σ such that

- Γ_Σ consists of one closed curve and k arcs with slope ∞, or
- Γ_Σ consists of one closed curve and k arcs with slope 1.

We claim that for the second case there is another isotopic copy of Σ such that there is a boundary parallel arc, or there are three isotopy classes of dividing arcs with slopes $\{0, 1, \infty\}$, $\mathrm{mult}(1) = k - 2$ and $\mathrm{mult}(0) = \mathrm{mult}(\infty) = 1$. This claim will compete the proof.

We remain to prove the claim. Let U be a small I-invariant neighborhood of Σ in $C_n(s)$. Then $C_n(s) \setminus U = \Sigma \times [0, 1]$. Let $\Sigma_i := \Sigma \times \{i\}$ for $i = 0, 1$ and Γ_i be a dividing set of Σ_i. Then we have $\Gamma_1 = \Gamma_\Sigma$ and $\Gamma_0 = \phi_n(\Gamma_1)$.

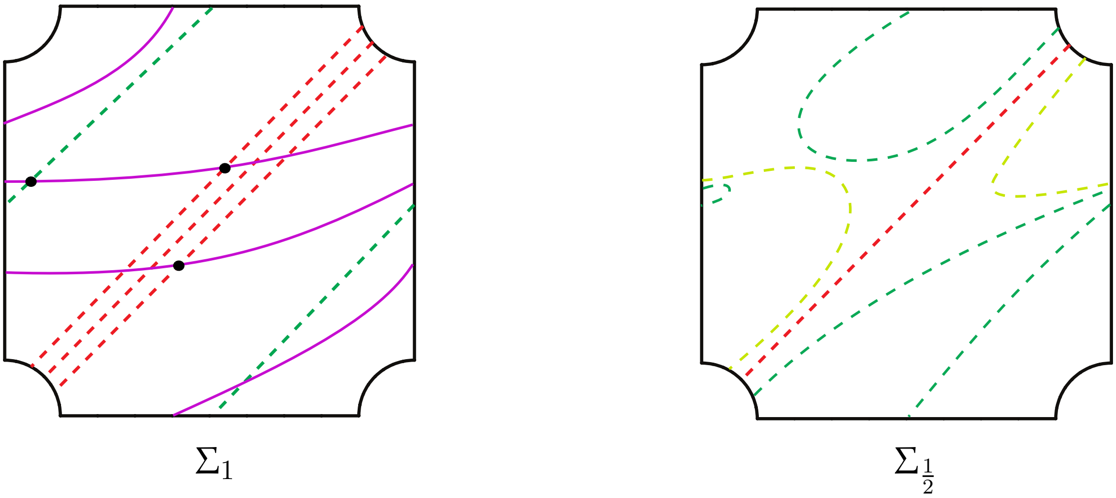

Figure 3.14: An example of a situation where the bypass straddles the closed dividing curve (on the left). The result of the bypass attachment is on the right. The figure refers to the case $n = 6$, and $k = 3$.

We first consider the case $n > 5$. Take a closed curve c on Σ_1 with slope $\frac{1}{n-3}$. Consider an annulus $c \times [0, 1]$ and let $c_i = c \times \{i\}$ for $i = 0, 1$. Assume c_i intersects Γ_i minimally. Then $|c_1 \cap \Gamma_1| = (n - 4)(k + 1)$ and $|c_0 \cap \Gamma_0| = 0$. Thus there is a bypass on A along c_1. If there is a bypass which does not straddle[7] the closed dividing curve, attaching the bypass results in a boundary parallel arc (here, we attach the bypass from the back). If all the available bypasses straddle the closed dividing curve, then there is a bypass attachment that results in the dividing set with slope $\{0, 1, \infty\}$ where $\text{mult}(1) = k - 2$ and $\text{mult}(0) = \text{mult}(\infty) = 1$ (see Figure 3.14).

Now if $n = 5$, take a closed curve c on Σ_1 with slope $\frac{2}{5}$. Consider an annulus $c \times [0, 1]$ and let $c_i = c \times \{i\}$ for $i = 0, 1$. Assume c_i intersects Γ_i minimally. Then $|c_1 \cap \Gamma_1| = 3(k+1)$ and $|c_0 \cap \Gamma_0| = k+1$. Thus there is a bypass on A along c_1. If there is a bypass which does not straddle the closed dividing curve, attaching the bypass results in a boundary parallel arc. If the bypasses straddle the closed dividing curve, one of the bypass attachments results in the dividing set with slope $\{0, 1, \infty\}$ where $\text{mult}(1) = k - 2$ and $\text{mult}(0) = \text{mult}(\infty) = 1$. $\square$

We also consider the case for $k = 1$ without boundary parallel half Giroux torsion.

Proposition 3.4.13. *Suppose there is no boundary parallel half Giroux torsion in $C_n(s)$ and Γ_Σ consists of one properly embedded arc and m closed curves. Then there exists an isotopic copy of Σ in $C_n(s)$ such that the new Γ_Σ consists of*

- *one arc and one closed curve with slope ∞.*
- *one boundary parallel arc without any other dividing curves.*

We will prove this proposition in Section 3.4.4.

[7]We will often use the word *straddle*, adopting the terminology used in [CM20]. A bypass straddles a dividing curve if the dividing curve sits in the middle of the local model of a bypass attachment – see Figure 3.14.

§ 3.4.3 | Thickening $C_n(s)$

Here, we will prove Lemma 3.4.1. We will thicken $C_n(s)$ to $C_n(s')$ by finding a bypass for $-\partial C_n(s)$ along $\partial\Sigma$. Recall that due to our slope conventions, this bypass has slope 0 on $\partial C_n(s)$ and s will change clockwise on the Farey graph.

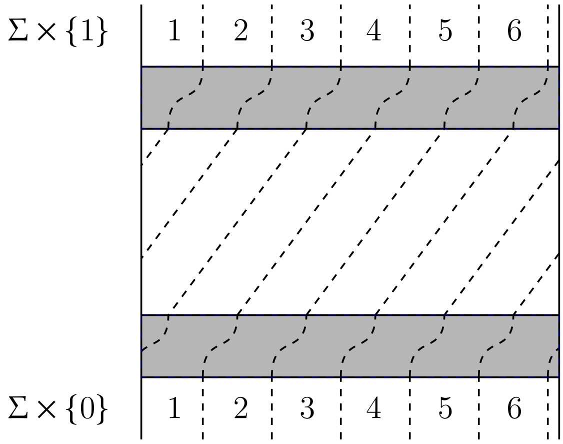

Figure 3.15: Edge rounding when $s = 3$. In this case $m = 3, k = 1$. $\partial\Sigma_i$ is divided into $2\times 3 = 6$ intervals. The left side is identified with the right side. We can see for example that the interval labelled with 5 is connected to the interval labelled with 2, and the interval labelled with 1 is connected to the interval labelled with 4.

Proposition 3.4.14. *Suppose $s \geq 2$ and $s \notin \{\frac{4k+1}{k} \mid k \in \mathbb{N}\}$. Then there is an isotopic copy of Σ in $C_n(s)$ such that Γ_Σ contains a boundary parallel arc.*

Proof. Let $s = \frac{m}{k}$ for a pair of relatively prime positive integers m, k. There are m properly embedded dividing arcs on Σ. We cut $C_n(s)$ along Σ to obtain a genus-2 handlebody $\Sigma\times[0,1]$ and round the edges to obtain a smooth convex boundary. Let Σ_i be $\Sigma\times\{i\}$ for $i = 0, 1$ and Γ_i the dividing set on Σ_i. Then $\Gamma_0 = \phi_n(\Gamma_1)$. After rounding the edges, the entire dividing set only contains closed curves, but we will keep calling the dividing curves that pass through $\partial\Sigma$ dividing arcs for convenience.

For $i = 0, 1$, the dividing arcs in Γ_i divide $\partial\Sigma_i$ into $2m$ intervals, which we will label by 1 through $2m$. The dividing curves on $\partial\Sigma\times[0,1]$ connect the i-th interval on Σ_1 to the $(i-2k-1)$-th interval (mod $2m$) on Σ_0. See Figure 3.15 for an example with $s = \frac{3}{1}$.

Remark 3.4.15. Note that technically speaking the dividing curves connect end of intervals, not the intervals themselves. What we mean here is: in the edge-rounded manifold, if we require curves to only intersect dividing curves on Σ_i and not along the vertical boundary, then they have to stay inside the region determined by the edge-rounding process. Basically, curves will have to twist as the dividing curve twist along $\partial\Sigma\times I$. Thus starting points in the i-th interval on Σ_1 correspond to end points in the $(i-2k-1)$-th interval (mod $2m$) on Σ_0.

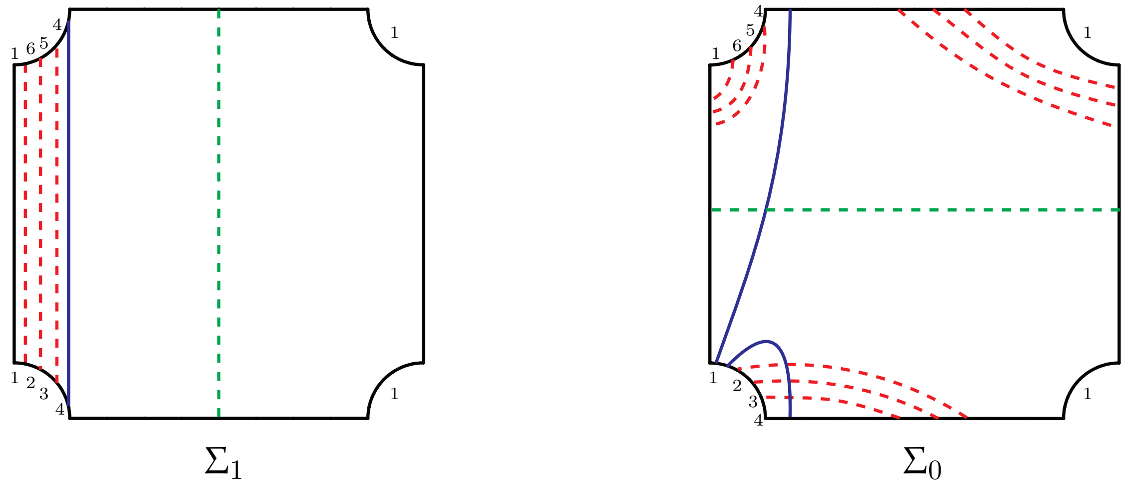

Figure 3.16: Σ_1 and Σ_0 in $C_n(3)$. The dotted lines are dividing curves. The blue lines are $\alpha \times \{1\}$ and $\alpha \times \{0\}$. In each drawing, the top and bottom sides are identified, and so are the left and right sides. In this figure, as well as in the rest of the chapter, we draw Σ_0 with the orientation induced from the fibration $C_n(s)$, which disagrees with that induced by $\Sigma \times [0, 1]$. Also in this picture (and this picture only), we have enumerated the regions of $\partial \Sigma$ to better see the twisting of the dividing set as it runs over $\partial \Sigma \times [0, 1]$. As mentioned, the blue lines witness a shift in their intersection with $\partial\Sigma$ dictated by the shift of the dividing curves.

Suppose there is no boundary parallel dividing arc in Γ_i for $i = 0, 1$. By Proposition 3.4.12 and Proposition 3.4.13, we need to consider two cases.

(1) Γ_1 *contains* m *arcs and one closed curve with slope* ∞: Let α be an arc on Σ_1 with slope ∞ that does not intersect Γ_1. Let $D_\alpha := \alpha \times [0, 1]$ be a compressing disk for $\Sigma \times [0, 1]$. Perturb D_α so that its boundary does not intersect any dividing curve on $\partial\Sigma \times [0, 1]$. This results in a shift of the basepoints of α on Σ_0 by $(2k + 1)$ intervals following the negative orientation of $\partial\Sigma$, see Figure 3.16 for example. Thus ∂D_α only intersects the dividing curves on Σ_0. We perturb D_α further so that it is convex with Legendrian boundary. We can also assume that ∂D_α intersects Γ_0 minimally, so it will intersect the closed dividing curve exactly once. Also, this intersection point separates $\alpha \times \{0\}$ into two sides. On one side it intersects $|2k + 1|$ dividing arcs, and on the other side it intersects $|m - (2k + 1)|$ dividing arcs. Since the total number of intersection points is greater than 2, there is a bypass in D_α by Theorem 3.2.5. The difference between the number of intersections is:

$$d = ||m - 2k - 1| - |2k + 1|| = \begin{cases} |m - 4k - 2| & m \geq 2k + 1 \\ |m| & m < 2k + 1 \end{cases}$$

If $d \neq 1$, then the dividing curves on D_α cannot be nested (as shown in the right drawing of Figure 3.17). This is not hard to prove. Draw a vertical line that divides the disk in two halves and passes through the intersection point (the green dot in Figure 3.17), creating the two sides of $\alpha \times \{0\}$. If $d \neq 1$ we can assume without loss of generality that the right hand side of the disk has at least two more red points than the left hand side. The extra pair of red points forces at least one dividing curve to be contained entirely in the right hand side (after isotopy if necessary). This implies we cannot have a completely nested dividing set: in that case all dividing curves would be forced to intersect the vertical line in the middle of the disk (see left side of Figure 3.17). Thus there is always a bypass which does not straddle the closed dividing curve.

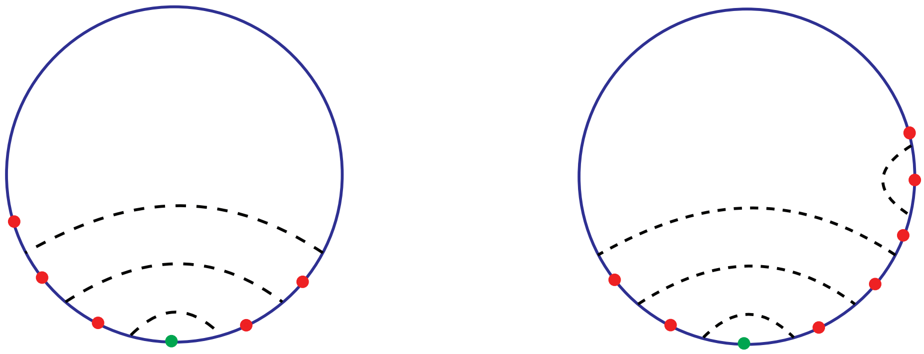

Figure 3.17: Dividing curves in D_α. The green dot is the intersection point of $\alpha \times \{0\}$ with the closed dividing curve on Σ_0 and the red dots are the intersections of $\alpha \times \{0\}$ with the dividing arcs on Σ_0.

After attaching this bypass, we obtain an isotopic copy of Σ containing a boundary parallel dividing arc. Notice that the bypass abuts Σ_0, since D_α only intersects dividing curves on Σ_0.

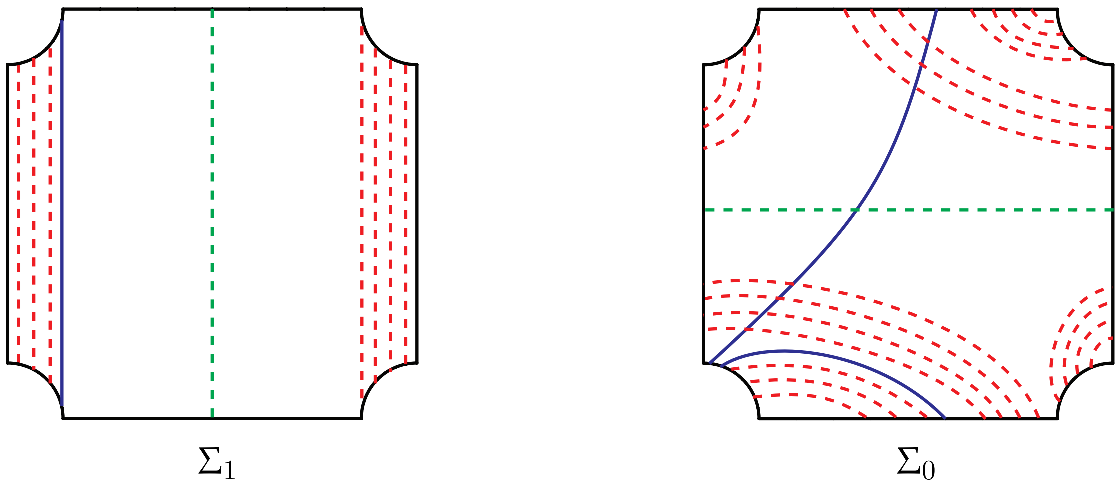

Figure 3.18: Σ_1 and Σ_0 in $C_n(7)$. The dotted lines are dividing curves and the blue lines are $\alpha \times \{1\}$ and $\alpha \times \{0\}$.

If $d = 1$, then $m = 1$, $m = 4k + 1$ or $m = 4k + 3$. Since we assume $s \geq 2$ and $s \neq \frac{4k+1}{k}$, we only need to consider the case $m = 4k + 3$. In this case, there are $2k + 2$ dividing curves on D_α and they can be nested as shown in the left drawing of Figure 3.17 in combination with Figure 3.18. Attach all $2k + 1$ bypasses to Σ_0 in sequence to obtain $\Sigma_{1/2}$ with dividing slopes $\{\infty, -1, 0\}$ such that $\text{mult}(\infty) = m - 2$

and $\mathrm{mult}(-1) = \mathrm{mult}(0) = 1$, see the right drawing of Figure 3.19. Then we can find an overtwisted disk as shown in Figure 3.19. Thus we can exclude this case too.

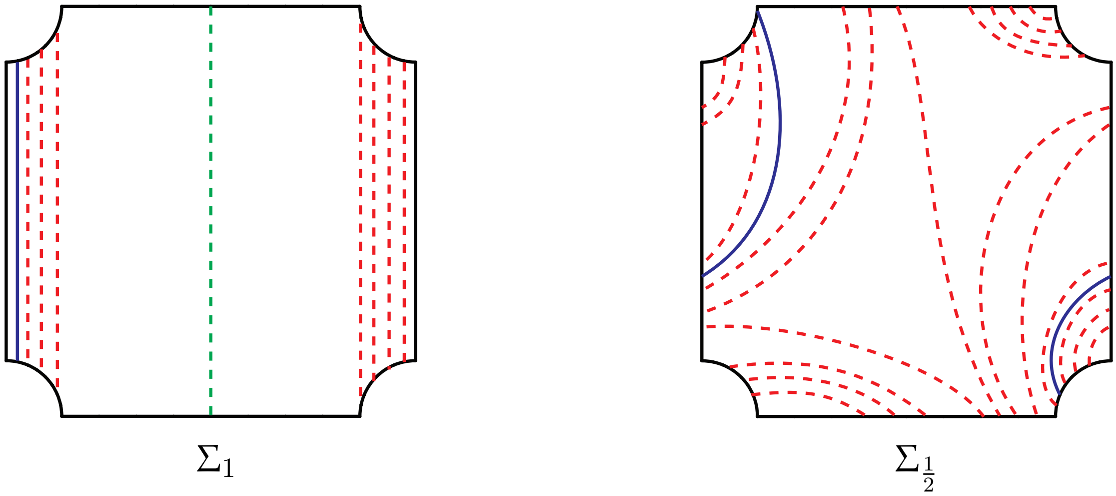

Figure 3.19: Σ_1 and $\Sigma_{\frac{1}{2}}$ in $C_n(7)$. The dotted lines are dividing curves and the blue lines are the intersections between an overtwisted disk and $\Sigma \times \{\frac{1}{2}, 1\}$. Note we can conclude the disk is overtwisted because the boundary does not intersect any dividing curve.

(2) *$m \geq 3$ and Γ_1 contains arcs with slope $\{0, 1, \infty\}$ where* $\mathrm{mult}(0) = \mathrm{mult}(\infty) = 1$ *and* $\mathrm{mult}(1) = m - 2$: Let β be an arc on Σ_1 with slope ∞ that does not intersect Γ_1, and $D_\beta := \beta \times [0, 1]$ be a compressing in $\Sigma \times [0, 1]$. We perturb D_β so that it is convex with Legendrian boundary, ∂D_β does not intersect the dividing curves on $\partial \Sigma \times [0, 1]$, and $\beta \times \{0\}$ intersects Γ_0 minimally, see Figure 3.20.

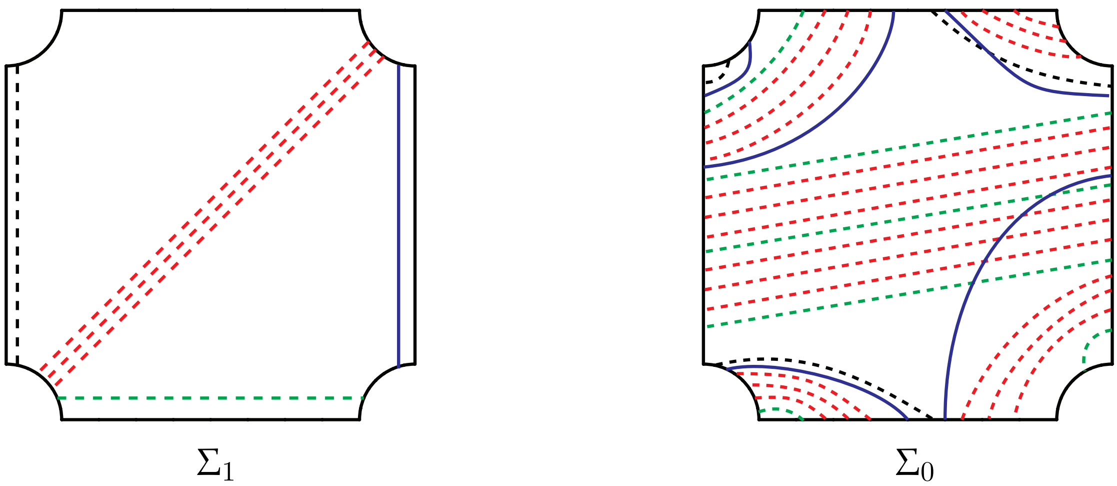

Figure 3.20: Σ_1 and Σ_0 in $C_n(\frac{5}{2})$. The dotted lines are dividing curves and the blue lines are $\alpha \times \{1\}$ and $\alpha \times \{0\}$.

Since $\beta \times \{0\}$ intersects more than four dividing curves in Γ_0, we can find a bypass in D_β whose attaching arc lies on $\beta \times \{0\}$ by Theorem 3.2.5. From now on, we call dividing curves on Σ_0 with slopes 0, $\frac{1}{n-2}$ and $\frac{1}{n-3}$ black, red and green dividing curves, respectively, see the right drawing of Figure 3.20. There are two cases we need to consider.

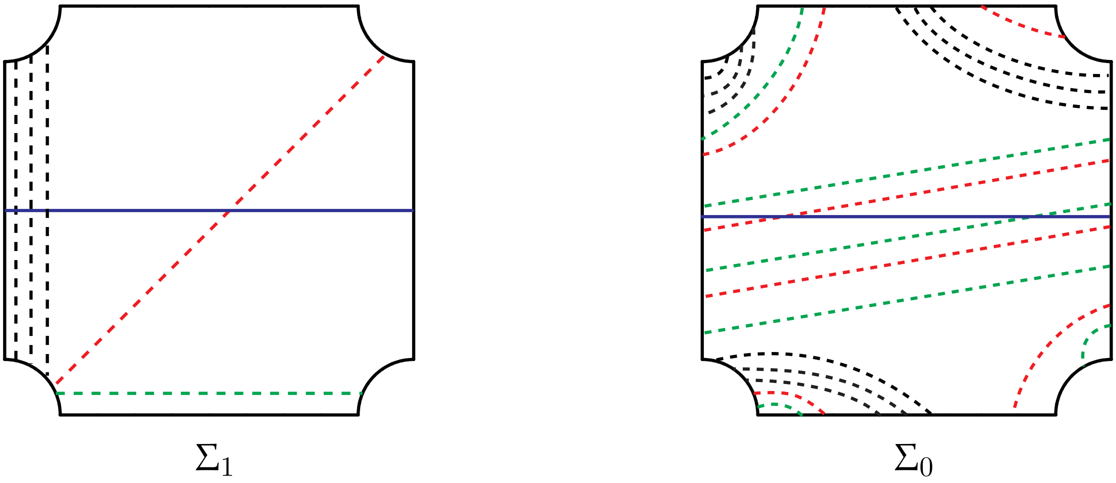

Figure 3.21: Σ_1 and Σ_0 in $C_n(\frac{5}{2})$. The dotted lines are dividing curves and the blue lines are $\gamma \times \{1\}$ and $\gamma \times \{0\}$.

First, suppose $m > 3$. Since $s \geq 2$, we can assume that $m > 2k-1$. In this case, the bypass cannot straddle the black dividing curve, see the right drawing of Figure 3.20. More precisely, there is no bypass passing through green, black, green dividing curves in order. Therefore, the only bypass that does not produce a boundary parallel arc is the one that straddles the green dividing curve. If the bypass straddles the green dividing curve, then attaching the bypass results in $\Sigma_{1/2}$ with $\Gamma_{1/2} = \{0, \frac{1}{n-2}, \frac{1}{n-3}\}$ where $\mathrm{mult}(0) = 3$, $\mathrm{mult}(\frac{1}{n-3}) = m-4$ and $\mathrm{mult}(\frac{1}{n-2}) = 1$. We can convert $\Gamma_{1/2}$ into $\{0, 1, \infty\}$ by acting on $\Sigma_{1/2}$ via ϕ_n^{-1}. Now we cut $C_n(s)$ along $\Sigma_{1/2}$ and obtain $\Sigma \times [0,1]$ again. We relable $\Sigma \times \{i\}$ as Σ_i for $i = \{0,1\}$. Then $\Gamma_1 = \{0, 1, \infty\}$ with $\mathrm{mult}(0) = 1$, $\mathrm{mult}(1) = m-4$, $\mathrm{mult}(\infty) = 3$. Take a closed curve γ with slope 0 and let $A_\gamma := \gamma \times [0,1]$ be a properly embedded annulus in $\Sigma \times [0,1]$. We perturb A_γ so that it is convex with Legendrian boundary and intersects $\Gamma_0 \cup \Gamma_1$ minimally, see Figure 3.21. Since $|\gamma \times \{1\} \cap \Gamma_1| = m-1$ and $|\gamma \times \{0\} \cap \Gamma_0| = m-3$, we can find a bypass whose attaching arc lies on Σ_1 by Theorem 3.2.4. Notice that we attach this bypass from the back. It is easy to check that any possible bypass attachment results in an isotopic copy of Σ that contains a boundary parallel dividing arc.

Now suppose $m = 3$. Since we assume $s \geq 2$, the only possible value of k is 1. In this case, there are exactly two possible bypass attachments on Σ_0 and both result in an isotopic copy of Σ containing boundary parallel dividing arc (see Figure 3.22). □

Now we consider the case $s < 0$.

Proposition 3.4.16. *Suppose $s < 0$. Then there is an isotopic copy of Σ in $C_n(s)$ such that Γ_Σ contains a boundary parallel arc.*

Proof. Let $s = -\frac{m}{k}$ for a pair of relatively prime positive integers m, k. Then there are m properly embedded dividing arcs on Σ. We cut $C_n(s)$ along Σ to obtain a genus-2

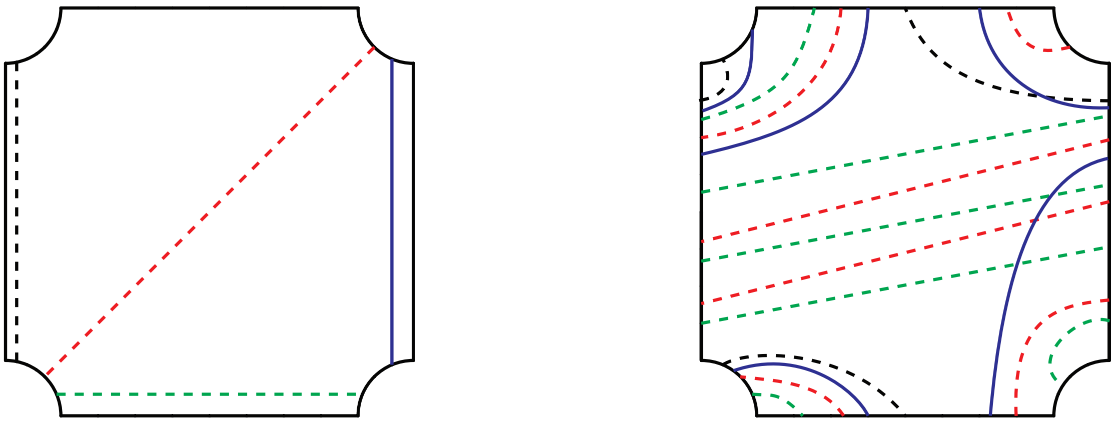

Σ_1 Σ_0

Figure 3.22: Σ_1 and Σ_0 in $C_n(3)$. The dotted lines are dividing curves and the blue lines are $\alpha \times \{1\}$ and $\alpha \times \{0\}$.

handlebody $\Sigma \times [0,1]$ and round edges to obtain a smooth convex boundary. Let Σ_i be $\Sigma \times \{i\}$ for $i = 0, 1$ and Γ_i the dividing set on Σ_i. Then $\Gamma_0 = \phi_n(\Gamma_1)$. After rounding the edges, the entire dividing set only contains closed curves, but we will keep calling the dividing curves that pass through $\partial \Sigma$ dividing arcs for convenience.

As in Proposition 3.4.14, the dividing arcs in Γ_i divide $\partial \Sigma_i$ into $2m$ intervals for $i = 0, 1$. The dividing curves on $\partial\Sigma \times [0, 1]$ connect the i-th interval on Σ_1 to the $(i + 2k - 1)$-th interval (mod $2m$) on Σ_0.

Suppose there is no boundary parallel dividing arc in Γ_i for $i = 0, 1$. By Proposition 3.4.12 and Proposition 3.4.13, we need to consider three cases.

(1) *$m > 1$ and Γ_1 contains m arcs and one closed curve with slope ∞*: As in Proposition 3.4.14, let α be an arc on Σ_1 with slope ∞ that does not intersect Γ_1. Let $D_\alpha := \alpha \times [0, 1]$ be a compressing disk for $\Sigma \times [0, 1]$. Perturb D_α so that its boundary does not intersect any dividing curve on $\partial\Sigma \times [0, 1]$. This results in a shift of the basepoints of α on Σ_0 by $(2k - 1)$ intervals following the positive orientation of $\partial\Sigma$. Thus ∂D_α only intersects the dividing curves in Γ_0. We perturb D_α further so that it is convex with Legendrian boundary. We can also assume that ∂D_α intersects Γ_0 minimally, so it will intersect the closed dividing curve exactly once. Also, this intersection point separates $\alpha \times \{0\}$ into two sides. On one side it intersects $|2k - 1|$ dividing arcs, and on the other side it intersects $|m + (2k - 1)|$ dividing arcs. Since the total number of intersection points is greater than 2, there is a bypass in D_α by Theorem 3.2.5. The difference between the number of intersections is:

$$d = |(m + 2k - 1) - (2k - 1)| = |m|.$$

Since we assume $m > 1$, we have $d \neq 1$ and the dividing curves in D_β cannot be nested as shown in the right drawing of Figure 3.17. This implies that there is always a bypass which does not straddle the closed dividing curve. After attaching this bypass, we obtain an isotopic copy of Σ containing a boundary parallel dividing arc.

(2) *$m \geq 3$ and Γ_1 contains arcs with slope $\{0, 1, \infty\}$ where* $\text{mult}(0) = \text{mult}(\infty) = 1$ *and* $\text{mult}(1) = m-2$: Let β be an arc on Σ_1 with slopes ∞ that does not intersects Γ_1 and $D_\beta := \beta \times [0,1]$ a compressing disk in $\Sigma \times [0,1]$. We perturb D_β so that it is convex with Legendrian boundary and does not intersect dividing curves on $\partial\Sigma \times [0,1]$. Since $\beta \times \{0\}$ intersects more than four dividing curves on Γ_0, we can find a bypass in D_β whose attaching arc lies on $\beta \times \{0\}$ by Theorem 3.2.5. Notice that there is no bypass passing through green, black, green dividing curves in order. Therefore, the only bypass that does not produce a boundary parallel arc is the one that straddles the green dividing curve.

Suppose $m > 3$. If the bypass straddles the green dividing curve, then attaching the bypass results in $\Sigma_{1/2}$ with $\Gamma_{1/2} = \{0, \frac{1}{n-2}, \frac{1}{n-3}\}$ where $\text{mult}(0) = 3$, $\text{mult}(\frac{1}{n-3}) = m-4$ and $\text{mult}(\frac{1}{n-2}) = 1$. We can convert $\Gamma_{1/2}$ into $\{0, 1, \infty\}$ by acting on $\Sigma_{1/2}$ via ϕ_n^{-1}. Now we cut $C_n(s)$ along $\Sigma_{1/2}$ and obtain $\Sigma \times [0,1]$ again. We relable $\Sigma \times \{i\}$ as Σ_i for $i = \{0, 1\}$. Then $\Gamma_1 = \{0, 1, \infty\}$ with $\text{mult}(0) = 1$, $\text{mult}(1) = m-4$, $\text{mult}(\infty) = 3$. Take a closed curve γ with slope 0 and let $A_\gamma := \gamma \times [0,1]$ be a properly embedded annulus in $\Sigma \times [0,1]$. We perturb A_γ so that it is convex with Legendrian boundary and intersects $\Gamma_0 \cup \Gamma_1$ minimally, see Figure 3.21. Since $|\gamma \times \{1\} \cap \Gamma_1| = m-1$ and $|\gamma \times \{0\} \cap \Gamma_0| = m-3$, we can find a bypass whose attaching arc lies on Σ_1 by Theorem 3.2.4. Notice that we attach this bypass from the back. It is easy to check that any possible bypass attachment results in an isotopic copy of Σ that contains a boundary parallel dividing arc.

Now suppose $m = 3$. If the bypass straddles the green dividing curve, attaching the bypass results in an isotopic copy of Σ containing one closed dividing curve and three dividing arcs with slope 0. We can covert this into the dividing set containing one closed curve and three arcs with slope ∞ by acting on Σ via ϕ_n^{-1}. We already dealt with this in Case (1).

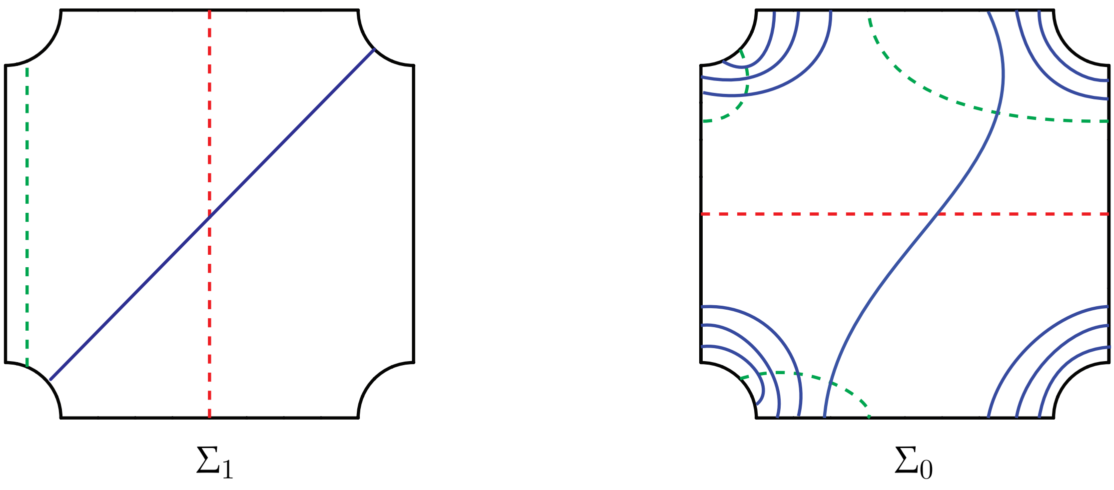

Figure 3.23: Σ_1 and Σ_0 in $C_n(-\frac{1}{2})$. The dotted lines are dividing curves and the blue lines are $\alpha \times \{1\}$ and $\alpha \times \{0\}$.

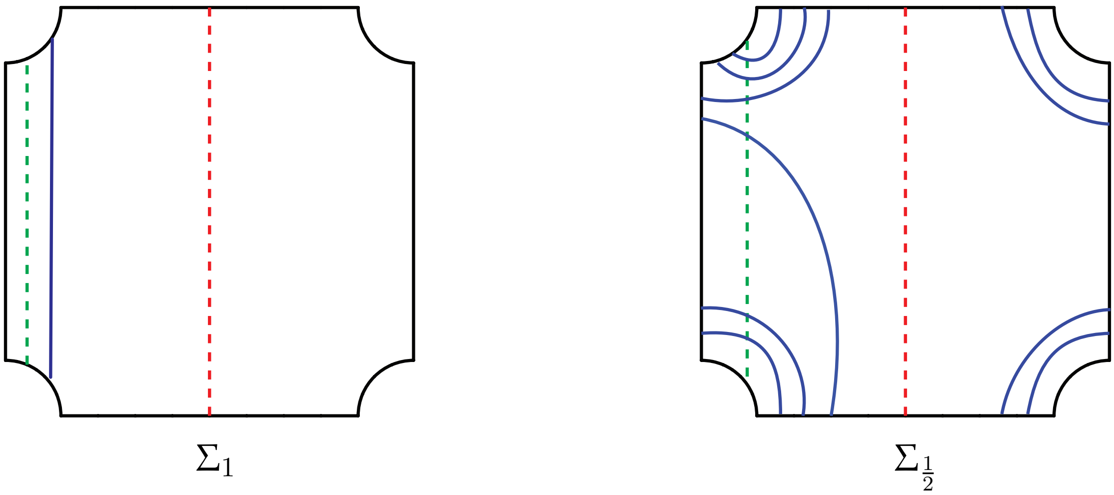

Figure 3.24: Σ_1 and $\Sigma_{\frac{1}{2}}$ in $C_n(-\frac{1}{2})$. The dotted lines are dividing curves and the blue lines are $\alpha \times \{1\}$ and $\alpha \times \{\frac{1}{2}\}$.

(3) $m = 1$ *and there is one closed curve and one arc with slope* ∞: First, suppose $k > 1$. Then take an arc on Σ with slope 1 and let D_α be a disk in $\Sigma \times [0, 1]$ as shown in Figure 3.23. The number of intersection between D_α and $\Gamma_0 \cup \Gamma_1$ is $4k + 2$, so we can find a bypass in D_α by Theorem 3.2.5. If the bypass does not straddle the closed dividing curve, then attaching the bypass results in a boundary parallel dividing arc. If the bypass straddles the closed dividing curve, then attaching the bypass results in $\Sigma_{1/2}$ with the dividing set identical to Γ_1, see Figure 3.24. Now take an arc β with slope ∞ and let D_β be a compressing disk for $\Sigma \times [\frac{1}{2}, 1]$ as shown in Figure 3.24. Since the number of intersection between D_β and $\Gamma_{1/2} \cup \Gamma_1$ is $4k - 2$ and $k > 1$, we can find a bypass in D_β. Here, any possible bypass does not straddle the closed dividing curve, so attaching the bypass will result in a boundary parallel dividing arc.

Now suppose $k = 1$. Take an arc on Σ with slope ∞ and let $D_\alpha = \alpha \times [0, 1]$ be a disk as shown in Figure 3.25.

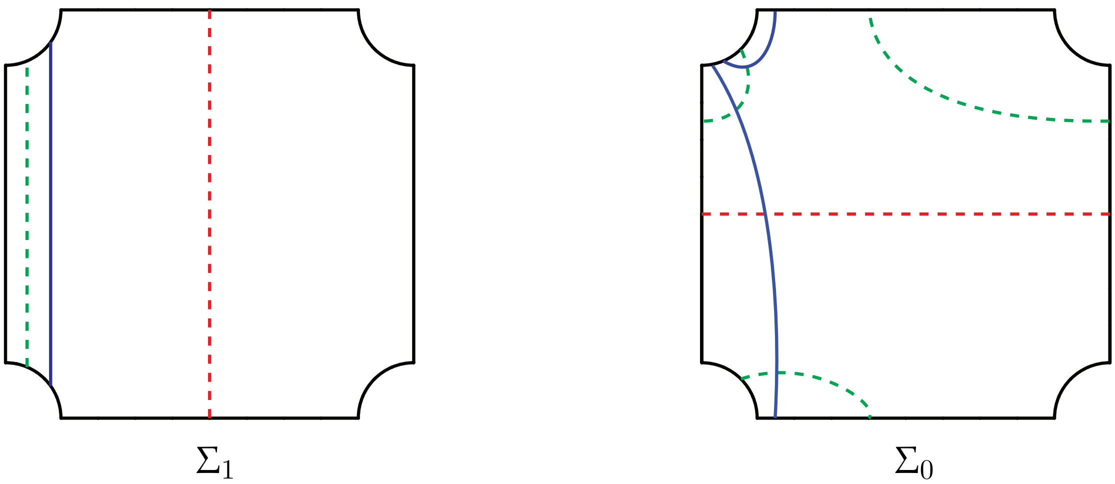

Figure 3.25: Σ_1 and Σ_0 in $C_n(-1)$. The dotted lines are dividing curves and the blue lines are $\alpha \times \{1\}$ and $\alpha \times \{0\}$.

We call the closed dividing curve and the dividing arc on Σ_0 red and green dividing curves, respectively. Since the number of intersections between D_β and $\Gamma_0 \cup \Gamma_1$ is 4, there are two possible dividing sets for D_β. These two dividing sets provide two different bypasses. One bypass passes through red, green, green dividing curves in order. Attaching this bypass results in a boundary parallel dividing arc. The attaching arc of the other bypass does not lie on Σ_0. The attaching arc only passes through two dividing curves on Σ_0, see the top left drawing of Figure 3.26. By Theorem 3.2.6, we can rotate this bypass and obtain a new bypass such that its attaching arc lies on Σ_0, see the top right drawing of Figure 3.26. Attaching this bypass results in a boundary parallel dividing arc. □

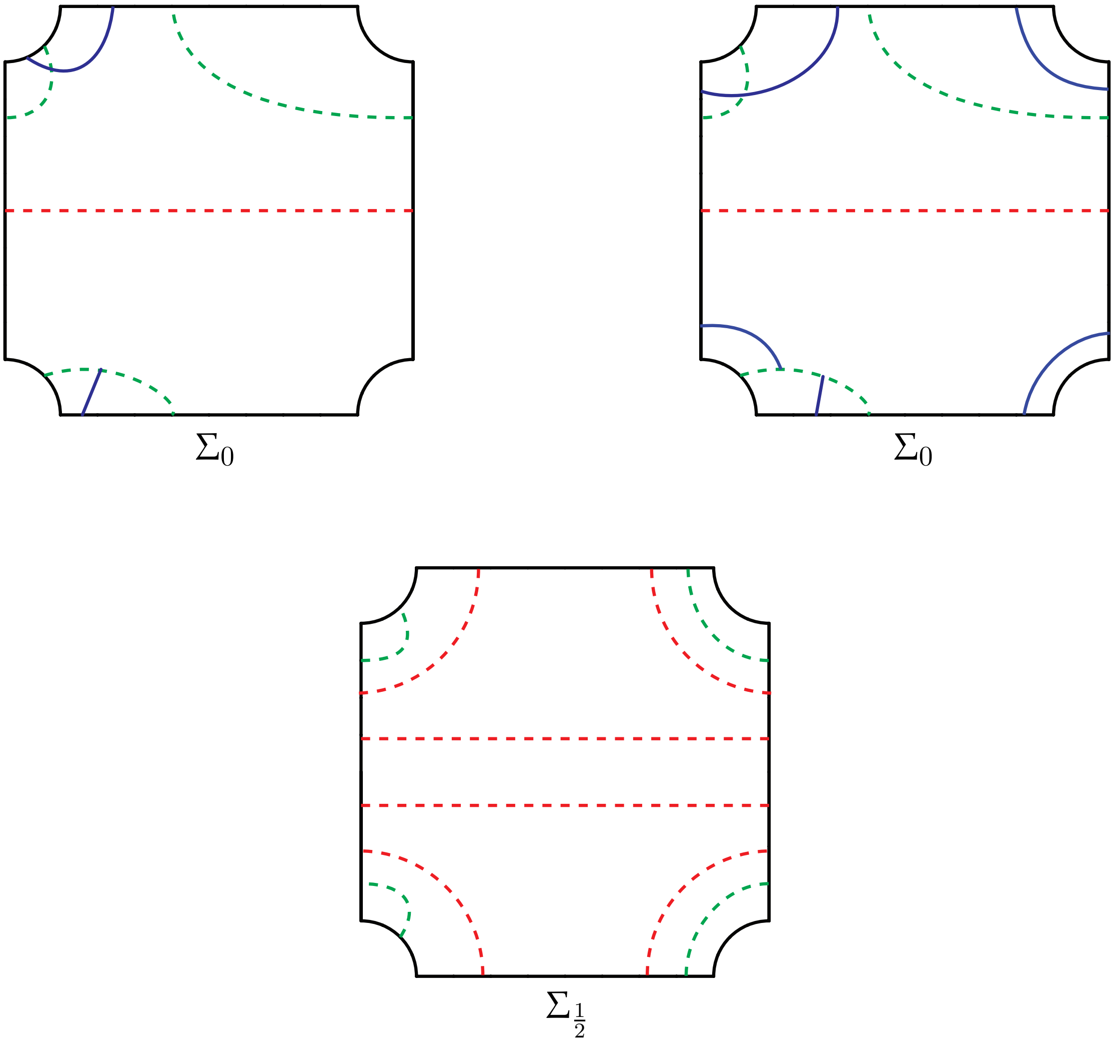

Figure 3.26: Top left: Σ_0 in $C_n(-1)$, before the bypass rotation. Top right: Σ_0 in $C_n(-1)$, after the bypass rotation. Bottom: $\Sigma_{\frac{1}{2}}$ in $C_n(-1)$, the result of the bypass attachment from the top right. The dotted lines are dividing curves and the blue lines are the attaching arcs of bypasses.

§ 3.4.4 | Analyzing tight contact structures on $C_n(\frac{1}{k})$ for $k \leq 0$

In this subsection, we will prove Lemma 3.4.1, Lemma 3.4.2, 3.4.4 and 3.4.5. To do so, we need to prove Proposition 3.4.13 first.

Proof of Proposition 3.4.13. Since there is only one dividing arc, we know $s = \frac{1}{k}$ for $k \in \mathbb{Z}$ (we consider $\infty = \frac{1}{0}$). We cut $C_n(s)$ along Σ to obtain a genus-2 handlebody $\Sigma\times[0,1]$. Let Σ_i be $\Sigma\times\{i\}$ for $i = 0, 1$ and Γ_i the dividing set on Σ_i. Then $\Gamma_0 = \phi_n(\Gamma_1)$. For $i = 0, 1$, the dividing arcs in Γ_i divide $\partial\Sigma_i$ into two intervals, which we will label by 1 and 2. The dividing curves on $\partial\Sigma \times [0, 1]$ connect the i-th interval on Σ_1 to the $(i - 2k - 1)$-th interval (mod 2) on Σ_0. Notice that $i - 2k - 1 \equiv i + 1 \pmod 2$. By Proposition 3.4.9, we need to consider two cases.

(1) Γ_1 *consists of one closed curve and one arc with slope* r: Recall from Proposition 3.4.12 that we calculated the slopes s_a^n and s_r^n of fixed points of ϕ_n and showed

$$0 < s_a^n < 1/2 \text{ and } 2 < s_r^n < \infty.$$

Before we cut $C_n(s)$ along Σ, we can change Γ by acting on Σ via $(\phi_n)^m$ for $m \in \mathbb{Z}$. Since $\phi_n(\infty) = 0$, we can assume r satisfies either

(a) $-\infty < r \leq 0$, or

(b) $s_a^n < r < 1 < s_r^n$.

For the case (a), we know $0 < \phi_n(r) < s_a^n$ since $\phi_n(\infty) = 0 < \phi_n(r)$ and s_n^a is the slope of the attracting fixed point. Assume r is not already 0. Let c be a closed curve on Σ with dividing slope $\phi_n(r)$ and $A_c := c \times [0, 1]$ be a properly embedded annulus in $\Sigma\times[0, 1]$. We perturb A_c so that it is convex with Legendrian boundary and intersects $\Gamma_0 \cup \Gamma_1$ minimally. Since $|c \times \{1\} \cap \Gamma_1| > 0$ and $|c \times \{0\} \cap \Gamma_0| = 0$, we can find a bypass whose attaching arc lies on Σ_1 by Theorem 3.2.4. We attach this bypass and keep track of dividing curves using Theorem 3.2.2. However, we should be careful according to Remark 3.2.3. First, we use the ordinary slope convention $\frac{q}{p} = \binom{p}{q}$ for Σ, so we should reverse the words "clockwise" and "anticlockwise". Also, since the bypass is attached from the back, we should reverse the words "clockwise" and "anticlockwise" again. Therefore, the slope of the dividing curves changes in a clockwise direction in the Farey graph. To summarize, attaching the bypass results in an isotopic copy of Σ with dividing slope r' that is clockwise of r, anticlockwise of $\phi_n(r)$ and closest to $\phi_n(r)$ with an edge to r. Simply, $r < r'$. We cut $C_n(s)$ again along this Σ and apply the same argument again. Repeat this procedure and we obtain an isotopic copy of Σ with slope 0 in the long run. By acting on Σ via ϕ_n^{-1}, we obtain Σ with dividing slope $\infty = \phi_n^{-1}(0)$.

Now consider the case (b). In this case, we know $0 < \phi_n(r) < r < 1$ since $\phi_n(r)$ is closer to s_a^n, the slope of the attracting fixed point of ϕ_n. Notice that the path in the Farey graph clockwise of r and anticlockwise of $\phi_n(r)$ contains 1 and ∞. Let c

be a closed curve on Σ with dividing slope $\phi_n(r)$ and $A_c := c \times [0,1]$ be a properly embedded annulus in $\Sigma \times [0,1]$. By the same argument in the case (a), we can find a bypass whose attaching arc lies on Σ_1. Again, according to Remark 3.2.3 this bypass changes the slope of the dividingcurves in a clockwise direction in the Farey graph. To summarize, attaching the bypass results in an isotopic copy of Σ with dividing slope r' that is clockwise of r, anticlockwise of $\phi_n(r)$ and closest to $\phi_n(r)$ with an edge to r. We cut $C_n(s)$ again along this Σ and apply the same argument again. Since the path in the Farey graph clockwise of r and anticlockwise of $\phi_n(r)$ contains 1, we can obtain an isotopic copy of Σ with dividing slope 1 by repeating this procedure. It is still true that $s_a^n < 1 < s_r^n$, so we can apply the same argument (attaching the bypass to Σ_1) again. Since 1 and ∞ are connected by an edge in the Farey graph, we obtain Σ with dividing slope ∞.

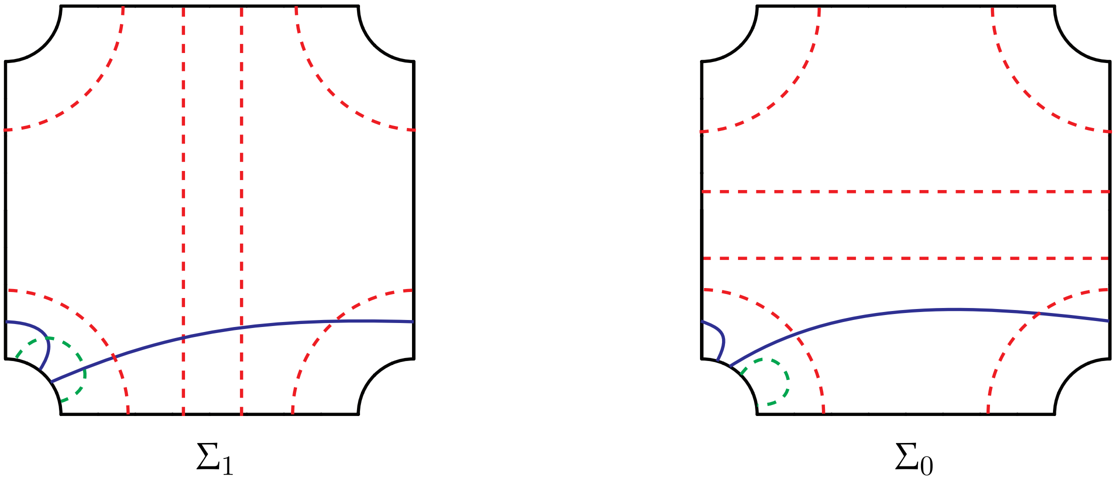

Figure 3.27: Σ_1 and Σ_0 in $C_n(\infty)$. The dotted lines are dividing curves and the blue lines are $\alpha \times \{1\}$ and $\alpha \times \{0\}$.

(2) Γ_1 *contains a boundary parallel arc*: In this case, Γ_1 may contain j boundary parallel closed curves and h essential closed curves, see Figure 3.27 for example, and we need to get rid of them. Observe that h is even. Let r be the slope of the essential dividing curves and α be an arc on Σ_1 with slope $\phi(r)$ that intersects the dividing arc twice, the closed boundary parallel dividing curves $2j$ times, and the essential closed curves $h|\phi(r) \bullet r|$ times, see the left drawing of Figure 3.27 for example. Observe that $|\phi(r) \bullet r| \geq 1$ since ϕ is pseudo-Anosov. Let $D_\alpha := \alpha \times [0,1]$ be a compressing disk for $\Sigma \times [0,1]$. Perturb D_α so that its boundary does not intersect any dividing curve on $\partial\Sigma \times [0,1]$. This results in a shift of the basepoints of α on Σ_0 by $(2k+1)$ intervals following the positive orientation of $\partial\Sigma$. We perturb D_α further so that it is convex with Legendrian boundary and $\alpha \times \{0\}$ intersects boundary parallel closed dividing curves $2j$ times as shown in the right drawing of Figure 3.27. To summarize, $\alpha \times \{1\}$ intersects at least $(2j+h+2)$ dividing curves and $\alpha \times \{0\}$ intersects exactly $2j$ dividing curves. If $h \geq 2$, then we have $|\Gamma_1 \cap D_\alpha| - |\Gamma_0 \cap D_\alpha| \geq 4$, so we can find a bypass in D_α of which the attaching arc lies in $\alpha \times \{1\}$, see the right drawing of Figure 3.28

for example. By attaching this bypass, we obtain an isotopic copy of Σ with 2 fewer dividing curves than the original one. We cut $C_n(s)$ along this new Σ and repeat this procedure until h becomes 0.

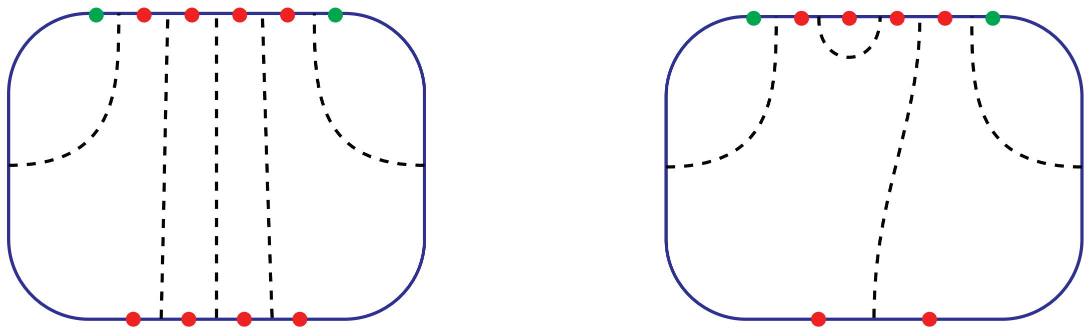

Figure 3.28: Dividing curves in D_α. Top sides: $\alpha \times \{1\}$. Bottom sides: $\alpha \times \{0\}$.

Now we can assume $h = 0$ and $j > 0$. Here, we assume $s = \infty$. For other $s = \frac{1}{k}$, we attach a minimally twisting contact structure on $T = T^2 \times [0, 1]$ with dividing slopes ∞ and $\frac{1}{k}$ to $C_n(\frac{1}{k})$ and obtain $C_n(\infty)$. Then remove T at the end of the proof. Also, fix a sign of the bypass on Σ_1 to be negative. The argument will be the same for the positive case. Now we have

$$|\Gamma_1 \cap D_\alpha| - |\Gamma_0 \cap D_\alpha| = (2j + h + 2) - 2j = 2,$$

so there is a dividing set on D_α that does not provide a bypass of which the attaching arc lies in $\alpha \times \{1\}$ as shown in the left drawing of Figure 3.28. Observe that all other dividing sets on D_α (up to isotopy) will give a bypass of which the attaching arc lies in $\alpha \times \{1\}$. Now take an arc β on Σ_1 such that $\Sigma \setminus (\alpha \cup \beta)$ is a disk and β intersects Γ_1 $(2j + 2)$ times, see the left drawing of Figure 3.29 for example ($j = 2$).

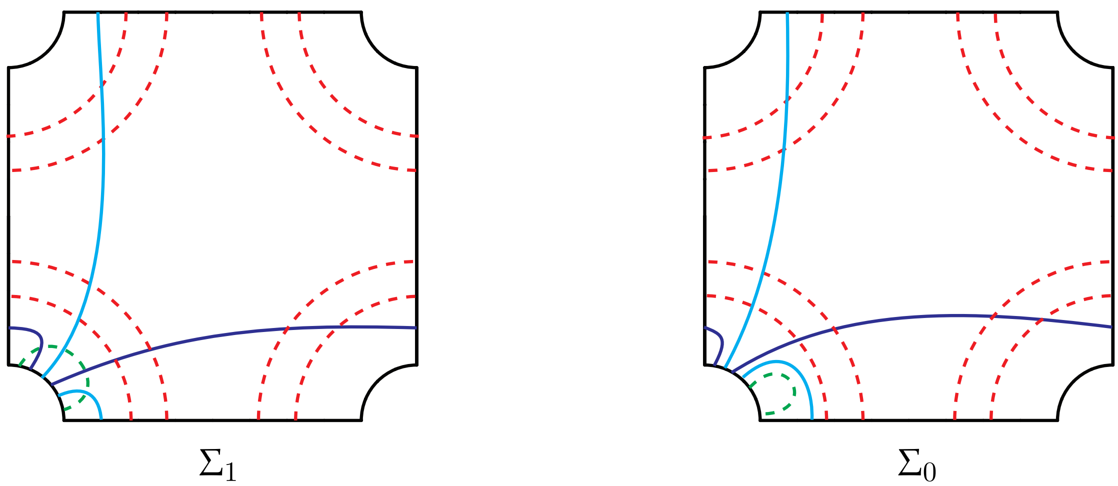

Figure 3.29: Σ_1 and Σ_0 in $C_n(\infty)$. The dotted lines are dividing curves, the blue lines are $\alpha \times \{1\}$ and $\alpha \times \{0\}$, and the sky blue lines are $\beta \times \{1\}$ and $\beta \times \{0\}$.

Let $D_\beta := \beta \times [0, 1]$ be a compressing disk for $\Sigma \times [0, 1]$. If we cut $\Sigma \times [0, 1]$ along D_α

and D_β and round the edges, then we obtain a 3-ball B^3 with convex boundary. Since there is a unique tight contact structure on a 3-ball with a fixed characteristic foliation, tight contact structures on $\Sigma\times[0,1]$ are completely determined by the dividing sets on D_α and D_β. As discussed above, all dividing sets on D_α (*resp.* D_β) contain a bypass of which the attaching arc lies in $\alpha\times\{1\}$ (*resp.* $\beta\times\{1\}$) except for the one shown in the left drawing of Figure 3.28. Therefore, in every tight contact structure on $\Sigma\times[0,1]$, except for (possibly) one, there is a bypass for Σ_1 of which the attaching arc lies in $\alpha\times\{1\}$ or $\beta\times\{1\}$. As we observed above, attaching this bypass reduces the number of dividing curves. Denote the contact structure that might not contain such a bypass by ξ. By the Thurston–Bennequin inequality for convex surfaces [Gir01], there is no bypass that decreases the number of dividing curves in an I-invariant neighborhood of a convex surface. Since the dividing curves on $\partial\Sigma\times[0,1]$ are vertical, the contact structure ξ should be contactomorphic to an I-invariant neighborhood of Σ_1.

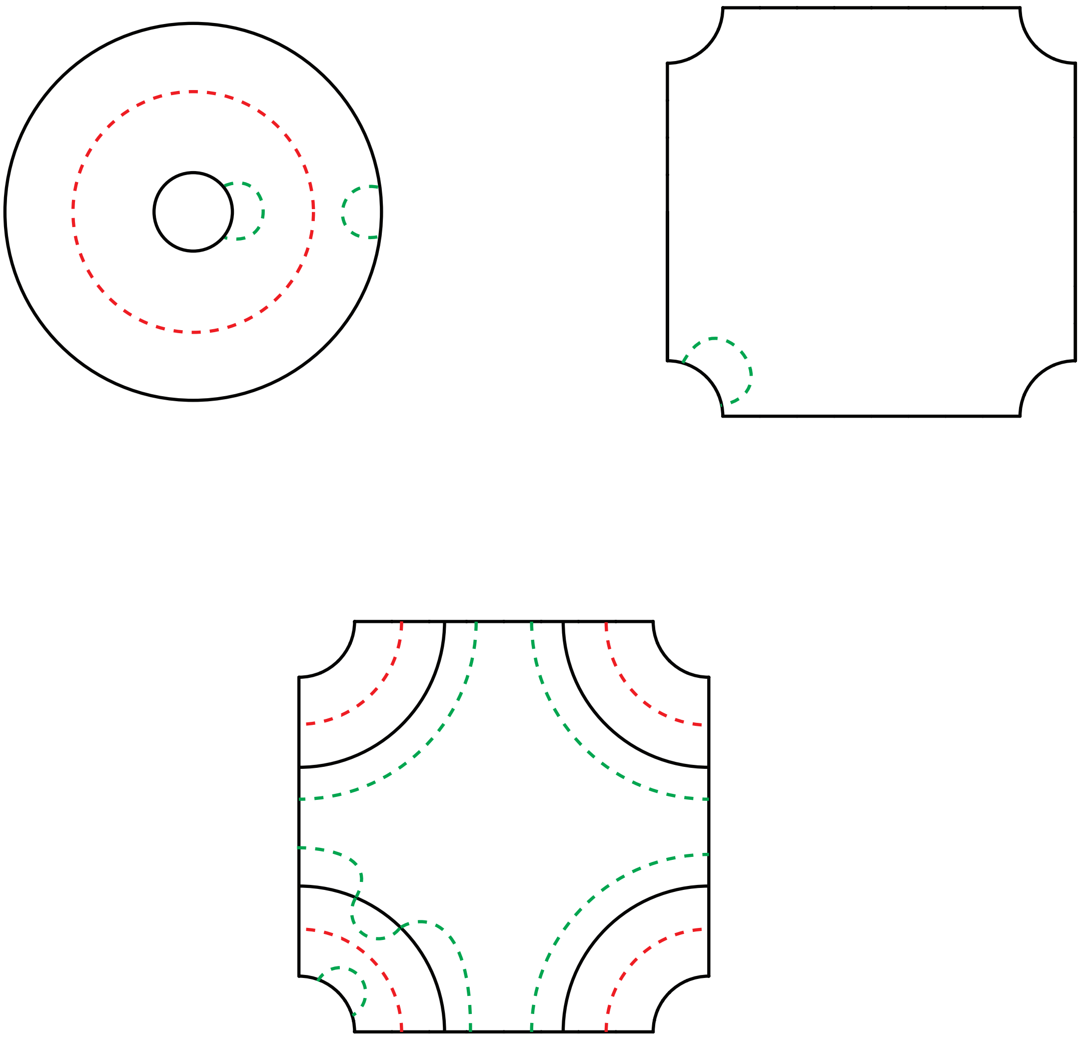

Figure 3.30: Top left: annulus in $T^2\times[0,1]$. Top right: Σ in $C_n(\infty)$. Bottom: Σ in $C_n(\infty)$ after gluing $T^2\times[0,1]$. The dotted lines are dividing curves.

Now consider a convex Giroux $\frac{j}{2}$-torsion layer $(T^2\times[0,1],\xi_{j/2})$ with boundary slope ∞. Since $T^2\times[0,1]=A\times S^1$, we cut $T^2\times[0,1]$ along A and obtain $A\times[0,1]$. It is well known (*c.f.* [Hon00b, Mat13]) that there is a convex annulus A in $\xi_{j/2}$ with a boundary parallel dividing arc on each boundary component and $(j-1)$ closed boundary parallel dividing curves, and $A\times[0,1]$ is an I-invariant neighborhood, see the top left drawing of Figure 3.30 for Giroux 1-torsion ($j=2$). We also consider a tight contact structure ξ_0 on $\Sigma\times[0,1]$, an I-invariant neighborhood of a convex surface Σ with a single dividing arc without any other dividing curves, see the top right drawing of Figure 3.30. With appropriate choices of the signs of the bypasses on Σ and A, we obtain an I-invariant neighborhood of a convex surface with one dividing arc and j boundary parallel closed curves by gluing two contact structures ξ_0 and $\xi_{j/2}$, see the bottom drawing of Figure 3.30. Therefore, ξ is contactomorphic to $\xi_{j/2}\cup\xi_0$. We glue the top and bottom of $(\Sigma\times[0,1],\xi)$ using ϕ_n and obtain $C_n(s)$. Then it clearly contains Giroux $\frac{j}{2}$-torsion. Thus we can exclude this case, and in any tight contact structure on $C_n(s)$ without boundary parallel half Giroux torsion, we can find a bypass for Σ_1 of which the attaching arc lies on $\alpha\times\{1\}$ or $\beta\times\{1\}$. By attaching this bypass we obtain an isotopic copy of Σ that contains 2 fewer dividing curves than Σ_1. We cut $C_n(s)$ along this new Σ and repeat the argument until we obtain Σ without closed dividing curves. □

According to Honda [Hon00a], there is a unique tight contact structure on $L(n,n-1)$ up to isotopy. We denote it by ξ_{std}. As explained in Section 3.4.1, K_2 can be considered as a knot in $L(n,n-1)$. Also, as shown in Figure 3.9, there is a Legendrian realization L of K_2 in $(L(n,n-1),\xi_{std})$ with $\mathrm{tb}=1$ and $\mathrm{rot}=0$ (which can be computed by using the formula from [LOSS09, Lemma 6.6]). We just have proved the following lemma.

Lemma 3.4.17. *There is a Legendrian representative L of K_2 in $(L(n,n-1),\xi_{std})$ such that* $\mathrm{tb}(L)=1$ *and* $\mathrm{rot}(L)=0$. □

Now we are ready to prove the lemmas in Section 3.4.1. We begin with Lemma 3.4.1

Proof of Lemma 3.4.1. Since $r\in\mathcal{R}_+$ and $s\in\mathcal{S}(r)$, we know $s>2$ and $s\notin(4,5]$. By Proposition 3.4.14, we can find a bypass for $-\partial C_n(s)$ with slope 0. By Theorem 3.2.2, we can thicken $C_n(s)$ to $C_n(s')$ such that $s'>2$ and $s'\notin(4,5]$. If $s'\neq\infty$, we can find a bypass again by Proposition 3.4.14 and repeat this until we obtain $C_n(\infty)$. □

Proof of Lemma 3.4.2. Again, after cutting $C_n(\infty)$ along Σ and rounding the edges, we obtain a genus-2 handlebody with convex boundary. Let Σ_i be $\Sigma\times\{i\}$ for $i=0,1$ and Γ_i the dividing set on Σ_i. Then $\Gamma_0=\phi_n(\Gamma_1)$. The dividing arc in each Γ_i divides $\partial\Sigma_i$ into two intervals, which we will label by 1 and 2. The dividing curves on $\partial\Sigma\times[0,1]$ connect the i-th interval on Σ_1 to the $(i-1)$-th interval (mod 2) on Σ_0. By Proposition 3.4.13, we need to consider two cases.

(1) Γ_1 *consists of a boundary-parallel arc without any other dividing curves*: First, we fix the sign of the bypass on Σ_1 to be negative. This will determine the signs of the regions of the entire $\partial(\Sigma\times[0,1])$. Also, the relative Euler class evaluated on Σ_1 is

-2. We observe that the dividing set on $\Sigma \times [0,1]$ is a single closed curve parallel to $\partial\Sigma$. Thus we can choose two convex compressing disks for the handlebody of which the Legendrian boundaries intersect the dividing curve exactly twice, see Figure 3.31. Thus there is a unique (possibly) tight contact structure on this handlebody, and thus a unique (possibly) tight contact structure on $C_n(\infty)$, which we denote by ξ_∞^-. Now we change the sign of the bypass on Σ_1 to be positive. Then the relative Euler class evaluated on Σ_1 is 2. By repeating the same argument, we can show that there is a unique (possibly) tight contact structure on $C_n(\infty)$, which we denote by ξ_∞^+.

It follows that any tight contact structure on $C_n(\infty)$ whose relative Euler class evaluated on Σ is ± 2 without boundary parallel half Giroux torsion is actually isotopic to $\xi_\infty^\pm$, respectively. Now Let ξ_{-1}^- be a contact structure on $C_n(-1)$, the complement of a standard neighborhood of $S_-(S_-(L))$, where S_- is the negative stabilization operator and L is a Legendrian representative of K_2 in $(L(n,n-1), \xi_{std})$ with $\mathrm{tb}(L) = 1$ and $\mathrm{rot}(L) = 0$ according to Lemma 3.4.17. Also, denote by ξ_B^- the contact structure on a negative basic slice $B_-(\infty, -1)$. Honda [Hon00a] showed that any basic slice is universally tight, so ξ_B^- is universally tight. Also ξ_{-1}^- is universally tight according to Colin's gluing theorem [Col99] since the gluing surfaces only contain boundary parallel dividing arcs (this condition is called *well-groomed*). If we glue ξ_0^- and ξ_B^- along the boundary torus T_{-1} with dividing slope -1, then we obtain a tight contact structure on $C_n(\infty)$ since T_{-1} is rotative and thus we can apply the gluing theorem for universally tight contact structures along a rotative torus [Col99, HKM02]. Clearly the relative Euler class evaluated on Σ in $\xi_0^- \cup \xi_B^-$ is -2, so the tight contact structure $\xi_0^- \cup \xi_B^-$ is isotopic to ξ_∞^-. By the same argument, $\xi_0^+ \cup \xi_B^+$ is isotopic to ξ_∞^+. Therefore, $(C_n(\infty), \xi_\infty^\pm)$ in fact thickens to $C_n(1)$.

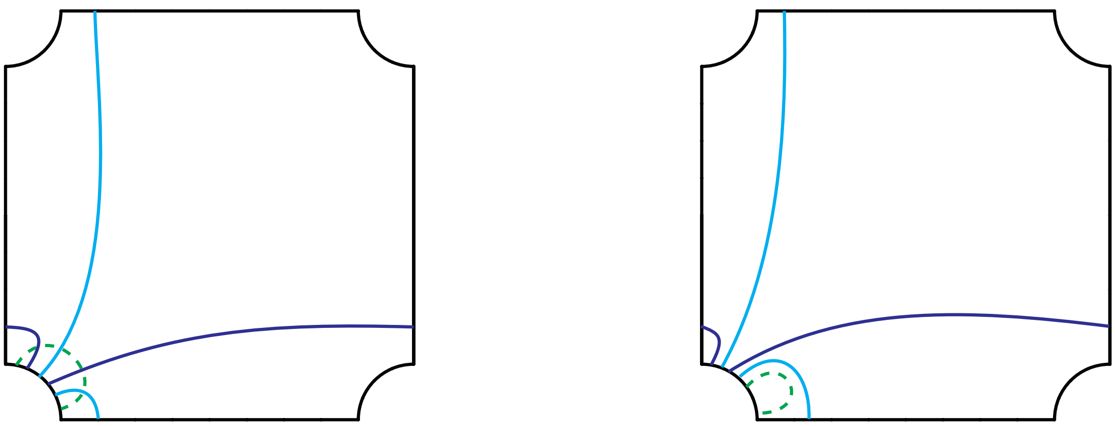

Σ_1 Σ_0

Figure 3.31: Σ_1 and Σ_0 in $C_n(\infty)$. The dotted lines are dividing curves, the blue lines are $\alpha \times \{1\}$ and $\alpha \times \{0\}$, and the sky blue lines are $\beta \times \{1\}$ and $\beta \times \{0\}$.

(2) Γ_1 *contains one arc and one closed curve with slope* ∞: In this case, the relative Euler class evaluated on Σ is 0. Fix the signs of the regions $\Sigma_1 \setminus \Gamma_1$. Take arcs α and β on Σ_1 with slopes ∞ and 0 as shown in the left drawing of Figure 3.32. Take

compressing disks $D_\alpha = \alpha \times [0,1]$ and $D_\beta = \beta \times [0,1]$ for $\Sigma \times [0,1]$. Perturb the disks so that their boundaries do not intersect any dividing curve on $\partial\Sigma \times [0,1]$. This results in a shift of the basepoints of α and β on Σ_0 by -1 intervals following the positive orientation of $\partial\Sigma$. Then ∂D_α and ∂D_β intersect the dividing curves on $\partial(\Sigma \times [0,1])$ exactly twice, respectively, as shown in Figure 3.32.

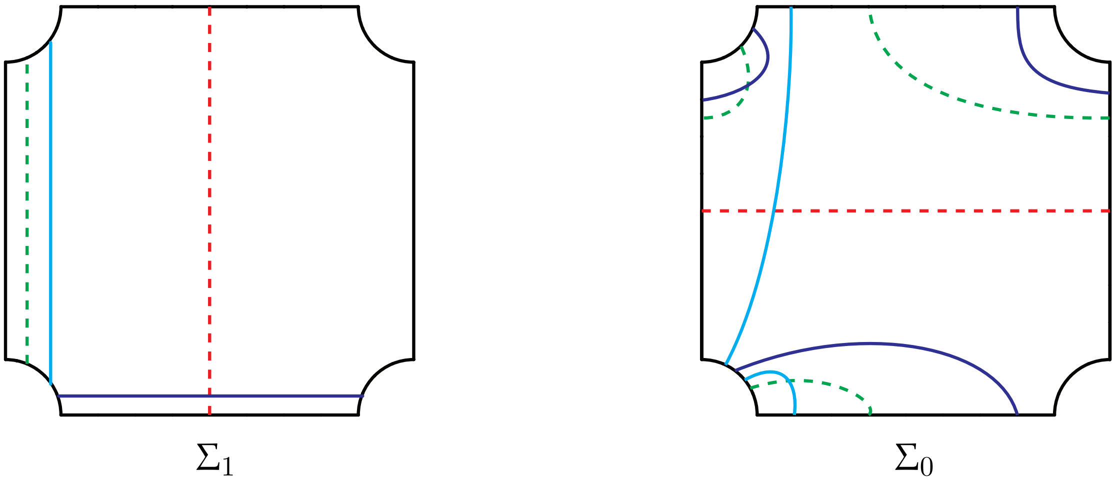

Figure 3.32: Σ_1 and Σ_0 in $C_n(\infty)$. The dotted lines are dividing curves, the blue lines are $\alpha \times \{1\}$ and $\alpha \times \{0\}$, and the sky blue lines are $\beta \times \{1\}$ and $\beta \times \{0\}$.

Thus there is a unique (possibly) tight contact structure on this handlebody, and thus a unique (possibly) tight contact structure on $C_n(\infty)$. Now we change the sign of the regions $\Sigma_1 \setminus \Gamma_1$. By repeating the same argument, we can show that there is a unique (possibly) tight contact structure on $C_n(\infty)$. In total, there are at most two (possibly) tight contact structures on $C(\infty)$. $\square$

Remark 3.4.18. Since the dividing curves on Σ may have some boundary twisting for the case (2), there could be infinitely many tight contact structures on $C_n(\infty)$ if we fix the boundary pointwise.

Now we will prove Lemma 3.4.4 and 3.4.5. The argument will be similar to the proof of [CM20, Lemma 3.1 and 3.4]. However, since ϕ_n is right veering, whereas the monodromy of the figure-eight knot is not, the maximal slope to which $C_n(s)$ can thicken is different.

Proof of Lemma 3.4.4 and 3.4.5. Since $r \in \mathbb{Q}_-$, $s \in \mathcal{S}(r)$ and $s \neq 0$, we know $s < 0$. Let $k \in \mathbb{N}$ such that $-\frac{1}{k-1} < s \leq -\frac{1}{k}$. Suppose $s \neq -\frac{1}{k}$. Then by Proposition 3.4.16 we can find a bypass for $-\partial C_n(s)$ with slope 0 and we can thicken $C_n(s)$ to $C_n(s')$ where $s < s' \leq -\frac{1}{k}$. Thus we can find a bypass again by Proposition 3.4.16 and repeat this until we obtain $C_n(-\frac{1}{k})$. Let Γ_Σ be a dividing set for Σ in $C_n(-\frac{1}{k})$. By Proposition 3.4.13, we need to consider two cases.

(1) Γ_Σ *contains one boundary parallel arc without any other dividing curves*: First, we fix the sign of the bypass on Σ to be negative. Then the relative Euler class

evaluated on Σ is -2. After cutting $C_n(-\frac{1}{k})$ along Σ and rounding the edges, we obtain $\Sigma \times [0,1]$ with a smooth convex boundary. Also, the dividing set consists of a single closed curve parallel to $\partial\Sigma$. By choosing convex compressing disks for this handlebody whose Legendrian boundaries intersect the dividing curve exactly twice as shown in Figure 3.31, we see that there is a unique (possibly) tight contact structure on this handlebody, and thus a unique (possibly) tight contact structure on $C_n(-\frac{1}{k})$, which we denote by $\xi^-_{-1/k}$.

It follows that any tight contact structure on $C_n(-\frac{1}{k})$ whose relative Euler class evaluated on Σ is -2 without boundary parallel half Giroux torsion is actually isotopic to $\xi^-_{-1/k}$. Hence the complement of a standard neighborhood of $S_-(S_-(L))$ in $(L(n,n-1),\xi_{std})$ is isotopic to ξ^-_{-1}, where S_- is the negative stabilization operator and L is a Legendrian representative of K_2 from Lemma 3.4.17. Therefore, $(C_n(-1),\xi^-_{-1})$ in fact thickens to $C_n(1)$, and $C_n(-1) = T_- \cup C_n(1)$, where $T_- = B_-(-1,0) \cup B_-(0,1)$ is a union of two negative basic slices with dividing slopes $s_0 = -1$ and $s_1 = 1$. We can further decompose T_- into $T^k_- \cup B_-(-\frac{1}{k},0) \cup B_-(0,1)$, where T^k_- is a minimally twisting contact $T^2 \times [0,1]$ with dividing slopes $s_0 = -1$ and $s_1 = -\frac{1}{k}$. Hence we obtain a tight contact structure on $C_n(-\frac{1}{k}) = B_-(-\frac{1}{k},0) \cup B_-(0,1) \cup C_n(1)$. It is straightforward to check that the relative Euler class evaluated on Σ in this $C_n(-\frac{1}{k})$ is -2, so this contact structure is isotopic to $\xi^-_{-1/k}$. Therefore, $(C_n(-\frac{1}{k}),\xi^-_{-1/k})$ also thickens to $C_n(1)$ for all $k \in \mathbb{N}$.

Next, change the signs of the regions of Σ so that the sign of the bypass is positive. In this case, the relative Euler class evaluated on Σ is 2. After repeating the above argument, we get a unique tight contact structure under these conditions, which we denote by $\xi^+_{-1/k}$. Similarly, we can build the tight contact structures isotopic to $(C_n(-\frac{1}{k}),\xi^+_{-1/k})$ that thicken to $C_n(1)$.

The above arguments show that these tight contact structures on $C_n(-\frac{1}{k})$ are determined by the sign of the bypass on Σ, which is in turn determined by the sign on the stacks of basic slices $B_\pm(-\frac{1}{k},0) \cup B_\pm(0,1)$, and are thus independent of the tight contact structure on $C_n(1)$.

(2) Γ_Σ *contains one closed curve and one arc with slope* ∞: In this case, the relative Euler class evaluated on Σ is 0. Fix the signs of the regions $\Sigma \setminus \Gamma_\Sigma$. We showed in the proof of Proposition 3.4.16 that there exists an isotopic copy of Σ in $C_n(-\frac{1}{k})$ with one boundary parallel dividing arc, one closed boundary parallel dividing curve and perhaps two closed essential curves, see the bottom drawing of Figure 3.26 for example. As in the proof of Proposition 3.4.13, we can remove the closed essential dividing curves and hence we can assume Γ_Σ consists of one boundary parallel arc and one boundary parallel closed curve. This implies that the dividing set of $\partial(\Sigma \times [0,1])$ consists of exactly three dividing curves parallel to $\partial\Sigma$. By Cofer [Cof04, Section 3], there exist two tight contact structures on this $\Sigma \times [0,1]$ (with a fixed characteristic foliation). Thus there exist at most two tight contact structures on $C_n(-\frac{1}{k})$.

According to the proof of Proposition 3.4.16, it is clear that one of these contact structures contains a boundary parallel half Giroux torsion layer. By repeating the same argument with the opposite signs on the regions on $\Sigma \setminus \Gamma_\Sigma$, we see that there are at most two tight contact structures on $C_n(-\frac{1}{k})$ without boundary parallel half Giroux torsion when the relative Euler class evaluated on Σ is 0, and that these contact structures are completely determined by the sign of the bypass on Σ. Denote these contact structures by $(C_n(-\frac{1}{k}), \xi'^{\pm}_{-1/k})$.

It follows that any tight contact structure on $C_n(-\frac{1}{k})$ whose relative Euler class evaluated on Σ is 0 without boundary parallel half Giroux torsion is actually isotopic (fixing boundary setwise) to either $\xi'^{+}_{-1/k}$ or $\xi'^{-}_{-1/k}$. Thus according to Lemma 3.4.17, the complement of a standard neighborhood of $S_+(S_-(L))$ (*resp.* $S_-(S_+(L))$) in $(L(n, n-1), \xi_{std})$ is isotopic to ξ'^{+}_{-1} (*resp.* ξ'^{-}_{-1}). Therefore, $(C_n(-1), \xi'^{\pm}_{-1})$ in fact thickens to $C_n(1)$, and $C_n(-1) = T'_\pm \cup C_n(1)$, where $T'_\pm = B_\pm(-1, 0) \cup B_\mp(0, 1)$ is a union of two negative basic slices with dividing slopes $s_0 = -1$ and $s_1 = 1$. We further decompose $T'_\pm$ into $T'^k_\pm \cup B_\pm(-\frac{1}{k}, 0) \cup B_\mp(0, 1)$, where $T'^k_\pm$ is a minimally twisting contact $T^2 \times [0, 1]$ with dividing slopes $s_0 = -1$ and $s_1 = -\frac{1}{k}$. Hence we obtain tight contact structures on $C_n(-\frac{1}{k}) = B_\pm(-\frac{1}{k}, 0) \cup B_\mp(0, 1) \cup C_n(1)$. It is straightforward to check that the relative Euler class evaluated on Σ is 0 and the sign of the bypass is $\pm$, so these contact structures are isotopic (fixing boundary setwise) to $\xi'^{\pm}_{-1/k}$. Therefore, $(C_n(-\frac{1}{k}), \xi'^{\pm}_{-1/k})$ also thickens to $C_n(1)$ for all $k \in \mathbb{N}$.

The above arguments show that these tight contact structures on $C_n(-\frac{1}{k})$ are determined by the sign of the bypass on Σ, which is in turn determined by the sign on the stacks of basic slices $B_\pm(-\frac{1}{k}, 0) \cup B_\mp(0, 1)$, and are thus independent of the tight contact structure on $C_n(1)$. □

§ 3.4.5 | Tight contact structures on a solid torus

In this subsection, we prove Lemma 3.4.7 by counting the number of tight contact structures on $N_r(\infty)$ and $N_r(1)$.

Proof of Lemma 3.4.7. By Proposition 3.2.15, there exist $\Phi(r)$ tight contact structures on $N_r(\infty)$.

Now we consider $N_r(1)$. Let $r = \frac{p}{q}$ and $r \neq 1$. We can change the coordinates of $\partial N_r(1)$ by the matrix

$$\begin{pmatrix} 0 & 1 \\ -1 & 1 \end{pmatrix}.$$

Then the dividing slope of $N_r(1)$ will become ∞ and the meridional slope will become $\frac{q}{q-p} = \frac{1}{1-r}$ (recall that we use the slope convention $\binom{p}{q} = \frac{p}{q}$ for a solid torus, see Remark 3.2.3). Therefore, there are $\Phi(\frac{1}{1-r}) = \Psi(r)$ tight contact structures on $N_r(1)$. □

§ 3.5 | Fillability and virtual overtwistedness

In this section, we will prove Theorem 3.1.8 and Theorem 3.1.9. We begin with the fillability of tight contact structures on $M(n, r)$.

Proof of Theorem 3.1.8. First, we consider the tight contact structures counted by Φ. As a consequence of [GLS06] we know that all the tight contact structures on $S^3_n(T_{2,3})$ are Stein fillable for $n \geq 5$. Recall from Section 3.3 that the tight contact structures counted by Φ can be constructed from the surgery diagram shown in Figure 3.11, which can be considered as a result of Legendrian surgeries on the knots in some tight contact structure on $S^3_n(T_{2,3})$. Since Legendrian surgery preserves Stein fillability (see Remark 3.2.18), all tight contact structures counted by Φ for $n \geq 5$ are Stein fillable.

Next we consider the tight contact structures counted by Ψ. We start by considering $M(n, 2)$. Observe that there is a unique tight contact structure on $M(n, 2)$ counted by Ψ and denote it by $(M(n, 2), \xi_2)$. We claim that $(M(n, 2), \xi_2)$ is Stein fillable and show that any tight contact structure on $M(n, r)$ for $r > 2$ counted by Ψ is obtained by some negative contact surgery on some Legendrian knot in $(M(n, 2), \xi_2)$. Since negative contact surgery preserves Stein fillability, these will complete the proof.

Lemma 3.4.5 and the proof of Theorem 3.4.8 implies that any contact structure on $M(n, r)$ for $n \geq 2$ and $r \geq 2$ counted by Ψ can be obtained by a positive contact surgery on a Legendrian push-off of the binding of an open book decomposition of $(L(n, n-1), \xi_{std})$, the unique tight contact structure on $L(n, n-1)$. This in fact implies that any tight contact structure on $M(n, r)$ for $r > 2$ counted by Ψ can be obtained by some negative contact surgery on some Legendrian knot in $(M(n, 2), \xi_2)$.

To be more precise, the open book is shown in the left drawing of Figure 3.33 where the monodromy of the open book is $\phi_n = D_\alpha D_\beta D_\alpha^{n-1}$, where D_α is a positive Dehn twist about α. This positive contact surgery is equivalent to an inadmissible transverse 2-surgery on the binding of the open book followed by a negative contact surgery on a Legendrian push-off of the surgery dual knot (*c.f.* [Con19]). Also this inadmissible transverse 2-surgery yields $(M(n, 2), \xi_2)$ – this is by definition of inadmissible transverse surgery (*c.f.* [Con19]) and by the construction of ξ_2 described in the proof of Lemma 3.4.2.

By applying an algorithm in [Con19] that converts the result of an inadmissible transverse surgery into an open book decomposition, we obtain an open book decomposition for $(M(n, 2), \xi_2)$ as shown in the right drawing of Figure 3.33 where the monodromy is

$$\widetilde{\phi}_n = D_\alpha D_\beta D_\alpha^{n-1} D_\gamma^{-1} \Delta$$

and Δ is the composition of positive Dehn twists about each boundary component. Korkmaz and Ozbagci [KO08] provided factorizations of Δ. In particular, they showed

$$\Delta = D_\alpha^{-2} D_\gamma D_\delta D_\sigma = D_\gamma D_\alpha^{-2} D_\delta D_\sigma$$

where δ, σ are some simple closed curves on the page. The second equality holds since α and γ are disjoint. Now we have

$$\begin{aligned}\widetilde{\phi}_n &= D_\alpha D_\beta D_\alpha^{n-1} D_\gamma^{-1} \Delta \\ &= D_\alpha D_\beta D_\alpha^{n-1} D_\gamma^{-1} D_\gamma D_\alpha^{-2} D_\delta D_\sigma \\ &= D_\alpha D_\beta D_\alpha^{n-3} D_\delta D_\sigma.\end{aligned}$$

Since $n \geq 5$, there is a factorization of $\phi\Delta$ which is a product of positive Dehn twists. Thus $(M(n,2), \xi_2)$ is Stein fillable. □

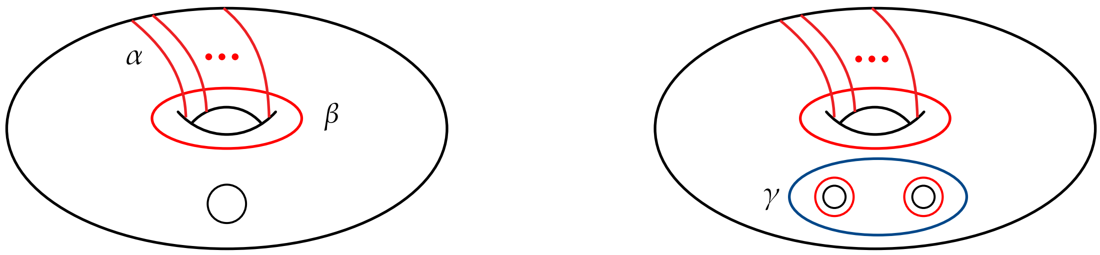

Figure 3.33: Left: an open book decomposition for $(L(n,n-1), \xi_{std})$. Right: an open book decomposition for $(M(n,2), \xi_2)$ counted by Ψ. The red curves represent positive Dehn twists and the blue curve represents a negative Dehn twist.

Lastly, we will consider the virtual overtwistedness of tight contact structures on $M(n,r)$.

Proof of Theorem 3.1.9. First, as shown in Figure 3.1, $M(n,r)$ can be obtained by r-surgery on K_2 in $L(n,n-1)$ and the surgery dual knot K_* represents a nontrivial element in $\pi_1(M(n,r))$. Thus there is a cover of $M(n,r)$ that unwraps K_*. Let N be a neighborhood of K_*. By Honda [Hon00a, Proposition 5.1.(2)], if ξ is a virtually overtwisted contact structure on N, then any cover of (N,ξ) contains an overtwisted disk. Thus if (N,ξ) is virtually overtwisted, then there is an overtwisted cover of (N,ξ) that embeds into some cover of $M(n,r)$.

Now according to the proof of Theorem 3.4.8, the tight contact structures counted by Ψ can be decomposed into $C(1)$ and $N_r(1)$. By Honda [Hon00a, Proposition 5.1.(2)], there are at most two universally tight contact structures on $N_r(1)$. Thus for any $r \in \mathcal{R}_+ \cup \mathbb{Q}_-$, there are at most two universally tight contact structures on $M(n,r)$ counted by Ψ and all others are virtually overtwisted. Also, the tight contact structures counted by Φ can be decomposed into $C(\infty)$ and $N_r(\infty)$. By Honda [Hon00a, Proposition 5.1.(2)] again, there are at most two universally tight contact structures on $N_r(\infty)$. Since there are two tight contact structures on $C_n(\infty)$ counted by Φ, there are at most four universally tight contact structures on $M(n,r)$ for $r \in \mathcal{R}_+$ counted by Φ, and all others are virtually overtwisted. □

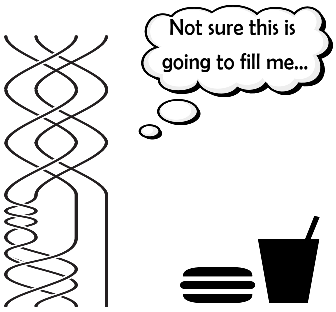

Chapter 4

L-space knots with positive surgeries that are not weakly symplectically fillable

The content of this chapter is taken from [Non24] with some changes done to fit the text more seamlessly in the fabric of this thesis.

§ 4.1 | Motivation: tightness versus symplectic fillability

As mentioned several times during this thesis, understanding whether a closed 3-manifold M admits a tight contact structure is one of the most relevant questions in 3-dimensional contact topology. As said in Chapter 3 the focus is on hyperbolic 3-manifolds. Moreover it is most natural to consider hyperbolic L-spaces to try and construct a hyperbolic 3-manifold with no tight contact structures, since they do not possess taut foliations.

Another relevant notion closely related to tightness is that of a *symplectic filling*, see Chapter 2. A contact manifold is *symplectically fillable* if it bounds a symplectic manifold with a certain boundary condition. Depending on the conditions imposed on the boundary we obtain different notions of symplectic fillability. We are mainly interested in *weakly symplectically fillable* manifolds, see Definition 2.3.2. For other fillability notions, see the discussion at the end of Chapter 2.

Trying to understand whether a manifold admits *weakly fillable* tight contact structures is an interesting question on its own. It is well known that weak fillability is stronger than tightness. Using convex surface theory Etnyre-Honda [EH02] produced the first examples of tight Seifert fibered manifolds without symplectic fillings. Later Lisca-Stipsicz [LS07c] produced larger families of tight manifolds without symplectic fillings. Their arguments rely on gauge theoretic obstructions.

Nonetheless, finding examples of manifolds *not* having weakly fillable contact structures is still a decent starting point to try and answer the existence question for hyperbolic 3-manifolds. In fact, our inspiration comes from the work of [DLW24, KT17, LL19]. The manifolds considered in [KT17, LL19] are hyperbolic L-spaces obtained via rational Dehn surgery on the *pretzel knots* $P(-2, 3, 2n + 1)$. This family of manifolds – living in the range of the slopes analyzed in [KT17, LL19] – is considered a potential source of hyperbolic manifolds without tight contact structures.

In this chapter we construct an obstruction for weak fillability of L-spaces obtained as surgery on L-space knots. We show how the strategy used in [DLW24, KT17, LL19] can be used for a more general L-space knot K[1]. In particular we are able to analyze the family of knots $\{K\}_n$ described in [BK22]. These are hyperbolic L-space knots which are not pretzel knots, whereas all the knots considered in [KT17, LL19] are of the form $P(-2, 3, 2n + 1)$.

Roughly speaking, the strategy goes as follows. If the L-space constructed via n-surgery on the knot K has symplectic fillings, such fillings need to be negative definite [OS04a]. On the other hand, if the surgered manifold has a negative definite symplectic filling and the surgery coefficient is square-free[2] its d-invariants have to satisfy some inequality (see Theorem 2.4.8). Therefore if the inequality does not hold, n-surgery on K cannot admit weakly symplectic fillings.

In this chapter we use an explicit description of the symmetrized Alexander polynomial $\Delta_K(T)$ of K to give a general computation of the d-invariants of the n-surgery on K. In short, the symmetrized Alexander polynomial of K can be *uniquely described* by the collection of its exponents (see Lemma 4.2.2 and the discussion below it). Using such collection and a formula from [OS12a] (see Theorem 4.2.1) we can then write down the values of the d-invariants using only the exponents n_i and n.

We show the following result.

Theorem 4.1.1 (General obstruction)**.** *Let K be an L-space knot of genus $g(K)$ and symmetrized Alexander polynomial described by the exponents $0, n_1, \cdots, n_k$. Let $n \in \mathbb{N}$ with $n \geq 2g(K) - 1$. Suppose n is square-free. The d-invariants can be computed as in Theorem 4.2.6 using only the exponents n_i and n. If the invariants fail to satisfy the inequalities in Theorem 2.4.8, then the manifold $K(n)$ has no weakly symplectically fillable contact structures.*

We then consider the infinite family of hyperbolic L-space knots $\{K_n\}_n$ described in [BK22] (see Figure 4.1). This is a quite interesting family of knots, since it might provide an infinite family of L-space knots that are *not* braid positive. In [MT23, Corollary 1.5] it is shown that any braid positive knot is *fillable*. We explain what this means.

Definition 4.1.2. A fillable knot is a knot that has *some* Legendrian representative with a *fillable positive surgery* in the sense of [MT23]. A fillable positive surgery is some n ($n > 0$) contact surgery so that the contact structure $\xi_n^{-1}(K)$ (the one obtained by all negative stabilizations, see Figure 2.5) is weakly fillable.

[1] Recall these are knots that admit a positive integral surgery to an L-space.

[2] We say that n is square-free if, for every p prime dividing, p^2 does not divide n.

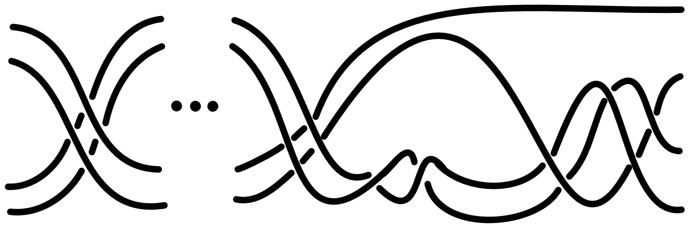

Figure 4.1: The braid β_n whose closure gives the knot K_n. This picture is taken from [BK22].

Question 4.1.3. *Are the knots $\{K_n\}_n$ fillable?*

In order to check whether the K_n's are fillable it suffices to check all the slopes in the range $[2g(K_n), 4g(K_n)]$. This is because in [MT23, Proposition 1.7] it is shown that if a knot is fillable then the minimal (smooth) slope that is fillable lies in the interval $[2g(K_n), 4g(K_n)]$.

In this chapter we do not show that the K_n's are not fillable. The interval we are able to study with our techniques is considerably smaller than $[2g(K_n), 4g(K_n)]$. In particular we prove the following result.

Theorem 4.1.4. *Let $n \geq 1 \in \mathbb{N}$ so that there is a square-free integer in the two-element set $\{8n+3, 8n+5\}$. Let m be the maximal such square-free number and q a rational number so that $q \in [8n+3, m]$. Let $K_n(q)$ denote the q rational Dehn surgery along the knot K_n. Then $K_n(q)$ is (generically) a hyperbolic 3-manifold that admits no weakly symplectically fillable contact structures.*

Here by *generically* we mean that we are excluding the exceptional (i.e. not producing an hyperbolic manifold) slopes that potentially live in the interval, since these are finite by Thurston's hyperbolic Dehn surgery theorem [Thu82]. We will be more specific with such exceptional slopes in Section 4.3.

Note that for K_n the interval $[2g(K_n), 4g(K_n)]$ corresponds to $[8n+4, 16n+8]$ (the genus of the knots K_n is computed in [BK22]). As we already stated, this interval is larger than the one studied in Theorem 4.1.4. However, it does give some partial evidence against the existence of fillable slopes for the K_n's. We point out that our obstruction is stronger than the one required for studying fillable slopes as per [MT23]. Here we show that certain slopes have no symplectic fillings at all. On the other hand [MT23, Proposition 1.7] only refers to a specific contact structure – the one obtained with only negative stabilizations. One could try show that the $\{K_n\}_n$ are not fillable just by obstructing fillability of that specific structure. This would require a different analysis from the one introduced in this chapter.[3]

Remark 4.1.5. For the interested reader, recent work of Himeno [Him25] introduced a family of L-space knots which are not braid positive. This family is distinct from the

[3]It is important to remark that even if the knots K_n were shown to be fillable this would not imply that they are braid positive.

one introduced in [BK22]. It would be interesting to understand whether the knots in [Him25] are fillable in the sense of [MT23].

After proving an existence result for tight contact structures, we obtain the following:

Theorem 4.1.6. *Let $n \geq 1$ and $q \in \mathbb{Q}$. Then the manifolds $K_n(q)$ admit a tight contact structure for $q \notin [8n+1, 8n+3]$.*

Moreover if $8n+5$ is square-free, the family $K_n(q)$, $q \in (8n+3, 8n+5] \cap \mathbb{Q}$, contains an infinite family of hyperbolic L-spaces that admit tight contact structures but do not admit weakly symplectically fillable contact structures.

Remark 4.1.7. There is still no clear way to understand whether the surgery coefficient $q = 8n+3$ produces a manifold admitting tight contact structures. The contact surgery with contact framing zero leads, by definition, to an overtwisted contact structure (Proposition 3.2.21). It is possible that $K_n(8n+3)$ provides an example of a manifold without tight contact structures.

§ 4.2 | L-space knots and a general obstruction for weak fillability

Let K be an L-space knot in S^3. Recall this is a knot that has a positive integral surgery to an L-space. By [LS07a], we know that for an L-space knot K of genus $g(K)$, every r surgery with $r \geq 2g(K)-1$ yields an L-space. We hence consider surgery coefficients $n \geq 2g(K)-1$ throughout the rest of the chapter.

Recall that due to work of [OS04a], when n is an integer we can enumerate the $Spin^c$ structures on the surgered 3-manifold $K(n)$ indexing them by integers i, with $|i| \leq n/2$. More precisely the set of $Spin^c$ structures t on a three-manifold Y is parameterized by $H_2(Y;\mathbb{Z}) \cong H_1(Y;\mathbb{Z})$. In the case of the surgered manifold $K(n)$ we have $H_1(K(n);\mathbb{Z}) \cong \mathbb{Z}/n\mathbb{Z}$, hence $Spin^c$ structures can be labeled by the elements of $\mathbb{Z}/n\mathbb{Z}$, where we interpret the latter as congruences modulo n. The exact labeling is described as follows. Attaching a 2-handle with framing n to $S^3 \times [0,1]$ along $K \subset S^3 \times \{1\}$ gives a cobordism W_n from S^3 to K_n. Note that $H_2(W_n;\mathbb{Z})$ is generated by the homology class of the core of the 2-handle attached to a Seifert surface for the knot K; denote this generator by f_n. A $Spin^c$ structure t on $K(n)$ is labeled by i if it admits an extension $\mathfrak{s}$ to W_n satisfying

$$\langle c_1(\mathfrak{s}), f_n\rangle - n \equiv 2i \pmod{2n}.$$

Additionally, if K is an L-space knot, then the d-invariants of integral surgeries can be computed by the following formula. The formula for the unknot can be found in [OS03, Proposition 4.8].

Theorem 4.2.1 ([OS12a, Theorem 6.1])**.** *Given $n \in \mathbb{N}$ and $\forall |i| \leq n/2$, we have:*

$$d(K(n),i) = d(U(n),i) - 2t_i(K) = \frac{(n-2|i|)^2}{4n} - \frac{1}{4} - 2t_i(K), \tag{4.1}$$

where U is the unknot, t_i the torsion coefficient :

$$t_i(K) = \sum_{j>0} j c_{|i|+j}, \tag{4.2}$$

and c_h is the coefficient of T^h in the symmetrized Alexander polynomial of K.

Theorem 2.4.8 gives us a strategy to study weak symplectic fillings of the surgered manifolds $K(n)$ when n is square-free. Suppose that all the d-invariants (which can be computed using Theorem 4.2.1) fail to satisfy the inequalities in Theorem 2.4.8. Since $K(n)$ is an L-space, by [OS04a] all of its symplectic fillings are negative definite. The existence of such a negative definite filling would then contradict our assumption on the d-invariants.

We therefore procede to describe a way to compute the d-invariants associated to $n \geq 2g(K) - 1$ surgeries on K for a general L-space knot.

First we note that for an L-space knot there is a specific description of its symmetrized Alexander polynomial.

Lemma 4.2.2 ([OS05b, Corollary 1.3],[HW18, Corollary 9]). *If $K \subset S^3$ is a knot which admits an L-space surgery, then:*

$$\Delta_K(T) = \sum_{i=-k}^{k} (-1)^{k+i} T^{n_i} \tag{4.3}$$

for some sequence of integers $n_{-k} < n_{-k+1} < \cdots < n_{k-1} < n_k$ satisfying $n_i = -n_{-i}$. Additionally we know that $n_k - n_{k-1} = 1$ and that $g(K)$ is the degree of the polynomial, i.e. $n_k = g(K)$.

Roughly speaking, since the coefficient associated to T^{n_i} is either 1 or -1 it is not hard to compute the torsion coefficients t_j using Equation (4.2). We provide a general algorithm to do it. This is discussed, albeit in different terms, in [OS12a].

We always assume in the following that $k = 2h$ is even. The odd case is similar and we do not discuss it here. Note that for $i = 1, \cdots, k$ the integers

$$n_{k+2-2i} - n_{k+1-2i} \tag{4.4}$$

encode a "jump" in the Alexander polynomial. By this we mean that $n_{k+2-2i} - n_{k+1-2i}$ determines the distance between two consecutive exponents appearing in $\Delta_K(T)$. These jumps are actually every second step. However since the polynomial is symmetric, the coefficients $n_{k+2-2i} - n_{k+1-2i}$ are enough to compute all the exponents appearing in $\Delta_K(T)$.

Remark 4.2.3. We point out that there is a result [Krc18, Theorem 1.5] that imposes additional conditions on the $n_{k+2-2i} - n_{k+1-2i}$'s for an L-space knot. As such, not all possible collections of $n_{k+2-2i} - n_{k+1-2i}$ for $i = 0, \cdots, k$ can arise from the Alexander polynomial of an L-space knot.

More precisely, if $\Delta_K(T)$ is the symmetrized Alexander polynomial of an L-space knot K with n_i and as above, then we have the following additional inequality for the values of $n_{k+2-2i} - n_{k+1-2i}$

$$\sum_{i=2}^{j} n_{k+2-2i} - n_{k+1-2i} \leq \sum_{i=k-j+2}^{k} n_{k+2-2i} - n_{k+1-2i} \tag{4.5}$$

for any $j \leq k$.

Back to our main question. By definition of the torsion coefficients $t_j = 0$ for $j \geq g(K)$, since the degree of the polynomial is $g(K)$. We need to understand when and how the torsion coefficients start to change. Using a recursive formula for torsion coefficients we derive an expression for $t_j(K)$ that is written in terms of the exponents. To help the reader visualise our computations we will end the discussion with an example. We first define the following quantity which is helpful to shorten the notation in the remainder of this section.

$$A_j : = \sum_{i=1}^{j} n_{k+2-2i} - n_{k+1-2i},$$

for $j = 1, \cdots, h$. Define $A_0 : = 0$.

Lemma 4.2.4. *Let K be an L-space knot with genus $g(K)$ and symmetrized Alexander polynomial described by exponents $0 = n_0, n_1, \cdots, n_k = g(K)$ with $k = 2h$. Then the difference between the torsion coefficients for $i \in \{1, \cdots, g(K)\}$ is given by the following equation:*

$$t_{i-1}(K) - t_i(K) = \sum_{j=0}^{h-1} \chi_{(n_{2j+1}, n_{2j+2}]}(i). \tag{4.6}$$

Here χ denotes the characteristic function. In words, the torsion coefficient increases if and only if i is contained in one of the (open on the left) intervals $(n_{2j+1}, n_{2j+2}]$. Note that the family of intervals $\bigsqcup_{j=0}^{h-1}(n_{2j+1}, n_{2j+2}]$ joint with the family of complementary intervals $\bigsqcup_{l=0}^{h-1}(n_{2l}, n_{2l+1}]$ covers $(0, g(K)]$.

Figure 4.2 visually represents the result in Lemma 4.2.4. The red dots correspond to the values of the torsion coefficients t_i.

Proof of Lemma 4.2.4. By definition of the torsion coefficients of K, we have the following recursive formula:

$$t_{i-1}(K) - t_i(K) = \sum_{j \geq i} c_j(K), \tag{4.7}$$

where we recall that $c_j(K)$ is the coefficient of T^j in $\Delta_K(T)$.

The result is obtained using Equation (4.7) and noticing the following: each interval $(n_{2j+1}, n_{2j+2}]$ contains exactly one index for which the corresponding coefficient in the Alexander polynomial is 1 (i.e. the index n_{2j+2}) and no indices corresponding to negative coefficients. On the other hand, each one of the complementary intervals behaves the opposite way – it contains exactly one index corresponding to -1 coefficient (i.e. the n_{2l+1}) and no indices corresponding to positive coefficients. Starting from $n_k = g(K)$ and $n_{k-1} = g(K) - 1$, with $c_{g(K)} = 1$, we obtain the desired equation by recursively applying Equation (4.7). ◻

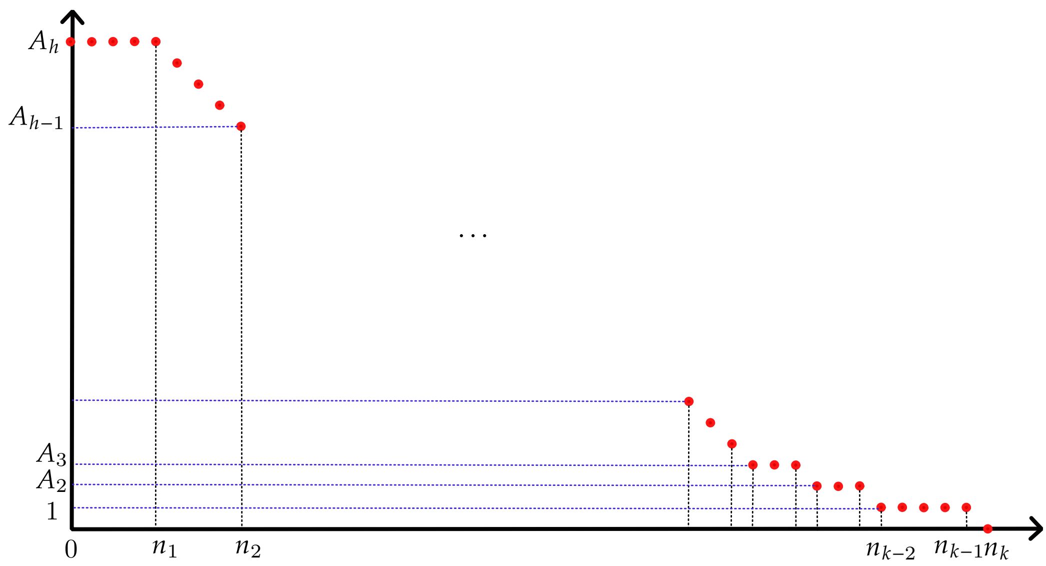

Figure 4.2: A visual representation of the torsion coefficients associated to K. To each red dot at $x = i$ is associated the value of t_i. The equality $A_i = t_{n_{k-2i}}$ is explained in Lemma 4.2.5.

Lemma 4.2.4 provides a way to compute the torsion coefficients starting from the exponents of the Alexander polynomial $\Delta_K(T)$.

Lemma 4.2.5. *Let K be an L-space knot with genus $g(K)$ and symmetrized Alexander polynomial with exponents $0 = n_0, \cdots, n_k = g(K)$. Let $i \in \{0, \cdots, g(K) - 1\}$. Then*

$$t_i(K) = \sum_{l=i+1}^{g(K)} \left(\sum_{j=0}^{h-1} \chi_{(n_{2j+1}, n_{2j+2}]}(l)\right). \tag{4.8}$$

Proof. We have an expression for $t_{i-1}(K) - t_i(K)$ for all i and we know that $t_{g(K)} = 0$. Note that $t_i = \sum_{j=i}^{g(K)-1}(t_j - t_{j+1})$. Simply plug in the expression in Lemma 4.2.4 to conclude. ◻

From Lemma 4.2.5 it is evident for example that $t_0(K) = A_h$. This is the maximum value for the torsion coefficients. In general, Lemma 4.2.5 shows that $t_{n_{k-2i}}(K) = A_i$ for $i = 0, \cdots, h$.

Now we can use Theorem 4.2.1 to give a general formula for the d-invariants.

Theorem 4.2.6. *Let K be an L-space knot with genus $g(K)$ and symmetrized Alexander polynomial of degree n_k, $k = 2h$. Let $n \in \mathbb{N}$ with $n = 2g(K) + (m-1)$, $m \geq 0$.*

For all $|j| \in \{0, \cdots, g(K)-1\}$ we have:

$$d(K(n), i) = \frac{(n-2|i|)^2}{4n} - \frac{1}{4} - 2\sum_{l=|i|+1}^{g(K)} \left(\sum_{j=0}^{h-1} \chi_{(n_{2j+1}, n_{2j+2}]}(l)\right). \tag{4.9}$$

If $|i| \in \{g(K), \cdots, g(K) + \lfloor \frac{m-1}{2} \rfloor\}$ then:

$$d(K(n), i) = \frac{(n-2|i|)^2}{4n} - \frac{1}{4}. \tag{4.10}$$

Although it would be a stretch to define the first equation in Theorem 4.2.6 as easy to visualize, it is important to notice that it is a quite simple linear expression. Once the exponents of $\Delta_K(T)$ are known it is then straightforward to use it to compute the desired values. As promised at the beginning, once we have computed the d-invariants we can obtain a general obstruction for weak fillability.

Theorem 4.1.1. *Let K be an L-space knot of genus $g(K)$ and symmetrized Alexander polynomial described by the exponents $0, n_1, \cdots, n_k$. Let $n \in \mathbb{N}$ with $n \geq 2g(K) - 1$. Suppose n is square-free. The d-invariants can be computed as in Theorem 4.2.6 using only the exponents n_i and n. If the invariants fail to satisfy the inequalities in Theorem 2.4.8, then the manifold $K(n)$ has no weakly symplectically fillable contact structures.*

To help the reader we now discuss an easy example to apply our calculations.

Example 4.2.7. Let K be the Pretzel knot $P(-2, 3, 11)$. This is an L-space knot whose symmetrized Alexander polynomial is given by:

$$\Delta_K(T) = T^7 - T^6 + T^4 - T^3 + T^2 - T + 1 - T^{-1} + T^{-2} - T^{-3} + T^{-4} - T^{-6} + T^{-7}.$$

In this case k – the number of non-negative exponents – is 6. We have $n_6 = 7$, $n_4 = 4$, $n_2 = 2$, $n_0 = 0$ and $n_5 = 6$, $n_3 = 3$, $n_1 = 1$.

Using Equation (4.8) we can write down the values of t_i for $i = 0, 1, \cdots, 6$. Clearly $t_7 = 0$. In general,

$$t_i(K) = \sum_{l=i+1}^{7} \left(\sum_{j=0}^{2} \chi_{(n_{2j+1}, n_{2j+2}]}(l)\right).$$

We can summarise everything in a graphic, see Figure 4.3.

Note that as shown in Figure 4.3 we can easily obtain an inequality for the d-invariants by considering the function $h(i) = -\frac{1}{3}i + \frac{7}{3}$. More precisely, we get

$$d(K(13), i) \leq \frac{(13-2i)^2}{44} - \frac{1}{4} + \frac{2}{3}i - \frac{14}{3}.$$

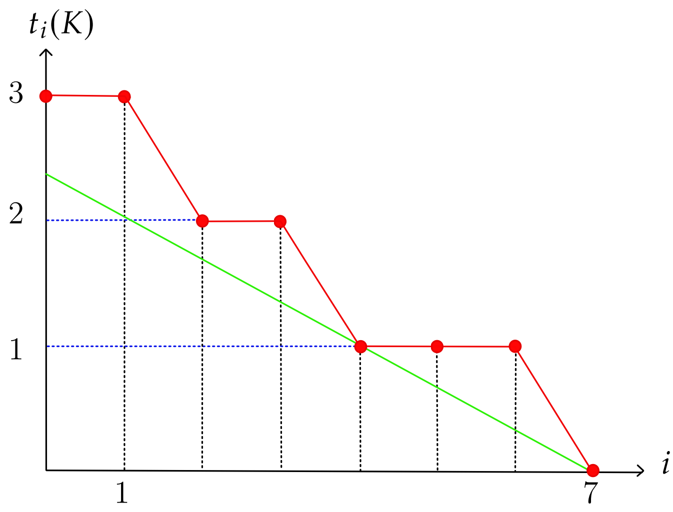

Figure 4.3: This graphic shows the values of $t_i(K)$. The red line is the linear interpolation between the points, the green line is the function $h(i) = -\frac{1}{3}i + \frac{7}{3}$.

Note $n = 2g(K) - 1 = 13$ it is square-free. The above inequality implies that:

$$d(K(13), i) \leq \frac{-142 + 4i^2 - 68i}{132} \leq 0$$

for $i = 0, \cdots, 7$. Hence we can apply Theorem 4.1.1 and conclude that $K(13)$ has no weakly symplectically fillable contact structures. This was already obtained in [LL19].

Definition 4.2.8. Given a knot K and $n \in \mathbb{N}$, we call a value for the d-invariant *weak* for the pair (K, n) if :

$$4d(K(n), i) \geq \begin{cases} 1 - \frac{1}{n} & \text{if } n \text{ is odd or} \\ 1 & \text{if } n \text{ is even.} \end{cases}$$

We say it is *non weak* for (K, n) if such inequality is not satisfied.

The terminology in Definition 4.2.8 is used in relation to the absence of weakly symplectic fillings. According to Theorem 4.1.1, we want all the d-invariants to be non weak in order to obstruct fillability. On the other hand, if some of the invariants are weak then our strategy cannot detect the absence of fillings.

Focusing on the second equation in Theorem 4.2.6 we can obtain an interesting bound on the surgery coefficient n that depends only on the genus of the knot.

Proposition 4.2.9. *Let $n = 2g(K) + (m - 1)$, with $m \geq 1$. Then the L-space $K(n)$ has non weak d-invariants* only if*:*

$$\begin{cases} (m-2)^2 < 4g(K) \text{ if } m \text{ is even} \\ (m-1)(m-3) < 4g(K) \text{ if } m \text{ is odd .} \end{cases} \tag{4.11}$$

Proof. We remark that the goal is to prove an "only if" statement. Hence it is only necessary to check whether the maximum possible value of $d(K(n), i)$ is non-weak.

Comparing Equation (4.9) and Equation (4.10) we see that we only need to consider indices $i \in \{g(K), \cdots, g(K) + \lfloor \frac{m-1}{2} \rfloor\}$. From Equation (4.10) the maximum value that $d(K(n), i)$ assumes for $i \in \{g(K), \cdots, g(K) + \lfloor \frac{m-1}{2} \rfloor\}$ corresponds to $i = g(K)$. We therefore check conditions for $d(K(n), g(K))$ to be non-weak.

- If m is even n is odd. Thus for a d-invariant to be non weak we need

$$\frac{(2g(K) + m - 1 - 2g(K))^2}{4(2g(K) + m - 1)} - \frac{1}{4} < \frac{1}{4} - \frac{1}{4(2g(K) + m - 1)}$$

$$\iff (m-2)^2 < 4g(K).$$

- If m is odd n is even. Thus for a d-invariant to be non weak we need

$$\frac{(2g(K) + m - 1 - 2g(K))^2}{4(2g(K) + m - 1)} - \frac{1}{4} < \frac{1}{4}$$

$$\iff (m-1)(m-3) < 4g(K).$$

□

This is just a rough upper bound. When considering Equation (4.9) we are quite likely introducing sharper bounds.

Remark 4.2.10. Theorem 4.1.1 does not imply that if the inequalities are satisfied the resulting surgered manifold has weak symplectic fillings – we just cannot detect their absence with our tools.

There is also another interesting result that can be obtained using a rough lower bound on the torsion coefficients. Remember we are considering an L-space knot K and symmetrized Alexander polynomial with degree n_k, $k = 2h$.

Proposition 4.2.11. *Let $n = 2g(K) - 1$. Let $j_{min} \in \{1, \cdots, h\}$ be the index minimising the quantity $\frac{A_j}{g(K) - n_{k-2j}}$. Then the L-space $K(n)$ has non weak d-invariants if:*

$$n_{k-2j_{min}} + 4A_{j_{min}} \geq g(K),$$

i.e. if the minimum value of $\frac{A_j}{g(K) - n_{k-2j}}$ is bigger than $\frac{1}{4}$.

Remark 4.2.12. One can rewrite the quantity $\frac{A_j}{g(K) - n_{k-2j}}$ as $\frac{t_{n_{k-2j}}}{g(K) - n_{k-2j}}$ (see Lemma 4.2.5) and write everything in terms of torsion coefficients. This notation is however quite cumbersome and we prefer to avoid using it.

Proof. The idea is to bound the values of the d-invariants of $K(n)$ from below using an adequate function. Let $j_{min} \in \{1, \cdots, k\}$ be the index minimising the quantity $\frac{A_j}{g(K) - n_{k-2j}}$. Consider the function:

$$h(i) = \left(-\frac{A_{j_{min}}}{g(K) - n_{k-2j_{min}}} \right) i + \left(\frac{A_{j_{min}}}{g(K) - n_{k-2j_{min}}} \right) g(K).$$

Here $t(i)$ is the linear interpolation between the values of t_i. Note that the line $h(i)$ is the result of the following construction. We choose the line with smallest slope between all the lines connecting $(g(K), 0)$ to a point (i, t_i). Hence, $h(i) \leq t(i)$ for $i \in [0, g(K)]$. For an example of such function see Figure 4.3. Then for $i = 0, \cdots, g(K)$ we have $d(K(n), i) \leq f(i)$, where $f(i) = \frac{(2g(K)-1-2i)^2}{4(2g(K)-1)} - \frac{1}{4} - 2h(i)$ (the inequality follows from Equation (4.9) and the definition of $h(i)$). $f(i)$ is a decreasing function from 0 to $i = (2g-1)\left(\frac{1}{2} - \frac{A_{j_{min}}}{g(K)-n_{k-2j_{min}}}\right)$ and then it increases until $i = g(K)$. We will compute the values of $f(i)$ at $i = 0, g(K)$ and show these are negative.

$$\begin{aligned}
f(0) &= \frac{2g(K)-1}{4} - \frac{1}{4} - 2\left(\frac{A_{j_{min}}}{g(K) - n_{k-2j_{min}}}\right) g(K) \\
&= \frac{g(K)-1}{2} - 2g(K)\left(\frac{A_{j_{min}}}{g(K) - n_{k-2j_{min}}}\right) \\
&= \frac{g(K)\left(1 - 4\left(\frac{A_{j_{min}}}{g(K)-n_{k-2j_{min}}}\right)\right) - 1}{2} \\
&= \frac{g(K)\left(\frac{g(K)-n_{k-2j_{min}}-4A_{j_{min}}}{g(K)-n_{k-2j_{min}}}\right) - 1}{2}
\end{aligned}$$

Since we are imposing $n_{k-2j_{min}} + 4A_{j_{min}} \geq g(K)$, we obtain that $f(0) < 0$. Moreover $f(g(K)) = \frac{1}{4(2g(K)-1)} - \frac{1}{4}$ which is negative as well. Thus $f(i) \leq 0$ for all $i \in [0, g(K)]$, which implies that $d(K(n), i) \leq 0$ for $i \in [0, g(K)]$. In other words, the d-invariants of $K(n)$ are non weak.

□

Remark 4.2.13. In our Example 4.2.7 with the pretzel knot $K = P(-2, 3, 11)$ the minimum value of $\frac{A_j}{g(K)-n_{k-2j}}$ is $\frac{1}{3}$. In particular the inequality in Proposition 4.2.11 is satisfied so we can immediately conclude that $K(11)$ has non weak d-invariants and hence it has no weakly symplectic fillings. Note that it is quite easy to tell whether Proposition 4.2.11 can be applied once we have the graphic representation of the torsion coefficients.

So far we only considered integral surgery coefficients. We now expand our results to rational coefficients as well. For this we need the following theorem.

Theorem 4.2.14 ([OS12b, Theorem 1.4])**.** *For all rational numbers $r > m(K)$, the r-surgered manifold $K(r)$ bounds a negative-definite manifold X_r, with $H^2(X_r) \to H^2(K(r))$ surjective, where $m(K)$ is:*

$$inf\,\{r \in \mathbb{Q}_{\geq 0} | K(r) \text{ bounds a negative-definite 4-manifold}\}.$$

We can combine this result with Theorem 4.1.1. In particular, we obtain:

Theorem 4.2.15. *Let K be an L-space knot of genus $g(K)$. Let $n \in \mathbb{N}$ with $n \geq 2g(K) - 1$. Suppose n is square-free. If $K(n)$ does not bound any negative-definite 4-manifold, then $K(q)$, $q \in \mathbb{Q}$ has no weak symplectic fillings for $q \in [2g(K) - 1, n]$.*

Proof. Assume by contradiction there is a slope $q \in [2g(K)-1, n]$ so that $K(q)$ has a weakly symplectically fillable tight structure. Then $K(q)$ bounds a negative-definite 4-manifold. By Theorem 4.2.14 every manifold $K(q')$ with $q' \geq q$ also bounds a negative-definite 4-manifold. However $K(n)$ cannot bound a negative-definite manifold by assumption. This concludes the proof. □

§ 4.3 | A family of hyperbolic L-spaces without weak symplectic fillings

In this section we apply the methods introduced in Section 4.2 a family of L-space knots which does not consist of pretzel knots. In our discussion regarding hyperbolicity we will use the terms *exceptional slopes, short slopes* and the 2π-*theorem*. We refer the reader to [Pur20] for an excellent discussion of such notions and other facets of hyperbolic geometry and knot theory.

Let $\{K_n\}_n$ be the family of knots obtained as the closure of the braids:

$$\beta_n = [(2,1,3,2)^{2n+1}, -1, 2, 1, 1, 2]. \tag{4.12}$$

See Figure 4.1. Here we adopt the notation from [BK22], where the numbers in the brackets denote the corresponding generator in the braid group with 4-strands.

Note this is a strongly quasi positive presentation of β_n that is *almost braid positive*, i.e. it is braid positive for all but one negative crossing.

This family of knots is particularly interesting for our present purposes due to the following result:

Theorem 4.3.1 ([BK22, Proposition 2.1])**.** *The knots K_n, $n \geq 1$, are hyperbolic L-space knots.*

The L-space surgery property in Theorem 4.3.1 is proved in [BK22] by showing that $(8n+6)$ surgery on K_n produces a Seifert fibered space that is known to be an L-space thanks to [LS07a]. In general we are interested in hyperbolic 3-manifolds. Our surgery coefficients lie in $[8n+3, 8n+5]$ (the interval bounds will become more clear after our computations). In this interval there might be exceptional surgeries. However we know there are only finitely many of them thanks to Thurston [Thu82]. Using the help of SnapPy [4] we can find the short slopes for the knots K_n. These are

$$[\infty, 8n+9, 8n+8, 8n+7, 8n+6, 8n+5, 8n+4, 8n+3, \frac{16n+13}{2}, \frac{16n+11}{2}].$$

By the "2π-Theorem" [Thu82] (or the "6 Theorem" by [Ago10, Lac00]), these short slopes are the only potentially non hyperbolic Dehn filling slopes for the knot K_n. One

[4] For this, one can find the description of the knots K_n in terms of a surgery link in [BK22]. In particular K_n has surgery description $L12n1739(-1, 2n+3)(0,0)(1, n+1)$. One then only needs to check the exceptional slopes for the non-filled cusp and set them in the correct homology basis.

can use SnapPy to check for a given knot which of above slopes is truly exceptional. For example in the case of $n = 2$ we check that the slopes

$$[\infty, 24, 23, 22, 21, 19]$$

are exceptional slopes. Note that this list includes 22, which is exactly $8n + 6$ in the case $n = 2$. As computed in [BK22], the symmetrized Alexander polynomial of the knot K_n is:

$$\Delta_{K_n}(T) = 1 + \sum_{k=0}^{n}(T^{4k+2} + T^{-4k-2}) - \sum_{j=0}^{n}(T^{4j+1} + T^{-4j-1}) \tag{4.13}$$

The Seifert genus of the knot K_n is given by the maximal exponent in $\Delta_{K_n}(T)$. Hence we have $g(K_n) = 4n + 2$.

By [LS07a], we know that for an L-space knot K of genus $g(K)$, every r surgery with $r \geq 2g(K) - 1$ yields an L-space. Thus, in our case, since $g(K_n) = 4n + 2$, we have that each $K_n(r)$ is an L-space for $r \in \mathbb{Q}$ and $r \geq 8n + 3$.

We now state the main result of this section.

Theorem 4.1.4. *Let $n \geq 1 \in \mathbb{N}$ so that there is a square-free integer in the two elements set $\{8n + 3, 8n + 5\}$. Let m be the maximal such square-free number and q a rational number so that $q \in [8n + 3, m]$. Let $K_n(q)$ denote the q rational Dehn surgery along the knot K_n. Then $K_n(q)$ is (generically) an hyperbolic 3-manifold that admits no weakly symplectically fillable contact structures.*

Consider for example the value $n = 2$. In this case, $8n + 5 = 21$ which is square-free. Thus for the hyperbolic L-space knot K_2 we have produced an infinite family $K_2(q)$, $q \in [11, 13] \cap \mathbb{Q}$, of 3-manifolds that do not admit weakly symplectically fillable tight contact structures.

Due to the considerations above about hyperbolicity, this family of manifolds $K_n(q)$ contains an infinite sub-family of hyperbolic 3-manifolds that are L-spaces and do not admit any weakly symplectically fillable contact structure. For example, the interval $[8n + 3, 8n + 5]$ for $n = 2$ translates to $[19, 21]$ and as mentioned above the only exceptional surgeries in $[19, 21]$ correspond to the slopes 19 and 21.

Remark 4.3.2. It is important to mention that there are *infinitely many primes* of the form $8k + 5$ (this is a special case of *Dirichlet's Prime Number Theorem*). Thus there are infinitely many values of $n \geq 1$ for which $8n + 5$ is prime and hence square-free. As such, there are infinitely many n for which the interval $[8n + 3, 8n + 5]$ does indeed contain a square-free number, and the maximum such number is $8n + 5$. So we actually produced a $(\mathbb{N} \times \mathbb{Q})$-infinite family (indexed both by n and q) of hyperbolic L-spaces not admitting weak symplectic fillings.

We now prove Theorem 4.1.4.

Proposition 4.3.3. *For the hyperbolic L-space knot K_n, the torsion coefficients $t_i(K_n)$ are given by:*

$$t_i(K_n) = \begin{cases} 0 \text{ for } i > 4n+2 \\ n - \lfloor \frac{i+2}{4} \rfloor + 1 \text{ for } i = 0, \cdots, 4n+2. \end{cases}$$

Proof. Recall that the symmetrized Alexander polynomial of K_n is given by

$$\Delta_{K_n}(T) = 1 + \sum_{k=0}^{n}(T^{4k+2} + T^{-4k-2}) - \sum_{i=0}^{n}(T^{4i+1} + T^{-4i-1}).$$

Here k is equal to $2n+2 = 2(n+1)$.

Then Equation (4.6) translates to the condition $t_{i-1}(K_n) = t_i(K_n)$ if j is contained in an interval of the form $(4m+2, 4m+5]$ for $m = 0, \cdots, n-1$ and $t_{i-1}(K_n) = t_i(K_n)+1$ if i is contained in an interval $(4m+1, 4m+2]$ for $m = 0, \cdots, n$. In other words $t_{i-1}(K_n) = t_i(K_n)$ if i is congruent to $0, 1, 3 \pmod 4$ and $t_{i-1}(K_n) = t_i(K_n) + 1$ if i is congruent to $2 \pmod 4$.

Clearly $t_{4n+2}(K_n) = 0$. Using the above considerations it is then straightforward to compute the value of t_i for $i \leq 4n+2$. See Figure 4.4 for the case K_2. □

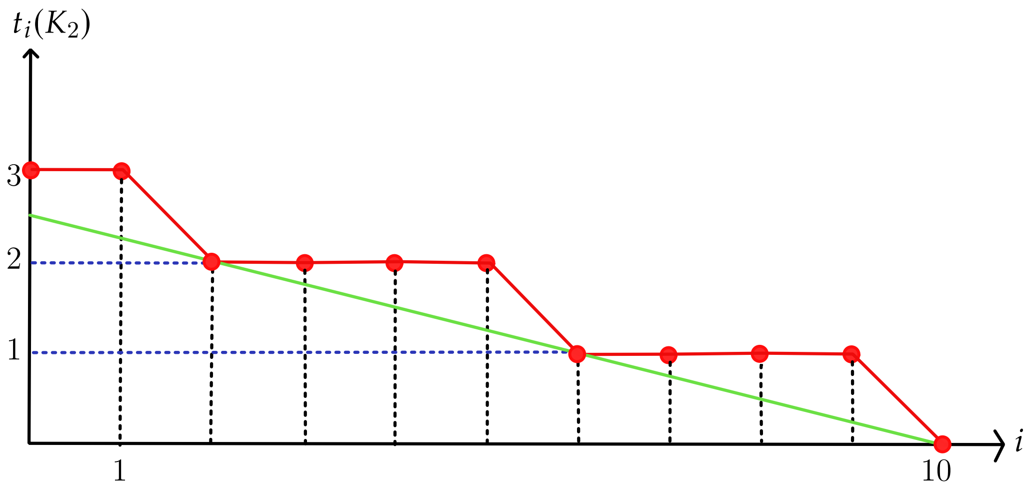

Figure 4.4: This graphic shows the values of $t_i(K_2)$ for $i = 0, \cdots, 10$. The red line is the linear interpolation between the values of $t_i(K_2)$. The green line is the function $h(i) = -\frac{i}{4} + \frac{5}{2}$ which we can use to obtain the desired inequalities.

Proposition 4.3.4. *Let $n \geq 1$ and $m \in \{8n+3, 8n+4, 8n+5\}$. Then all the d-invariants of $K_n(m)$ are negative.*

Proof. We use Theorem 4.2.1 to compute the d-invariants for $m = 8n+k$ with $k \in \{3, 4, 5\}$. Recall that we have to check negativity for the d-invariants corresponding to all the indices $|i| \leq 4n + \lfloor \frac{k}{2} \rfloor$.

Since our k is in $\{3, 4, 5\}$, we can split the calculations in two cases. We first assume that $k = 3$. Then the coefficients we have to consider are $0 \leq i \leq 4n+1$ (the negative case is identical).

If $k \neq 3$, then we also have to consider the torsion coefficient t_h with $h = 4n + 2$, which is equal to 0 by Proposition 4.3.3.

First let $0 \leq i \leq 4n + 1$. We have:

$$d(K_n(8n+k), \pm i) = \frac{(8n+k-2i)^2}{4(8n+k)} - \frac{1}{4} - 2(n - \lfloor \frac{i+2}{4} \rfloor + 1) \tag{4.14}$$
$$\leq \frac{(8n+k)}{4} - \frac{i}{2} - \frac{5}{4} + \frac{i^2}{(8n+k)} - 2n \tag{4.15}$$
$$= \frac{i^2}{(8n+k)} - \frac{i}{2} + \frac{(k-5)}{4}. \tag{4.16}$$

If we evaluate the last expression at 0 we obtain $\frac{k-5}{4}$, which by assumption on k is negative. Note that in passing from the first to the second step we bounded the values of the torsion coefficients from below using the function $h(i) = -\frac{i}{4} + n + \frac{1}{2}$. Note that $h(i) \leq t_i$ since $-\frac{i}{4} + n + \frac{1}{2} \leq n - \lfloor \frac{i+2}{4} \rfloor + 1$. See Figure 4.4 for the case K_2.

Let $f(i) = \frac{i^2}{(8n+k)} - \frac{i}{2} + \frac{(k-5)}{4}$. Here we are extending the domain so that i is varying on the real line. This is a decreasing function from 0 to $i = \frac{8n+k}{4}$, after which it starts increasing.

The value at $i = 4n + 1$ is:

$$\frac{(4n+1)^2}{(8n+k)} - \frac{(4n+1)}{2} + \frac{(k-5)}{4} = \frac{-24n + k^2 - 7k + 4}{4(8n+k)}.$$

From the above equality we see that if $k \in \{3, 4, 5\}$ then the value of $f(4n + 1)$ is negative. Thus we have showed that all the d-invariants up to $i = 4n + 1$ are negative. If $k = 3$, this is sufficient to conclude the proof.

On the other hand, assume $k \in \{4, 5\}$. Then the d-invariant corresponding to $4n+2$ can be easily shown to be negative as well.

$$\frac{(8n+k-2(4n+2))^2}{4(8n+k)} - \frac{1}{4} = \frac{(k-4)^2}{4(8n+k)} - \frac{1}{4} < 0 \tag{4.17}$$

for our values of k.

Thus we have shown that all the d-invariants for integral $8n + k$ surgery on K_n with $k \in \{3, 4, 5\}$ are negative. □

We have thus shown that all the d-invariants in this case are non weak.

Proof of Theorem 4.1.4. The proof is a direct application of Theorem 4.2.15. □

Remark 4.3.5. Note that to conclude the non weakness of the d-invariants of $K_n(8n+3)$ we could have used Proposition 4.2.11 directly.

§ 4.4 | Existence of tight contact structures

We now show that the family of hyperbolic L-spaces introduced in Section 3 does admit tight contact structures. First recall that the braid presentation in Figure 4.12 shows that the knots K_n are strongly-quasi positive. As such, the slice genus $g_s(K_n)$ and the Seifert genus $g(K_n)$ of the knot agree [Hed10]. As we showed in Section 3, the Seifert genus $g(K_n) = 4n + 2$.

Moreover, we know that for quasi-positive knots the slice Bennequin inequality is sharp. In particular:

$$tb(\tilde{K}_n) + |rot(\tilde{K}_n)| = 2g_s(K_n) - 1$$

for some Legendrian representative $\tilde{K}_n$ of K_n in S^3. In our case, this translates to:

$$tb(\tilde{K}_n) + |rot(\tilde{K}_n)| = 8n + 3$$

for some Legendrian representative $\tilde{K}_n$ of K_n. An explicit example of this can be

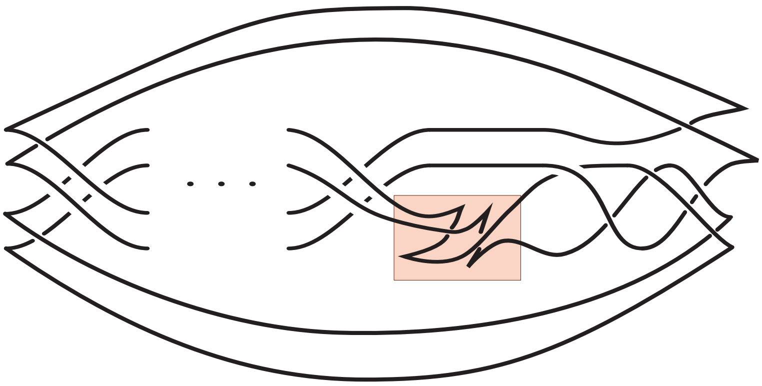

Figure 4.5: The Legendrian representative $\tilde{K}_n$. In orange we highlight the region where a pair of stabilizations is inserted.

directly seen by taking the Legendrian knot diagram in Figure 4.5.

It is a straightforward calculation to show that indeed $tb(\tilde{K}_n) + |rot(\tilde{K}_n)| = 8n + 3$ for the Legendrian knot $\tilde{K}_n$, where $tb = 8n + 1$ and $|rot| = 2$.

In [MT18] the authors prove the following result:

Theorem 4.4.1 ([MT18, Theorem 1.3])**.** *Let $K \subset S^3$ be a knot with slice genus $g_s(K) >$ 0 that admits a Legendrian representative K with $tb(K) + |rot(K)| = 2g_s(K) - 1$. Then the manifold $S^3_{\frac{p}{q}}(K)$ obtained by smooth $(\frac{p}{q})$-surgery along K admits a tight contact structure for every $\frac{p}{q} \notin [2g_s(K) - |rot(K)| - 1, 2g_s(K) - 1]$.*

In our case the family of strongly-quasi positive knots K_n satisfies the hypothesis of Theorem 4.4.1. Hence we obtain the following theorem:

Theorem 4.1.6. *Let $n \geq 1$ and $q \in \mathbb{Q}$. Then the manifolds $K_n(q)$ admit a tight contact structure for $q \notin [8n + 1, 8n + 3]$.*

Moreover if $8n+5$ is square-free, the family $K_n(q)$, $q \in (8n+3, 8n+5] \cap \mathbb{Q}$, contains an infinite family of hyperbolic L-spaces that admit tight contact structures but do not admit weakly symplectically fillable contact structures.

Proof. The proof is a combination of Theorem 4.1.4 and Theorem 4.4.1. ◻

Hence we have constructed an infinite family of hyperbolic L-spaces $K_n(q)$ that do admit tight contact structures but none of them can be weakly symplectically fillable.

Remark 4.4.2. In the proof of Theorem 4.4.1 the tight structures constructed by smooth $(\frac{p}{q})$-surgery along the knot K have *non-vanishing* contact invariant. They cannot contain Giroux torsion since a contact structure ξ with non-trivial torsion has vanishing contact invariant $c(\xi)$. Recall that having non-trivial torsion is the first obvious obstruction to weak fillability. The family of manifolds $K_n(q)$ constructed here is however an example of torsion-free tight manifolds without weakly symplectic fillings.

Bibliography

[Ago10] Ian Agol. Bounds on exceptional Dehn filling. II. *Geom. Topol.*, 14(4):1921–1940, 2010.

[Bak14] Kenneth L. Baker. Counting genus one fibered knots in Lens spaces. *Mich. Math. J.*, 63(3):553–569, 2014.

[BE12] Kenneth Baker and John Etnyre. Rational linking and contact geometry. In *Perspectives in analysis, geometry, and topology*, volume 296 of *Progr. Math.*, pages 19–37. Birkhäuser/Springer, New York, 2012.

[BEM15] Matthew Strom Borman, Yakov Eliashberg, and Emmy Murphy. Existence and classification of overtwisted contact structures in all dimensions. *Acta Math.*, 215(2):281–361, 2015.

[Ben83] Daniel Bennequin. Links and Pfaffian equation. Astérisque 107/108, 87-161 (1983)., 1983.

[BGW13] Steven Boyer, Cameron McA. Gordon, and Liam Watson. On L-spaces and left-orderable fundamental groups. *Math. Ann.*, 356(4):1213–1245, 2013.

[BK22] Kenneth L. Baker and Marc Kegel. Census L-space knots are braid positive, except for one that is not, 2022.

[BSZ25] John A. Baldwin, Steven Sivek, and Jonathan Zung. Pseudo-Anosov flows on hyperbolic L-spaces. Preprint, arXiv:2505.21113 [math.GT] (2025), 2025.

[CGH09] Vincent Colin, Emmanuel Giroux, and Ko Honda. Finitude homotopique et isotopique des structures de contact tendues. *Publ. Math. Inst. Hautes Études Sci.*, (109):245–293, 2009.

[CK24] Rima Chatterjee and Marc Kegel. Contact surgery numbers of Sigma(2,3,11) and L(4m+3,4). Preprint, arXiv:2404.18177 [math.SG] (2024), 2024.

[CM20] James Conway and Hyunki Min. Classification of tight contact structures on surgeries on the figure-eight knot. *Geom. Topol.*, 24(3):1457–1517, 2020.

[Cof04] Tanya Cofer. A class of tight contact structures on $\Sigma_2 \times I$. *Algebr. Geom. Topol.*, 4:961–1011, 2004.

[Col97] Vincent Colin. Chirurgies d'indice un et isotopies de sphères dans les variétés de contact tendues. *C. R. Acad. Sci. Paris Sér. I Math.*, 324(6):659–663, 1997.

[Col99] Vincent Colin. Recollement de variétés de contact tendues. *Bull. Soc. Math. France*, 127(1):43–69, 1999.

[Con19] James Conway. Transverse surgery on knots in contact 3-manifolds. *Trans. Amer. Math. Soc.*, 372(3):1671–1707, 2019.

[CPP15] Roger Casals, Dishant M. Pancholi, and Francisco Presas. Almost contact 5-manifolds are contact. *Ann. Math. (2)*, 182(2):429–490, 2015.

[DG04] Fan Ding and Hansjörg Geiges. A Legendrian surgery presentation of contact 3-manifolds. *Math. Proc. Cambridge Philos. Soc.*, 136(3):583–598, 2004.

[DG07] Fan Ding and Hansjörg Geiges. A unique decomposition theorem for tight contact 3-manifolds. *Enseign. Math. (2)*, 53(3-4):333–345, 2007.

[DGS04] Fan Ding, Hansjörg Geiges, and András I. Stipsicz. Surgery diagrams for contact 3-manifolds. *Turkish J. Math.*, 28(1):41–74, 2004.

[DLW24] Fan Ding, Youlin Li, and Zhongtao Wu. Nonexistence and existence of fillable contact structures on 3-manifolds. *Asian J. Math.*, 28(5):617–652, 2024.

[EH01a] John B. Etnyre and Ko Honda. Knots and contact geometry. I. Torus knots and the figure eight knot. *J. Symplectic Geom.*, 1(1):63–120, 2001.

[EH01b] John B. Etnyre and Ko Honda. On the nonexistence of tight contact structures. *Ann. of Math. (2)*, 153(3):749–766, 2001.

[EH02] John B. Etnyre and Ko Honda. Tight contact structures with no symplectic fillings. *Invent. Math.*, 148(3):609–626, 2002.

[Eli89] Y. Eliashberg. Classification of overtwisted contact structures on 3-manifolds. *Invent. Math.*, 98(3):623–637, 1989.

[Eli90] Yakov Eliashberg. Topological characterization of Stein manifolds of dimension > 2. *Int. J. Math.*, 1(1):29–46, 1990.

[Eli92] Yakov Eliashberg. Contact 3-manifolds twenty years since J. Martinet's work. *Ann. Inst. Fourier (Grenoble)*, 42(1-2):165–192, 1992.

[Eli96] Yasha Eliashberg. Unique holomorphically fillable contact structure on the 3-torus. *Int. Math. Res. Not.*, 1996(2):77–82, 1996.

[ET98] Yakov M. Eliashberg and William P. Thurston. *Confoliations*, volume 13 of *Univ. Lect. Ser.* Providence, RI: American Mathematical Society, 1998.

[Etn] John B. Etnyre. Convex surfaces in contact geometry: Class notes.

[Etn00] John B. Etnyre. Tight contact structures on lens spaces. *Commun. Contemp. Math.*, 2(4):559–577, 2000.

[Etn03] John B. Etnyre. Introductory lectures on contact geometry. *Proc. Sympos. Pure Math.*, 71:81–107, 2003.

[Etn13] John B. Etnyre. On knots in overtwisted contact structures. *Quantum Topol.*, 4(3):229–264, 2013.

[Gei08] Hansjörg Geiges. *An introduction to contact topology*, volume 109 of *Camb. Stud. Adv. Math.* Cambridge: Cambridge University Press, 2008.

[Ghi05] Paolo Ghiggini. Strongly fillable contact 3-manifolds without Stein fillings. *Geom. Topol.*, 9:1677–1687, 2005.

[Ghi06] Paolo Ghiggini. Ozsváth-Szabó invariants and fillability of contact structures. *Math. Z.*, 253(1):159–175, 2006.

[Gir91] Emmanuel Giroux. Convexité en topologie de contact. *Comment. Math. Helv.*, 66(4):637–677, 1991.

[Gir99] Emmanuel Giroux. Une infinité de structures de contact tendues sur une infinité de variétés. *Invent. Math.*, 135(3):789–802, 1999.

[Gir00] Emmanuel Giroux. Structures de contact en dimension trois et bifurcations des feuilletages de surfaces. *Invent. Math.*, 141(3):615–689, 2000.

[Gir01] Emmanuel Giroux. Structures de contact sur les variétés fibrées en cercles audessus d'une surface. *Comment. Math. Helv.*, 76(2):218–262, 2001.

[Gir02] Emmanuel Giroux. Contact geometry: From dimension three to higher dimensions. In *Proceedings of the International Congress of Mathematicians, ICM 2002, Beijing, China, August 20–28, 2002. Vol. II: Invited lectures*, pages 405–414. Beijing: Higher Education Press; Singapore: World Scientific/distributor, 2002.

[GLS06] Paolo Ghiggini, Paolo Lisca, and András I. Stipsicz. Classification of tight contact structures on small Seifert 3-manifolds with $e_0 \geq 0$. *Proc. Am. Math. Soc.*, 134(3):909–916, 2006.

[GLS07] Paolo Ghiggini, Paolo Lisca, and András I. Stipsicz. Tight contact structures on some small Seifert fibered 3-manifolds. *Amer. J. Math.*, 129(5):1403–1447, 2007.

[GMM09] David Gabai, Robert Meyerhoff, and Peter Milley. Minimum volume cusped hyperbolic three-manifolds. *J. Amer. Math. Soc.*, 22(4):1157–1215, 2009.

[GO89] David Gabai and Ulrich Oertel. Essential laminations in 3-manifolds. *Ann. Math. (2)*, 130(1):41–73, 1989.

[Gol15] Marco Golla. Ozsváth-Szabó invariants of contact surgeries. *Geom. Topol.*, 19(1):171–235, 2015.

[Gom98] Robert E. Gompf. Handlebody construction of Stein surfaces. *Ann. of Math. (2)*, 148(2):619–693, 1998.

[Gra59] John W. Gray. Some global properties of contact structures. *Ann. Math. (2)*, 69:421–450, 1959.

[GS99] Robert E. Gompf and András I. Stipsicz. *4-manifolds and Kirby calculus*, volume 20 of *Graduate Studies in Mathematics*. American Mathematical Society, Providence, RI, 1999.

[GS03] Paolo Ghiggini and Stephan Schönenberger. On the classification of tight contact structures. In *Topology and geometry of manifolds (Athens, GA, 2001)*, volume 71 of *Proc. Sympos. Pure Math.*, pages 121–151. Amer. Math. Soc., Providence, RI, 2003.

[Hed10] Matthew Hedden. Notions of positivity and the Ozsváth-Szabó concordance invariant. *J. Knot Theory Ramifications*, 19(5):617–629, 2010.

[Him25] Keisuke Himeno. Non-braid positive hyperbolic L-space knots. Preprint, arXiv:2506.22934 [math.GT] (2025), 2025.

[HKM02] Ko Honda, William H. Kazez, and Gordana Matić. Convex decomposition theory. *Int. Math. Res. Not.*, (2):55–88, 2002.

[HKM03] Ko Honda, William H. Kazez, and Gordana Matić. Tight contact structures on fibered hyperbolic 3-manifolds. *J. Differential Geom.*, 64(2):305–358, 2003.

[HKM05] Ko Honda, William H. Kazez, and Gordana Matic. Pinwheels and bypasses. *Algebr. Geom. Topol.*, 5:769–784, 2005.

[HKM07] Ko Honda, William H. Kazez, and Gordana Matić. Right-veering diffeomorphisms of compact surfaces with boundary. *Invent. Math.*, 169(2):427–449, 2007.

[HM18] Matthew Hedden and Thomas E. Mark. Floer homology and fractional Dehn twists. *Adv. Math.*, 324:1–39, 2018.

[HMW92] Craig D. Hodgson, G. Robert Meyerhoff, and Jeffrey R. Weeks. Surgeries on the Whitehead link yield geometrically similar manifolds. *Topology '90 (Columbus, OH, 1990)*, 1:195–206, 1992.

[Hon00a] Ko Honda. On the classification of tight contact structures. I. *Geom. Topol.*, 4:309–368, 2000.

[Hon00b] Ko Honda. On the classification of tight contact structures. II. *J. Differential Geom.*, 55(1):83–143, 2000.

[Hon02] Ko Honda. Gluing tight contact structures. *Duke Math. J.*, 115(3):435–478, 2002.

[Hoz20] Surena Hozoori. Dynamics and topology of conformally Anosov contact 3-manifolds. *Differ. Geom. Appl.*, 73:16, 2020. Id/No 101679.

[HW18] Matthew Hedden and Liam Watson. On the geography and botany of knot Floer homology. *Sel. Math., New Ser.*, 24(2):997–1037, 2018.

[Juh15] András Juhász. A survey of Heegaard Floer homology. In *New ideas in low dimensional topology*, pages 237–296. Hackensack, NJ: World Scientific, 2015.

[Kan97] Yutaka Kanda. The classification of tight contact structures on the 3-torus. *Comm. Anal. Geom.*, 5(3):413–438, 1997.

[KO08] Mustafa Korkmaz and Burak Ozbagci. On sections of elliptic fibrations. *Michigan Math. J.*, 56(1):77–87, 2008.

[Krc18] David Krcatovich. A restriction on the Alexander polynomials of L-space knots. *Pac. J. Math.*, 297(1):117–129, 2018.

[KT17] Amey Kaloti and Bülent Tosun. Hyperbolic rational homology spheres not admitting fillable contact structures. *Math. Res. Lett.*, 24(6):1693–1705, 2017.

[Lac00] Marc Lackenby. Word hyperbolic Dehn surgery. *Invent. Math.*, 140(2):243–282, 2000.

[Liu17] Yajing Liu. L-space surgeries on links. *Quantum Topol.*, 8(3):505–570, 2017.

[LL19] Youlin Li and Yajing Liu. Hyperbolic 3-manifolds admitting no fillable contact structures. *Proc. Am. Math. Soc.*, 147(1):351–360, 2019.

[LOSS09] Paolo Lisca, Peter Ozsváth, András I. Stipsicz, and Zoltán Szabó. Heegaard Floer invariants of Legendrian knots in contact three-manifolds. *J. Eur. Math. Soc. (JEMS)*, 11(6):1307–1363, 2009.

[LS04] Paolo Lisca and András I. Stipsicz. Ozsváth-Szabó invariants and tight contact three-manifolds. I. *Geom. Topol.*, 8:925–945, 2004.

[LS07a] Paolo Lisca and András I. Stipsicz. Ozsváth-Szabó invariants and tight contact 3-manifolds, III. *J. Symplectic Geom.*, 5(4):357–384, 2007.

[LS07b] Paolo Lisca and András I. Stipsicz. Ozsváth-Szabó invariants and tight contact 3-manifolds. III. *J. Symplectic Geom.*, 5(4):357–384, 2007.

[LS07c] Paolo Lisca and András I. Stipsicz. Ozsváth-Szabó invariants and tight contact three-manifolds. II. *J. Differ. Geom.*, 75(1):109–141, 2007.

[LS09] Paolo Lisca and András I. Stipsicz. On the existence of tight contact structures on Seifert fibered 3-manifolds. *Duke Math. J.*, 148(2):175–209, 2009.

[LW19] Youlin Li and Zhongtao Wu. A bound for rational Thurston-Bennequin invariants. *Geom. Dedicata*, 200:371–383, 2019.

[Mar71] J. Martinet. Formes de contact sur les variétés de dimension 3. Proc. Liverpool Singularities-Symp. II, Dept. Pure Math. Univ. Liverpool 1969-1970, 142-163 (1971)., 1971.

[Mar21] Bruno Martelli. Dehn surgery on the minimally twisted seven-chain link. *Comm. Anal. Geom.*, 29(7):1597–1641, 2021.

[Mas24] Thomas Massoni. Taut foliations and contact pairs in dimension three. 2024.

[Mat13] Daniel V. Mathews. Sutured TQFT, torsion and tori. *Internat. J. Math.*, 24(5):1350039, 35, 2013.

[MN26] Hyunki Min and Isacco Nonino. Tight contact structures on a family of hyperbolic L-spaces. *Geom. Dedicata*, 220(4):42, 2026. Id/No 45.

[MNW13] Patrick Massot, Klaus Niederkrüger, and Chris Wendl. Weak and strong fillability of higher dimensional contact manifolds. *Invent. Math.*, 192(2):287–373, 2013.

[MO07] Ciprian Manolescu and Brendan Owens. A concordance invariant from the Floer homology of double branched covers. *Int. Math. Res. Not.*, 2007(20):21, 2007. Id/No rnm077.

[Mor89] Kanji Morimoto. Genus one fibered knots in lens spaces. *J. Math. Soc. Japan*, 41(1):81–96, 1989.

[MT18] Thomas E. Mark and Bülent Tosun. Naturality of Heegaard Floer invariants under positive rational contact surgery. *J. Differ. Geom.*, 110(2):281–344, 2018.

[MT23] Thomas Mark and Bülent Tosun. Fillable contact structures from positive surgery, 2023.

[Non24] Isacco Nonino. L-space knots with positive surgeries that are not weakly symplectically fillable. Preprint, arXiv:2404.17308 [math.GT] (2024), 2024.

[Ona18] Sinem Onaran. On overtwisted contact surgeries. *Bull. Aust. Math. Soc.*, 98(1):144–148, 2018.

[OS03] Peter Ozsváth and Zoltán Szabó. Absolutely graded Floer homologies and intersection forms for four-manifolds with boundary. *Adv. Math.*, 173(2):179–261, 2003.

[OS04a] Peter Ozsváth and Zoltán Szabó. Holomorphic disks and genus bounds. *Geom. Topol.*, 8:311–334, 2004.

[OS04b] Peter Ozsváth and Zoltán Szabó. Holomorphic disks and three-manifold invariants: properties and applications. *Ann. of Math. (2)*, 159(3):1159–1245, 2004.

[OS04c] Peter Ozsváth and Zoltán Szabó. Holomorphic disks and topological invariants for closed three-manifolds. *Ann. of Math. (2)*, 159(3):1027–1158, 2004.

[OS05a] Peter Ozsváth and Zoltán Szabó. Heegaard Floer homology and contact structures. *Duke Math. J.*, 129(1):39–61, 2005.

[OS05b] Peter Ozsváth and Zoltán Szabó. On knot Floer homology and lens space surgeries. *Topology*, 44(6):1281–1300, 2005.

[OS06] Brendan Owens and Sašo Strle. Rational homology spheres and the four-ball genus of knots. *Adv. Math.*, 200(1):196–216, 2006.

[OS12a] Brendan Owens and Sašo Strle. A characterization of the $\mathbb{Z}^n \oplus \mathbb{Z}(\delta)$ lattice and definite nonunimodular intersection forms. *Am. J. Math.*, 134(4):891–913, 2012.

[OS12b] Brendan Owens and Sašo Strle. Dehn surgeries and negative-definite four-manifolds. *Sel. Math., New Ser.*, 18(4):839–854, 2012.

[Pla04] Olga Plamenevskaya. Contact structures with distinct Heegaard Floer invariants. *Math. Res. Lett.*, 11(4):547–561, 2004.

[Pur20] Jessica S. Purcell. *Hyperbolic knot theory*, volume 209 of *Grad. Stud. Math.* Providence, RI: American Mathematical Society (AMS), 2020.

[Thu82] William P. Thurston. Three-dimensional manifolds, Kleinian groups and hyperbolic geometry. *Bull. Amer. Math. Soc. (N.S.)*, 6(3):357–381, 1982.

[Thu22] William P. Thurston. *The geometry and topology of three-manifolds. Vol. IV.* American Mathematical Society, Providence, RI, [2022] ©2022. Edited and with a preface by Steven P. Kerckhoff and a chapter by J. W. Milnor.

[Tos20] Bülent Tosun. Tight small Seifert fibered manifolds with $e_0 = -2$. *Algebr. Geom. Topol.*, 20(1):1–27, 2020.

[Tri06] James J. Tripp. Contact structures on open 3-manifolds. *J. Symplectic Geom.*, 4(1):93–116, 2006.

[Wan15] Andy Wand. Tightness is preserved by Legendrian surgery. *Ann. Math. (2)*, 182(2):723–738, 2015.

[Wei91] Alan Weinstein. Contact surgery and symplectic handlebodies. *Hokkaido Math. J.*, 20(2):241–251, 1991.

[Wu06] Hao Wu. Legendrian vertical circles in small Seifert spaces. *Commun. Contemp. Math.*, 8(2):219–246, 2006.